

EUROPEAN ORGANISATION FOR NUCLEAR RESEARCH (CERN)



Submitted to: JHEP



CERN-EP-2024-315
17th December 2024

Test of lepton flavour universality in W -boson decays into electrons and τ -leptons using pp collisions at $\sqrt{s} = 13$ TeV with the ATLAS detector

The ATLAS Collaboration

A measurement of the ratio of the branching fractions, $R_{\tau/e} = B(W \rightarrow \tau\nu)/B(W \rightarrow e\nu)$, is performed using a sample of W bosons originating from top-quark decays to final states containing τ -leptons or electrons. This measurement uses pp collisions at $\sqrt{s} = 13$ TeV, collected by the ATLAS experiment at the Large Hadron Collider during Run 2, corresponding to an integrated luminosity of 140 fb^{-1} . The $W \rightarrow \tau\nu_\tau$ (with $\tau \rightarrow e\nu_e\nu_\tau$) and $W \rightarrow e\nu_e$ decays are distinguished using the differences in the impact parameter distributions and transverse momentum spectra of the electrons. The measured ratio of branching fractions $R_{\tau/e} = 0.975 \pm 0.012$ (stat.) ± 0.020 (syst.), is consistent with the Standard Model assumption of lepton flavour universality in W -boson decays.

© 2024 CERN for the benefit of the ATLAS Collaboration.

Reproduction of this article or parts of it is allowed as specified in the CC-BY-4.0 license.

arXiv:2412.11989v1 [hep-ex] 16 Dec 2024

Contents

1	Introduction	2
2	ATLAS detector	3
3	Data and simulated events samples	4
4	Event reconstruction and selection	7
5	Electron impact parameter calibration	9
6	Background estimation	11
7	Statistical analysis and systematic uncertainties	16
8	Results	18
9	Conclusion	25

1 Introduction

The Standard Model (SM) [1–3] posits that the electroweak interactions of charged leptons (electrons, muons and τ -leptons) are identical. This feature, known as lepton flavour universality (LFU), is one of the foundational principles of the SM. Differences in the rates of electroweak processes among charged leptons are induced only via their mass differences, manifesting in phase space and radiative effects. Any violation of LFU would be an unambiguous signal of physics beyond the SM and would help to identify the principles that can be used to build a more comprehensive theory.

LFU has been extensively tested by measuring the couplings of the different generations of leptons to the W boson. Such studies have been performed in decays of τ -leptons, charged π and K mesons [4], and in leptonic decays of the W bosons [5]. No significant deviations from LFU have been observed in the charged-current decays of τ -leptons, π and K mesons, with experimental precision reaching about 0.1–0.2%. The precision of LFU tests in the decays of on-shell W bosons is lower. The ratios of the branching fractions of the W -boson decays into leptons are consistent with LFU, and the world-average values have a precision of 0.6–2%. Despite higher experimental uncertainties, probes of LFU in decays of on-shell W bosons offer sensitivity to different possible new physics effects compared to the decays of light particles [6–8].

The ratio of branching fractions $R_{\tau/\mu} \equiv B(W \rightarrow \tau\nu_\tau)/B(W \rightarrow \mu\nu_\mu)$ was measured at the LEP collider [9] and at the Large Hadron Collider (LHC) by the ATLAS [10] and CMS [11] collaborations. The measurements at LEP deviate from unity by more than two standard deviations, but the more precise subsequent measurements from ATLAS and CMS agree with the SM expectation. The Particle Data Group (PDG) average of all the measurements of $R_{\tau/\mu}$, accounting for the tension between them, is 1.002 ± 0.020 [5]. Recently, the ATLAS Collaboration published a measurement of $R_{\mu/e} \equiv B(W \rightarrow \mu\nu_\mu)/B(W \rightarrow e\nu_e) = 0.9995 \pm 0.0044$ [12] with an improved precision compared to the current world average $R_{\mu/e} = 1.002 \pm 0.006$ [5]. The combined LEP result of $R_{\tau/e} \equiv B(W \rightarrow \tau\nu_\tau)/B(W \rightarrow e\nu_e) =$

1.063 ± 0.027 deviates from the SM by more than two standard deviations like the LEP $R_{\tau/\mu}$ measurement [9]. The result of the CMS Collaboration $R_{\tau/e} = 0.994 \pm 0.021$ [11] agrees with the SM expectation and differs from the corresponding LEP measurement.

This paper presents the first measurement of the ratio $R_{\tau/e}$ with the ATLAS detector using top-quark decays as a source of W bosons. The analysis complements the previous ATLAS measurement of $R_{\tau/\mu}$ and $R_{\mu/e}$ in W -boson decays by including another decay channel. Top-quark pair-production yields a clean source of W bosons, owing to the large $t\bar{t}$ production cross-section relative to expected background processes and efficient triggering. The SM predicts that the top quark decays almost exclusively into a Wb final state, and thus a measurement of the ratio of branching fractions $B(t \rightarrow \tau\nu b)/B(t \rightarrow e\nu b)$ provides a measurement of $R_{\tau/e}$. For the τ -lepton selection, the leptonic decay $\tau \rightarrow e\nu_e\nu_\tau$ is chosen over hadronic τ decays due to the smaller experimental uncertainties associated with the leptonic channel. In addition, selecting the electron in both the $W \rightarrow \tau\nu_\tau$ and $W \rightarrow e\nu_e$ final states results in a substantial reduction of the systematic uncertainties in the ratio $R_{\tau/e}$.

This paper is organised as follows. Section 2 presents the ATLAS detector, followed by a description of the data and Monte Carlo simulation samples used in the analysis in Section 3. Section 4 details the physical objects and event selection criteria. The calibration of the signal modelling is discussed in Section 5, and Section 6 describes the estimate of background contributions. The statistical analysis and systematic uncertainties are covered in Section 7, with the results and conclusions presented in Sections 8 and 9, respectively.

2 ATLAS detector

The ATLAS detector [13] at the LHC covers nearly the entire solid angle around the collision point.¹ It consists of an inner tracking detector surrounded by a thin superconducting solenoid, electromagnetic and hadronic calorimeters, and a muon spectrometer incorporating three large superconducting air-core toroidal magnets.

The inner-detector system (ID) is immersed in a 2 T axial magnetic field and provides charged-particle tracking in the range of $|\eta| < 2.5$. The high-granularity silicon pixel detector covers the vertex region and typically provides four measurements per track, the first hit generally being in the insertable B-layer (IBL) installed before Run 2 [14, 15]. It is followed by the SemiConductor Tracker (SCT), which usually provides eight measurements per track. These silicon detectors are complemented by the transition radiation tracker (TRT), which enables radially extended track reconstruction up to $|\eta| = 2.0$. The TRT also provides electron identification information based on the fraction of hits (typically 30 in total) above a higher energy-deposit threshold arising from transition radiation.

The calorimeter system covers the pseudorapidity range $|\eta| < 4.9$. Within the region $|\eta| < 3.2$, electromagnetic calorimetry is provided by barrel and endcap high-granularity lead/liquid-argon (LAr) calorimeters, with an additional thin LAr presampler covering $|\eta| < 1.8$ to correct for energy loss in material

¹ ATLAS uses a right-handed coordinate system with its origin at the nominal interaction point (IP) in the centre of the detector and the z -axis along the beam pipe. The x -axis points from the IP to the centre of the LHC ring, and the y -axis points upwards. Polar coordinates (r, ϕ) are used in the transverse plane, ϕ being the azimuthal angle around the z -axis. The pseudorapidity is defined in terms of the polar angle θ as $\eta = -\ln \tan(\theta/2)$ and is equal to the rapidity $y = \frac{1}{2} \ln \left(\frac{E+p_z}{E-p_z} \right)$ in the relativistic limit. Angular distance is measured in units of $\Delta R \equiv \sqrt{(\Delta y)^2 + (\Delta\phi)^2}$. The transverse momentum p_T is defined as the projection of the momentum of a particle on the plane perpendicular to the beam pipe in the centre of ATLAS detector.

upstream of the calorimeters. Hadronic calorimetry is provided by the steel/scintillator-tile calorimeter, segmented into three barrel structures within $|\eta| < 1.7$, and two copper/LAr hadronic endcap calorimeters. The solid angle coverage is completed with forward copper/LAr and tungsten/LAr calorimeter modules optimised for electromagnetic and hadronic energy measurements, respectively.

The muon spectrometer (MS) comprises separate trigger and high-precision tracking chambers measuring the deflection of muons in a magnetic field generated by the superconducting air-core toroidal magnets. The field integral of the toroids ranges between 2.0 and 6.0 T m across most of the detector. Three layers of precision chambers, each consisting of layers of monitored drift tubes, cover the region $|\eta| < 2.7$, complemented by cathode-strip chambers in the forward region, where the background is highest. The muon trigger system covers the range $|\eta| < 2.4$ with resistive-plate chambers in the barrel, and thin-gap chambers in the endcap regions.

The luminosity is measured mainly by the LUCID-2 [16] detector that records Cherenkov light produced in the quartz windows of photomultipliers located close to the beampipe.

Events are selected by the first-level trigger system implemented in custom hardware, followed by selections made by algorithms implemented in software in the high-level trigger [17]. The first-level trigger accepts events from the 40 MHz bunch crossings at a rate below 100 kHz, which the high-level trigger further reduces to record complete events to disk at about 1 kHz.

A software suite [18] is used in data simulation, in the reconstruction and analysis of real and simulated data, in detector operations, and in the trigger and data acquisition systems of the experiment.

3 Data and simulated events samples

The measurement uses pp collision data recorded by the ATLAS detector from 2015 to 2018 at a centre-of-mass energy of $\sqrt{s} = 13$ TeV. Each recorded event includes on average 33 additional inelastic collisions because of the high instantaneous luminosity of the LHC. These background collisions are referred to as *pile-up*. After the application of data-quality requirements [19], the data sample corresponds to an integrated luminosity of $140.1 \pm 1.2 \text{ fb}^{-1}$ [20].

Samples of simulated events were produced using Monte Carlo (MC) techniques to model different SM processes. After event generation of the process of interest for each sample, the detector response was modelled using either the full ATLAS detector simulation based on GEANT4 toolkit [21] or a fast simulation that relied on a parametrisation of the calorimeter response [22]. The effect of pile-up was modelled by overlaying the simulated hard-scattering event with inelastic pp collisions generated with PYTHIA 8.186 [23] using the NNPDF2.3LO [24] set of parton distribution functions (PDF) and the A3 set of tuned parameters [25]. The data and MC simulated events were passed through the same reconstruction and analysis procedures.

For all MC samples simulating the production of top quarks, the mass of the top quark was set to $m_{\text{top}} = 172.5$ GeV. The mass of the Higgs boson was set to 125 GeV. In all samples where PYTHIA was used to simulate the parton shower (PS) and hadronisation, it used the A14 set of tuned parameters [26] and the NNPDF2.3LO set of PDFs. In all samples where the PYTHIA or HERWIG [27, 28] generators were used to simulate the PS and hadronisation, the decays of bottom and charm hadrons were simulated using the EVTGEN program [29].

The production of $t\bar{t}$ events was modelled using the POWHEG BOX v2 [30–33] generator, which provides matrix elements (ME) at next-to-leading order (NLO) in the strong coupling constant α_s , and the NNPDF3.0_{NLO} [34] PDF set. The h_{damp} parameter, which effectively regulates the high-transverse momentum (p_T) radiation against which the $t\bar{t}$ system recoils, was set to $1.5 m_{\text{top}}$ [35]. The functional form of the renormalisation and factorisation scales was set to $\sqrt{m_{\text{top}}^2 + p_T^2}$. The events were passed through PYTHIA 8.230 [36] for the PS and hadronisation.

An additional re-weighting was applied to the $t\bar{t}$ events to match the calculations at next-to-next-to-leading-order (NNLO) in α_s and NLO in α_{EW} [37]. The applied weights are based on the parton-level distributions, after final state radiation, and are derived as a function of the top-quark and anti-top-quark p_T , and the mass and transverse momentum of the $t\bar{t}$ system. The re-weighting improves the agreement between data and MC simulation.

The $t\bar{t}$ sample was normalised to the cross-section prediction at NNLO in α_s including the resummation of next-to-next-to-leading logarithmic (NNLL) soft-gluon terms calculated using TOP++ 2.0 [38–44]. For pp collisions at a centre-of-mass energy of $\sqrt{s} = 13$ TeV, this cross-section corresponds to $\sigma(t\bar{t})_{\text{NNLO+NNLL}} = 832 \pm 45$ pb. The uncertainties in the cross-section due to the PDF and α_s were calculated using the PDF4LHC15 prescription [45] with the MSTW2008_{NNLO} [46, 47], CT10_{NNLO} [48, 49] and NNPDF2.3_{LO} PDF sets in the five-flavour scheme, and were added in quadrature to the effect of the scale uncertainty.

In addition to $t\bar{t}$ events, the contribution of the Wt and $t\bar{t} + X$ ($X = W, Z, H$) production processes are treated as signal. For the Wt process, the leptons (electron or τ -lepton) coming from the top-quark and W -boson decays are included in the analysis as in both cases they are produced in the decays of a real W boson.

Single-top Wt associated production was modelled using POWHEG BOX v2 and PYTHIA 8.230. The renormalisation and factorisation scales were set to m_{top} . A diagram removal scheme [50] was employed to handle the interference with $t\bar{t}$ production [35]. The inclusive cross-section of Wt production was corrected to the theory prediction calculated at NLO in α_s with NNLL soft-gluon corrections [51, 52] yielding $\sigma(Wt)_{\text{NLO+NNLL}} = 71.7 \pm 3.8$ pb. The uncertainty in the cross-section due to the PDF was calculated using the MSTW2008_{NNLO} PDF set, and was added in quadrature to the uncertainty of $\sigma(Wt)$.

The production of $t\bar{t}V$ ($V = W, Z$) events was modelled using the MADGRAPH5_AMC@NLO 2.3.3 [53] generator, which provided MEs at NLO in α_s with the NNPDF3.0_{NLO} PDF set. The functional form of the renormalisation and factorisation scales was set to $0.5 \times \sum_i \sqrt{m_i^2 + p_{T,i}^2}$, where the sum runs over all the particles generated from the ME calculation. Top quarks were decayed at leading-order (LO) using MADSPIN [54, 55]. The events were passed through PYTHIA 8.210 for the PS and hadronisation. The cross-sections were calculated at NLO in α_s and NLO in α_{EW} accuracy using MADGRAPH5_AMC@NLO as reported in Ref. [56]. In the case of $t\bar{t}l^+l^-$ ($l = e, \mu, \tau$), the cross-section was scaled by an off-shell correction estimated at the one-loop level in α_s . The predicted values at $\sqrt{s} = 13$ TeV are $0.88_{-0.11}^{+0.09}$ pb and $0.60_{-0.07}^{+0.08}$ pb for $t\bar{t}Z$ and $t\bar{t}W$, respectively, where the uncertainties were estimated from variations of α_s and the renormalisation and factorisation scales.

The production of $t\bar{t}H$ events was modelled using the POWHEG BOX v2 [30–33, 57] generator. The functional form of the renormalisation and factorisation scales was set to $\sqrt[3]{m_T(t) \cdot m_T(\bar{t}) \cdot m_T(H)}$, where $m_T = \sqrt{m^2 + p_T^2}$ is the transverse mass of a generated particle, m is its mass, and p_T is its transverse momentum. The events were passed through PYTHIA 8.230. The cross-section was calculated at NLO in α_s and NLO in α_{EW} accuracy using MADGRAPH5_AMC@NLO as reported in Ref. [56]. The predicted

value at $\sqrt{s} = 13$ TeV is 507^{+35}_{-50} fb, where the uncertainties were estimated from variations of α_s and the renormalisation and factorisation scales.

The background for this analysis comes from two main sources. The first is the production of Z bosons decaying to pairs of leptons. The second source includes all processes in which the probe electrons do not come from the decays of real W or Z bosons. Such electrons are referred to as *fake* electrons.

The production of most V +jets ($V = Z, W$) events was simulated with the SHERPA 2.2.11 [58] generator. For the simulation of $Z \rightarrow \tau^+ \tau^-$ events SHERPA 2.2.14 was used. The simulation setup involved MEs with NLO accuracy in α_s for up to two partons, and LO accuracy for up to four partons calculated with the COMIX [59] and OPENLOOPS [60–62] libraries. The default SHERPA PS [63] based on Catani–Seymour dipole factorisation and the cluster hadronisation model [64] were used. They employed the dedicated set of tuned parameters developed by the SHERPA authors and the NNPDF3.0NNLO [34] PDF set. The NLO MEs for a given jet multiplicity were matched to the PS using a colour-exact variant of the MC@NLO algorithm [65]. Different jet multiplicities were then merged into an inclusive sample using an improved CKKW matching procedure [66, 67] which was extended to NLO accuracy using the MEPS@NLO prescription [68].

The production of diboson final states (VV) was simulated with the SHERPA 2.2.1 or 2.2.2 generator depending on the process, including off-shell effects and Higgs boson contributions, where appropriate. Fully leptonic final states and semileptonic final states, where one boson decays leptonically and the other hadronically, were generated using MEs at NLO in α_s for up to one additional parton and at LO in α_s for up to three additional parton emissions. Samples for the loop-induced processes $gg \rightarrow VV$ were generated using LO-accurate MEs for up to one additional parton emission for both the cases of fully leptonic and semileptonic final states. The ME calculations were matched and merged with the SHERPA PS based on Catani–Seymour dipole factorisation [59, 63] using the MEPS@NLO prescription [65–68]. The virtual QCD corrections were provided by the OPENLOOPS library [60–62]. The NNPDF3.0NNLO set of PDFs was used, along with the dedicated set of tuned PS parameters developed by the SHERPA authors.

Events featuring at least one fake lepton originate from $t\bar{t}$, $t\bar{t} + X$ ($X = W, Z, H$), or Wt production processes. The simulation of such events was described above. Single-top-quark s - and t -channel production can also produce dilepton events with at least one fake lepton. These processes were modelled using the POWHEG BOX v2 [31–33, 69] generator. The functional form of the renormalisation and factorisation scales was set to $\sqrt{m_b^2 + p_{T,b}^2}$ for t -channel following the recommendation of Ref. [69], and to m_{top} for s -channel. The events were processed through PYTHIA 8.230.

Any possible contribution of other sources of fake leptons was taken into account in the correction factors measured using data as explained in Section 6.

The uncertainties related to the modelling of the signal and background production were estimated by comparing the baseline MC samples described above with different MC generators or a modified configuration of the baseline MC generators. More details of these studies are given in Section 7. Here, the description of the alternative MC samples is given.

The uncertainty due to the choice of the PS and hadronisation model used in $t\bar{t}$ and Wt production was evaluated with a sample generated with POWHEG BOX v2 for the hard-scatter simulation but passed through HERWIG 7.1.3 for the PS and hadronisation. The samples employ the HERWIG 7.1 default set of tuned parameters and the MMHT2014LO [70] PDF set.

The baseline $t\bar{t}$ and Wt samples were generated with $h_{\text{damp}} = 1.5 m_{\text{top}}$. A variation of the h_{damp} value to $3.0 m_{\text{top}}$ was used to evaluate the systematic uncertainty related to this parameter.

The NLO matching uncertainty was evaluated by comparing the baseline $t\bar{t}$ and Wt samples with alternative samples obtained by setting the $p_{\text{T}_{\text{hard}}}$ parameter of PYTHIA 8 to one (the default value is zero). This parameter regulates the definition of the vetoed region of the showering, important to avoid holes or overlap in the phase space filled by POWHEG and PYTHIA. This follows the recommendation of Refs. [71, 72].

An additional source of uncertainty in the PS is the modelling of the recoil for gluons emitted from b -quarks in the $t \rightarrow Wb$ process. The baseline $t\bar{t}$ sample employs a scheme where partons recoil against b -quarks. An alternative sample was generated with identical settings to the baseline ones, except for a modified recoil scheme. Here, the gluon emissions from the PS of the b -quark were made to recoil against the top quark itself. This scheme changes the modelling of second and subsequent gluon emissions.

The baseline POWHEG+PYTHIA 8 sample of Wt production was generated using the diagram removal scheme to model the interference between the $t\bar{t}$ and Wt production. To evaluate the corresponding uncertainty, the baseline simulation was compared with an alternative sample generated using the diagram subtraction scheme [35, 50].

To estimate the systematic uncertainty related to the electron reconstruction efficiency, an alternative sample of $Z(\rightarrow e^+e^-)+$ jets events was used, which was simulated with MADGRAPH5_AMC@NLO 2.2.2 [53], using MEs at NLO in α_s with up to four final-state partons. The ME calculation employed the NNPDF2.3LO set of PDFs. Events were passed through PYTHIA 8.186 for the modelling of the PS and hadronisation. The overlap between ME and PS emissions was removed using the CKKW-L merging procedure [73, 74]. The Z +jets samples were normalised to a NNLO prediction [75].

4 Event reconstruction and selection

A sample of $t\bar{t}$ events, in which the W bosons from both t and \bar{t} quarks decay to leptons, is selected for the measurement. With this selection, the tag-and-probe approach is used. One charged lepton (muon or electron) from the decay of the $t\bar{t}$ pair is used as the *tag*. The other lepton (electron), which is called the *probe*, is used in an unbiased way to determine whether the electron is directly produced in the decay $W \rightarrow e\nu_e$ or via an intermediate decay $W \rightarrow \tau\nu_\tau \rightarrow e\nu_e\nu_\tau\nu_\tau$. In the first case, the probe electrons are called *prompt* and denoted by $W \rightarrow e$, while in the second case they are denoted by $W \rightarrow \tau \rightarrow e$.

To distinguish between electrons from $W \rightarrow e$ and $W \rightarrow \tau \rightarrow e$ decays, the analysis exploits differences in the p_{T} spectra of the probe electrons together with the displacement of the intermediate τ -lepton decays from the pp collision point (primary vertex) owing to the τ -lepton lifetime. The quantity reflecting the displacement of the vertex of the τ -lepton decay from the primary vertex is the transverse impact parameter (d_0) of the electron track with respect to the beamline. This quantity is defined as the distance of closest approach of the extrapolated track to the beamline in the transverse plane. Electrons originating from the $W \rightarrow \tau\nu_\tau \rightarrow e\nu_e\nu_\tau\nu_\tau$ decays generally have lower p_{T} due to energy lost to undetected neutrinos. These electrons also have on average a larger $|d_0|$ because of the non-zero lifetime of the τ -lepton. In contrast, the electrons from prompt decays are produced directly at the primary vertex, and therefore their measured value of d_0 depends mainly on the detector resolution.

Electrons are reconstructed using the clusters of energy deposits in the electromagnetic calorimeter matched to tracks in the ID. They must pass the *tight* (for both isolation and quality) requirements of Refs. [76, 77].

Muons are reconstructed by combining tracks from the ID with matching tracks reconstructed in the MS. They must pass the *medium* quality and *tight* isolation criteria defined in Ref. [78]. The charged tracks of the selected electrons and muons must be consistent with the primary vertex and have $|d_0| < 0.5$ mm. These requirements reduce the contribution of fake leptons, which becomes large compared to the signal for $|d_0| > 0.5$ mm. The pseudorapidity of the electromagnetic cluster associated with the electron (η_{cl}) must be $|\eta_{cl}| < 2.47$. The electrons with $1.37 < |\eta_{cl}| < 1.52$ are not used in the analysis to exclude the transition region between the barrel and endcap electromagnetic calorimeters. The pseudorapidity of the selected muons must be $|\eta| < 2.5$. All these requirements are applied to both tag and probe leptons. The tag lepton must pass a suite of single-muon or single-electron triggers [79–81]. No trigger requirement for the probe electron is applied. The lowest electron p_T trigger threshold is 24 GeV in 2015 and 26 GeV in 2016–2018. The lowest muon p_T trigger threshold is 20 GeV in 2015 and 26 GeV in 2016–2018. The efficiency of the triggers reached the plateau for electrons with $p_T > 27$ GeV and muons with $p_T > 27.3$ GeV. Consequently, the tag electrons must have $p_T > 27$ GeV and tag muons must have $p_T > 27.3$ GeV. The probe electrons must have $7 < p_T < 250$ GeV. The fraction of electrons with $p_T > 250$ GeV from $W \rightarrow \tau\nu_\tau$ is much smaller than from other sources, and the upper cut on p_T of probe electrons is applied to simplify the measurement without loss in accuracy.

Jets are reconstructed using the anti- k_r algorithm [82, 83] with a radius parameter $R = 0.4$ applied to particle flow objects based on tracks and topological clusters calibrated as specified in Ref. [84]. The jet energy scale and resolution are calibrated using simulations with in situ corrections obtained from data [85]. Jets are required to have $p_T > 25$ GeV and $|\eta| < 2.5$. To reduce the pile-up contribution, an additional requirement for jets with $p_T < 60$ GeV and $|\eta| < 2.4$ is applied based on a dedicated jet vertex tagger (JVT) algorithm which is designed to discriminate between jets produced in the hard-scatter process and those from pile-up [86].

To avoid double counting electrons and muons within jets, an overlap removal procedure is implemented. Specifically, all electrons that share a track with another electron are removed, as are electrons sharing a track with a muon. Additionally, the closest jet found within a $\Delta R = 0.2$ of a reconstructed electron is removed. Any electron subsequently found within $\Delta R = 0.4$ of a jet is also removed. Any jet with fewer than three tracks associated to it and found within $\Delta R = 0.2$ of a muon is removed. Any muon subsequently found within $\Delta R = 0.4$ of a jet is removed.

Jets likely to contain b hadrons are identified as b -jets using the DL1r algorithm [87], which employs a deep neural network. Such jets are referred to as b -tagged in the following. The network utilises distinctive features of b -hadrons, such as the impact parameters of tracks and the displaced vertices reconstructed in the ID. The b -tagging efficiency in simulated $t\bar{t}$ events is approximately 70%.

Events containing exactly one tag lepton (muon or electron), one probe electron, and at least two b -tagged jets are selected for this measurement. The tag and probe leptons must have opposite electric charge. The events with μ_{tag} and e_{probe} , and with e_{tag} and e_{probe} are analysed separately. These channels are referred to as μe and ee , respectively. To further refine the selection, several criteria based on the invariant mass of the tag and probe leptons ($m_{\ell\ell}$) are applied. Only events with $m_{\ell\ell} > 15$ GeV are selected to suppress the contribution from fake probe electrons. Additionally, the ee channel events with $|m_{e^+e^-} - m_Z| < 5$ GeV are excluded, to remove events that could come from Z -boson production.² Finally, the ee events where both electrons satisfied the tag criteria are analysed twice, with each electron considered in turn the tag or probe.

The sample of events passing this selection is referred to as *nominal* in the following.

² The mass of Z boson is taken to be $m_Z = 91.188$ GeV [5].

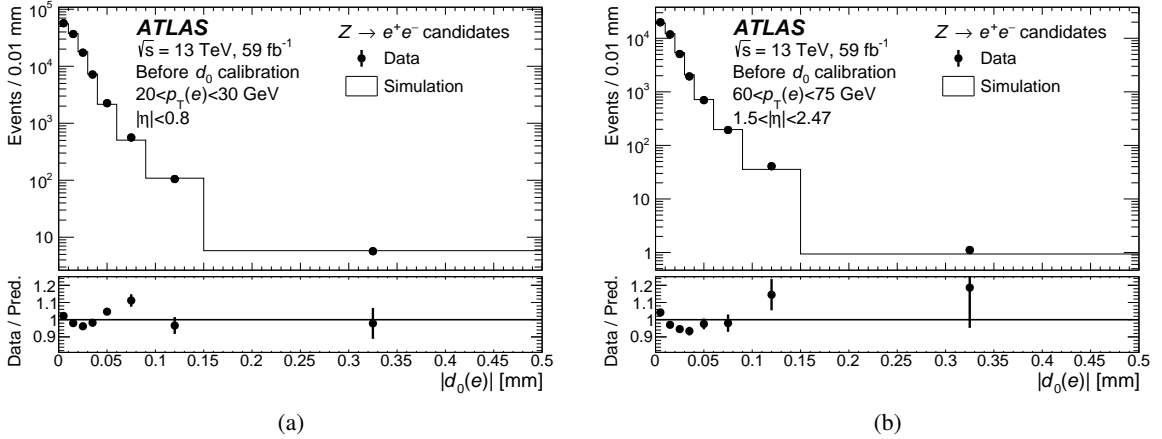


Figure 1: Example distributions of $|d_0|$ of the probe electrons for two kinematic bins in the Z data and simulation samples (before $|d_0|$ calibration) collected in the 2018 data-taking period. The data are represented by black markers and the simulation prediction as the histogram. Only the statistical uncertainties in the data are shown. The distribution of the simulated events in each kinematic bin is normalised to the number of data events in that bin. The bottom panels show the ratio of the data to the simulation prediction.

5 Electron impact parameter calibration

The impact parameter d_0 is one of the two quantities used to separate the electrons produced in τ -lepton decays from other sources. An accurate calibration of the d_0 distribution in simulation is essential for the measurement of $R_{\tau/e}$. The impact parameter d_0 is measured relative to the beamline. Therefore, the shape of the d_0 distribution of prompt electrons is mainly determined by the detector resolution and the precision of the beamspot measurement, and can be obtained in data using the $Z \rightarrow e^+e^-$ decay. A clean sample of such events is obtained by requiring that two electrons satisfy the same criteria as in the nominal event selection, but with the invariant mass of the e^+e^- pair satisfying $|m_{e^+e^-} - m_Z| < 10$ GeV. At least two jets are required in the event to reproduce the track activity around the electron as in the nominal sample. However, no b -tagging condition must be fulfilled. This selection results in a sample of 4.3 million electrons, which is referred to in the following as the Z data sample. The contribution of non-prompt electrons is estimated by using the MC simulation to be about 0.4%. By using the Z data sample to calibrate the d_0 distribution of prompt electrons, the uncertainties due to the shape of the d_0 distribution are considerably reduced.

The d_0 distribution depends on the electron p_T and η . Consequently, the shape of the d_0 distribution of prompt electrons is determined separately in 39 kinematic bins of p_T and $|\eta|$. These bins are obtained by dividing the p_T range of 7–250 GeV into 13 bins and the $|\eta|$ range of 0–2.47 into three bins. The boundaries are optimised to have reasonable statistics in each bin. Figure 1 shows the comparison of $|d_0|$ distributions in data and MC simulation in two kinematic bins before the $|d_0|$ calibration is applied.

For the measurement of $R_{\tau/e}$, the d_0 distribution in each kinematic bin is taken from the Z data sample after subtracting the contribution of non-prompt electrons estimated from MC simulation. The resulting distributions $T_{ij}^{\text{pr}}(d_0)$, which are referred to as d_0 templates, are normalised to unity. Here the indices i and j refer to the p_T and $|\eta|$ bins, respectively. Separate templates are used for data collected in different years

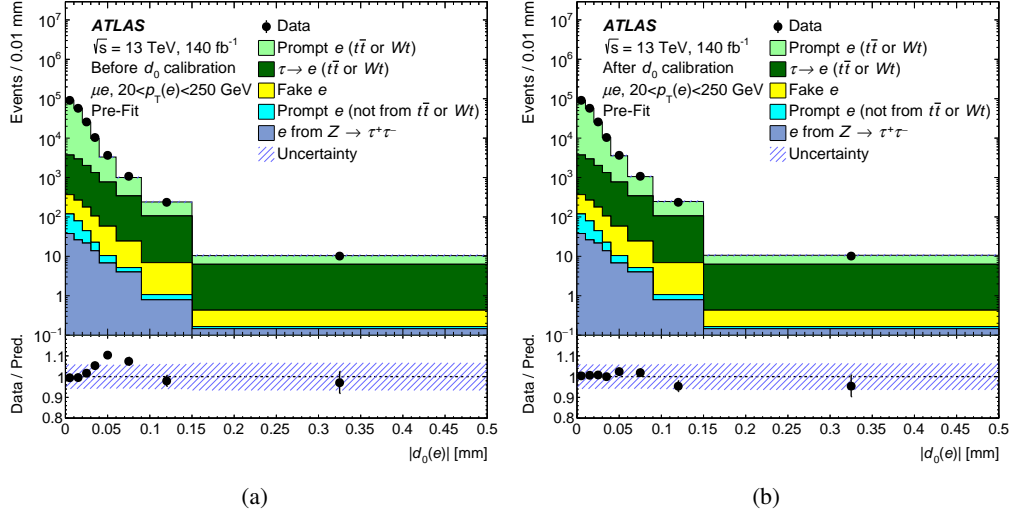


Figure 2: Distributions of $|d_0|$ for the μe channel of the nominal sample for $20 < p_T(e) < 250$ GeV (a) before and (b) after the d_0 calibration is applied. The data are represented by black markers. The different contributions to the nominal sample, are shown by stacked histograms. The bottom panels show the ratio of the data to the simulation prediction. The systematic uncertainties in the prediction are represented by the blue hatched bands.

(2015–2016, 2017, and 2018) because of the variation of the beam conditions and the alignment of the ID from year to year.

The d_0 distribution of prompt electrons with p_T in a range $p_T^{\min} \leq p_T < p_T^{\max}$ is computed as

$$D^{\text{Pr}}(d_0, p_T^{\min}, p_T^{\max}) = \sum_{i=i_{\min}}^{i_{\max}} \sum_{j=1}^3 f_{ij}^{\text{Pr}} T_{ij}^{\text{Pr}}(d_0). \quad (1)$$

Here, f_{ij}^{Pr} is the fraction of prompt probe electrons produced in the $W \rightarrow e$ decay and contained in the kinematic bin ij relative to the total number of prompt probe electrons from the $W \rightarrow e$ decay in all bins. The outer sum ranges from i_{\min} to i_{\max} , the indices of the bins containing p_T^{\min} and p_T^{\max} . The values of p_T^{\min} and p_T^{\max} correspond to the definition of p_T bins used for the measurement of $R_{\tau/e}$ ($7 < p_T < 10$ GeV, $10 < p_T < 20$ GeV, and $20 < p_T < 250$ GeV) as defined in Section 7. The same method and d_0 templates are used to obtain the d_0 distribution of prompt electrons from other sources (i.e., non-resonant Drell-Yan production of e^+e^- and VV production), with the fractions f_{ij} being computed from MC simulation for each source separately. Figure 2 shows the comparison of $|d_0|$ distributions of the probe electrons with $20 < p_T < 250$ GeV in the nominal sample before and after the d_0 calibration is applied. A significant improvement in the agreement between data and MC simulation is observed.

The d_0 templates of electrons from $W \rightarrow \tau \rightarrow e$ decays are determined using simulated events and corrected for the difference in resolution of d_0 in data and simulation following the method employed in Ref. [10]. For these electrons, the d_0 distribution is the convolution of the d_0 resolution and the d_0 distribution due to the lifetime of the τ -lepton. This lifetime is known with good precision [88]. Therefore, only the correction of d_0 resolution is necessary to calibrate the d_0 templates of electrons from $W \rightarrow \tau \rightarrow e$ decays in simulation. To quantify the difference in resolution of d_0 in data and simulation, the $|d_0|$ distribution of the probe electrons in the Z data sample is fitted using a Gaussian function with the mean

fixed at zero. The fit is performed in each kinematic bin in the range of $|d_0| < 0.02$ mm. For $p_T = 20$ GeV, the d_0 resolution is about $15 \mu\text{m}$. The d_0 resolution is determined separately for 2015-2016, 2017, and 2018 data-taking periods. The d_0 templates of the electrons from τ -lepton decays in the MC simulation are corrected using the measured $|d_0|$ resolution. The corrected templates are then used to measure $R_{\tau/e}$. The resulting correction due to the d_0 resolution is small and varies within 1% for different values of d_0 . The d_0 templates of fake electrons are similarly taken from simulated events and corrected using the d_0 resolution from data events with corrections also at the 1% level.

6 Background estimation

Drell-Yan production of an e^+e^- pair in association with jets is a large background at small values of $|d_0|$. The resonant $Z \rightarrow e^+e^-$ decay is suppressed by applying a selection on the e^+e^- invariant mass $|m_{e^+e^-} - m_Z| > 5$ GeV. However, non-resonant e^+e^- production is an irreducible background. Its contribution is determined using a control sample of e^+e^- events containing the resonant $Z \rightarrow e^+e^-$ contribution. This sample is obtained by removing the Z -mass window veto ($|m_{e^+e^-} - m_Z| > 5$ GeV), whilst keeping all other requirements as specified in Section 4. Figure 3 shows the $m_{e^+e^-}$ distribution for the data control sample in the range of $55 < m_{e^+e^-} < 115$ GeV which is used to determine the $Z \rightarrow e^+e^-$ contribution.

The control sample in data and MC simulation is partitioned into three subsamples, depending on p_T of the probe electron ($7 < p_T < 10$ GeV, $10 < p_T < 20$ GeV, and $20 < p_T < 250$ GeV). This binning in p_T matches the one used in the measurement of $R_{\tau/e}$, as detailed in Section 7. A binned extended maximum-likelihood fit [89] of the $m_{e^+e^-}$ distribution in the range of $55 < m_{e^+e^-} < 115$ GeV is used to estimate the number of Z +jets events in each p_T bin i , $N_{Z,i}$, of the control sample. The distribution is modelled by the function

$$F(m_{e^+e^-} | m_Z, \Gamma_Z, s, N_{Z,i}, N_{\text{bkg},i}) = N_{Z,i} V(m_{e^+e^-} | m_Z, \Gamma_Z, s) + N_{\text{bkg},i} P(m_{e^+e^-}). \quad (2)$$

Here, $V(m_{e^+e^-} | m_Z, \Gamma_Z, s)$ is the Voigt profile [90] describing the $Z \rightarrow e^+e^-$ signal and $P(m_{e^+e^-})$ is the second-degree Chebyshev polynomial corresponding to the background under the Z -boson peak. The parameters $N_{Z,i}$ and $N_{\text{bkg},i}$ are the numbers of Z and background events, respectively. The parameters m_Z and Γ_Z are the mass and width of the Z boson, respectively, and s is the standard deviation of the mass resolution. The Z boson's width is fixed to the PDG value $\Gamma_Z = 2.4955$ GeV [5], while the other parameters in Eq. (2) are varied freely in the fit.

The numbers of $Z \rightarrow e^+e^-$ events in data and MC, $N_{Z,i}^{\text{data}}$ and $N_{Z,i}^{\text{MC}}$, are obtained from the fit to the $m_{e^+e^-}$ distribution in data and MC simulation, respectively. The simulated non-resonant Drell-Yan contribution in the nominal sample is then scaled in each p_T bin i by the factor $C_i^Z \equiv N_{Z,i}^{\text{data}} / N_{Z,i}^{\text{MC}}$. The scaling factors C_i^Z are also applied to the $Z(\rightarrow \tau^+\tau^-)$ +jets sample, which contributes to both μe and ee channels.

The values of C_i^Z in all p_T groups are found to be statistically consistent across all p_T bins. The average value of C_i^Z is 1.117 ± 0.013 , where the uncertainty reflects the limited size of the data and simulation samples.

The solid blue line in Figure 3 shows the result of the fit to the full data control sample using the model function specified in Eq. (2). The parametrisation of the background, which comes mainly from $t\bar{t}$ and Wt production, is shown as the dashed line.

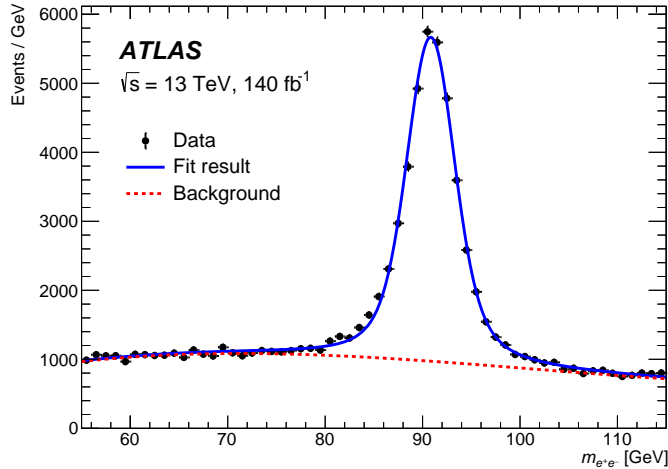


Figure 3: Distribution of the invariant mass of the electron-positron system, $m_{e^+e^-}$, in the control sample. The data are represented by black markers. The result of the fit by the sum of the Voigt profile for the Z-boson peak and the second-degree Chebyshev polynomial for the background is shown by the solid line. The dashed line corresponds to the parametrisation of the background contribution.

Fake electrons are another important source of background. They mainly arise from two processes: the decay of b - or c -hadrons, and photon conversions. The number of fake electrons in the nominal sample in simulation is corrected by a factor derived from the comparison of data and simulation. A control sample is defined by applying the nominal selections, but requiring two leptons with the same electric charge. The fake electrons contribute to both the nominal (i.e., opposite-sign) and control (i.e., same-sign) samples, while the contribution of non-fake leptons to the same-sign sample is reduced. For electrons with $p_T < 10$ GeV the fraction of fake electrons in the same-sign sample is about 97%, and for electrons with $20 < p_T < 250$ GeV it is about 50%. The extrapolation of the correction factor from the same-sign to opposite-sign sample is evaluated from simulated events.

In addition to the fake electrons from hadron decays and photon conversions, prompt electrons from W - and Z -boson decays also contribute to the same-sign sample, especially at high p_T and small values of $|d_0|$. The main processes yielding prompt same-sign electrons are $t\bar{t} + V$ and VV production, where the leptons from the V boson and one of the top-quark decays can have the same electric charge. There is also a 3% contribution of events with a wrong measurement of the charge of the electron due to bremsstrahlung.

The correction factors for the number of fake electrons from hadron decays (C^{HAD}), from photon conversions (C^{PH}), and for the number of prompt electrons (C^{PR}), are derived from the comparison of the number of same-sign events as a function of probe lepton p_T in data and simulation. In addition to the events with probe electrons, the same-sign events with probe muons are also used. The probe muons are selected using the same requirements as the tag muons but changing the p_T condition to $5 < p_T(\mu) < 250$ GeV. No trigger requirements are applied to the probe muons. The addition of the events with a probe muon increases the statistical precision of the correction factors. The same C^{PR} value is applied to the events with prompt probe muons and electrons, and the same C^{HAD} value is applied to the events with fake muons and electrons from hadron decays. It was verified that the separate treatment of electrons and muons from these sources had no statistically significant impact on the result.

The same-sign sample is divided into 12 groups depending on the channel (ee , μe , $e\mu$, and $\mu\mu$) and

p_T of the probe lepton ($p_T < 10$ GeV, $10 < p_T < 20$ GeV, and $20 < p_T < 250$ GeV), and a binned maximum-likelihood fit is performed to these groups. The free parameters in the fit are C^{HAD} , C^{PH} , and C^{PR} . The statistical and systematic uncertainties related to the limited size of the simulation samples are taken into account. Other systematic uncertainties are discussed in Section 7. Figure 4 shows the results of the fit. A good agreement between data and simulation is obtained for all 12 groups of same-sign events with the p -value of the global goodness of the fit [91] being equal to 0.7. The obtained values of C^{HAD} , C^{PH} , and C^{PR} are 1.41 ± 0.03 , 0.84 ± 0.05 , and 1.45 ± 0.08 , respectively.

Figure 5 shows the p_T and $|d_0|$ distributions of the probe electrons after the fit to the same-sign data. A reasonably good agreement between data and simulation is observed after applying the measured correction factors. The remaining differences are in the regions where the contribution of prompt electrons from $t\bar{t}V$ and VV production is dominant. These differences are taken into account by the uncertainties in the $t\bar{t}V$ and VV production together with the systematic uncertainties of fake-lepton contribution.

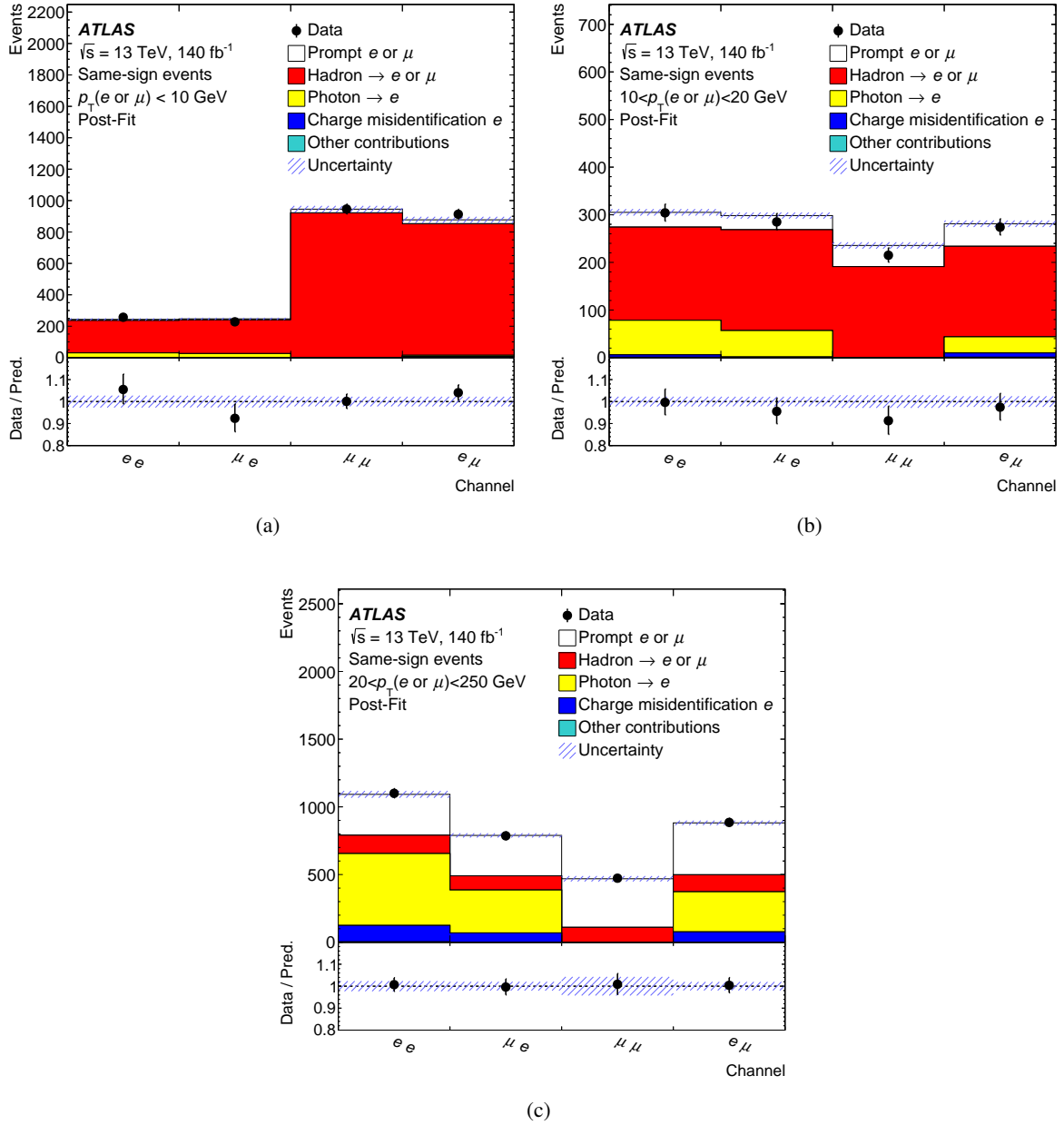


Figure 4: Number of same-sign events in the ee , μe , $e\mu$, and $\mu\mu$ channels where the first lepton is the tag lepton and the second is the probe lepton. The sub-figures correspond to (a) $p_T < 10 \text{ GeV}$, (b) $10 < p_T < 20 \text{ GeV}$, and (c) $20 < p_T < 250 \text{ GeV}$ of the probe lepton (electron or muon). The data are represented by black markers and the different components contributing to the sample, taken from simulation after the fit ('Post-Fit'), are shown by stacked histograms. The component 'Other contributions' contains events with both fake leptons or with charge misidentification of both leptons. Distributions are shown after the fit to the same-sign data has been performed. The systematic uncertainties related to the limited size of the simulation samples are included in the fit, and represented by the blue hatched bands. The bottom panels show the ratio of the data to the simulation prediction.

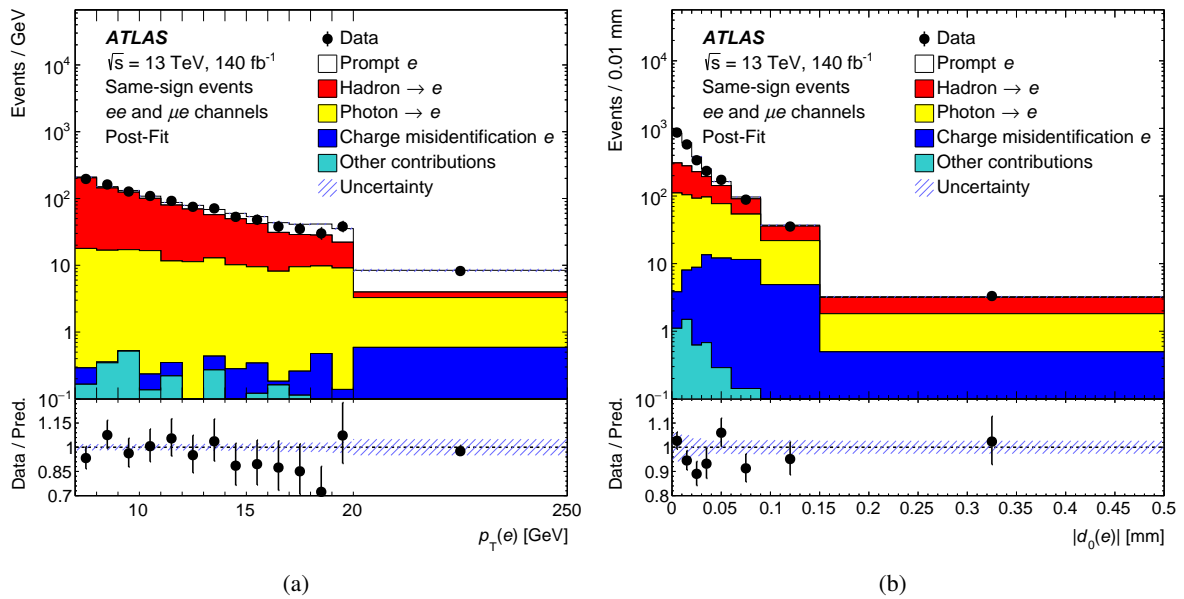


Figure 5: Distributions of (a) p_T and (b) $|d_0|$ of the probe electrons for the sum of the μe and ee channels of the same-sign sample. The last bin in the p_T distribution includes all events with $20 < p_T(e) < 250$ GeV. The data are represented by black markers and the different components contributing to the sample, taken from simulation after the fit ('Post-Fit'), are shown by stacked histograms. The component 'Other contributions' contains events with both fake leptons or with charge misidentification of both leptons. Distributions are shown after the fit to the same-sign data has been performed. The systematic uncertainties related to the limited size of the simulation samples and the cross-section of $t\bar{t}V$ production are represented by the blue hatched bands. The bottom panels show the ratio of the data to the simulation prediction.

7 Statistical analysis and systematic uncertainties

To measure $R_{\tau/e}$, a two-dimensional binned template profile likelihood fit is performed to the p_T and $|d_0|$ distributions. The bin boundaries are optimised to provide the best sensitivity to $R_{\tau/e}$ given the available data. This optimisation resulted in three bins in p_T ($7 < p_T < 10$ GeV, $10 < p_T < 20$ GeV, and $20 < p_T < 250$ GeV) and eight bins in $|d_0|$ ($|d_0| < 0.01$ mm, $0.01 < |d_0| < 0.02$ mm, $0.02 < |d_0| < 0.03$ mm, $0.03 < |d_0| < 0.04$ mm, $0.04 < |d_0| < 0.06$ mm, $0.06 < |d_0| < 0.09$ mm, $0.09 < |d_0| < 0.15$ mm, $0.15 < |d_0| < 0.5$ mm) in both the ee and μe channels. In total 48 bins are used in the fit.

The fit is set up such that a negative-log-likelihood minimization is performed with the parameter of interest, $R_{\tau/e}$, two other unknown parameters k_{sig} and $k(\mu/e)$ defined below, and systematic uncertainties included as nuisance parameters (NP), θ . The likelihood function is defined as a product of Poisson probabilities for each bin in each channel and a probability density function for systematic uncertainties.

$$L(\mathbf{n}, \theta^0 | R_{\tau/e}, k_{\text{sig}}, k(\mu/e), \theta) = \prod_{i \in \text{bins}} P(n_i | R_{\tau/e}, k_{\text{sig}}, k(\mu/e), \theta) \times \prod_{j \in \text{NPs}} G(\theta_j^0 | \theta_j). \quad (3)$$

Here n_i is the number of events in bin i and G is a Gaussian distribution that constrains the nuisance parameter θ_j to the nominal value θ_j^0 .

The scaling factors $R_{\tau/e}$, k_{sig} , $k(\mu/e)$ and more than 300 nuisance parameters representing various statistical and systematic uncertainties are varied in the fit. The parameter of interest $R_{\tau/e}$ is applied to the $W \rightarrow \tau \rightarrow e$ events. The SM value of $R_{\tau/e} = 1$ is set in the MC simulation. The parameter k_{sig} is the normalisation scaling factor of the $t\bar{t}$ and Wt processes contributing to the signal. It is applied to both the $W \rightarrow \tau \rightarrow e$ and $W \rightarrow e$ components of the signal. The parameter $k(\mu/e)$ takes into account any residual difference in the modelling of the selection efficiencies of the tag muon and electron. It is applied to both the signal and background contributions to the μe channel.

The fit is performed after applying the correction factors to the main components of the background events as explained in Section 6. Other background processes are normalised to their theoretical cross-sections.

The main systematic uncertainties in $R_{\tau/e}$ are discussed in detail below.

For the measurement of $R_{\tau/e}$ the $t\bar{t}$ simulation with NNLO re-weighting is used as explained in Section 3. The uncertainty due to re-weighting of the NNLO matrix element calculations is estimated by comparing the result with and without this re-weighting applied.

The uncertainties related to the modelling of $t\bar{t}$ and Wt signals are estimated by comparing the baseline POWHEG + PYTHIA 8 generator to alternative MC generators of $t\bar{t}$ and Wt production or to modified configurations of the baseline MC generators. The NNLO re-weighting is available only for some of the alternative MC generators. For consistency, the systematic uncertainties related to the $t\bar{t}$ and Wt modelling are derived from the comparison of the baseline and alternative MC generators without NNLO re-weighting.

To evaluate the uncertainty of $t\bar{t}$ production due to the h_{damp} parameter, the PS and hadronisation model, the NLO matching, and the gluon recoil scheme, the templates obtained with the POWHEG+PYTHIA 8 generator are compared with the simulation obtained with the alternative MC samples described in Section 3.

To estimate the sensitivity of $t\bar{t}$ production to the amount of parton radiation and potential missing higher-order QCD corrections, the renormalisation and factorisation scales of the baseline MC generator are varied up by a factor of 2.0 and down by a factor of 0.5 from the default values. The uncertainties in

initial-state-radiation (ISR) are estimated by using the Var3c eigen-tune variations of the A14 tune [26]. The impact of final-state-radiation (FSR) uncertainties is evaluated using weights which vary the renormalisation scale for QCD emission in the FSR by factors of 0.5 and 2.0, respectively. The difference between up and down variations divided by two is taken as a symmetric uncertainty related to these variations of the MC generators.

The modelling uncertainties of Wt production related to the PS and hadronisation model, h_{damp} parameter, NLO matching, ISR and FSR are estimated similarly to $t\bar{t}$ events. The uncertainty related to the interference between the $t\bar{t}$ and Wt processes is evaluated by comparing the baseline Wt simulation, which was generated using the diagram removal scheme, and the alternative MC sample generated using the diagram subtraction scheme [35, 50] as described in Section 3.

The uncertainty of 5% in the Wt cross-section is included as a separate contribution to the systematic uncertainty. The relative uncertainties of the $t\bar{t}V$ and VV production cross-section are set to 15% and 30%, respectively. The relative uncertainties in the t - and s -channel single-top-quark production are set to 5%. These uncertainties produce a negligible impact on $R_{\tau/e}$.

To estimate the systematic uncertainty due to the proton PDFs, 30 nuisance parameters corresponding to 30 different variations of PDF defined by the PDF4LHC15 set [45] are included in the fit.

The modelling uncertainties are estimated separately for $t\bar{t}$ and Wt processes, and treated as correlated between these processes and between $W \rightarrow e$ and $W \rightarrow \tau \rightarrow e$ contributions.

To build the d_0 templates of prompt electrons from $W \rightarrow e$ decays, the Z sample containing mainly $Z \rightarrow e^+e^-$ events is used as explained in Section 5. The electrons from these two processes originate in the hard-scatter primary vertex and therefore their d_0 distributions are expected to be the same. However, second-order effects related to track reconstruction and differences in kinematics of electrons coming from Z -boson decay and from $t\bar{t}$ result in residual differences between the templates employed in the fit and the actual d_0 distributions. To evaluate the impact of this difference on the result, the d_0 templates are modified as

$$T'_{ij}(d_0) = N T_{ij}^{\text{pr}}(d_0) \frac{D_{ij}^{W \rightarrow e}(d_0)}{D_{ij}^Z(d_0)}. \quad (4)$$

Here, $D_{ij}^Z(d_0)$ and $D_{ij}^{W \rightarrow e}(d_0)$ are the normalised d_0 distributions of prompt electrons produced in $Z \rightarrow e^+e^-$ and $t\bar{t}$ processes, respectively, which are obtained in simulation. The coefficient N normalises the modified templates $T'_{ij}(d_0)$ to unity. The difference in the value of $R_{\tau/e}$ obtained with the $T'_{ij}(d_0)$ and $T_{ij}^{\text{pr}}(d_0)$ templates is taken as the systematic uncertainty due to the calibration of d_0 of prompt electrons.

Three sources of uncertainty in the evaluation of the correction factors to the number of fake electrons are considered. These include the limited size of the same-sign sample, the choice of PS and hadronisation model, and the possible variation of the fraction of electrons from photon conversion. The uncertainty due to the parton shower and hadronisation model is obtained by comparing the expected number of fake electrons evaluated using the baseline PYTHIA and alternative HERWIG algorithms. The fraction of electrons from photon conversions is evaluated using the MC simulation. The effect of the uncertainty in this quantity is estimated by using the fraction in the same-sign sample instead of the nominal opposite-sign sample when measuring $R_{\tau/e}$.

The electron energy scale and resolution, the reconstruction, isolation, and identification efficiencies and their corresponding uncertainties are measured using $Z \rightarrow e^+e^-$ and $J/\psi \rightarrow e^+e^-$ events [76, 77, 92]. In particular, J/ψ events are used to measure the identification efficiency for electrons with $p_T < 20$ GeV. The

reconstruction efficiency is not measured for electrons with $p_T < 15$ GeV with the standard tag-and-probe method because of large backgrounds which make the measurement unreliable. The agreement between data and MC in p_T dependence of electron efficiency is essential for this measurement. This agreement is tested using the Z sample of events described in Section 5. The dominant contribution to this sample originates from $Z \rightarrow e^+e^-$ events accompanied with two or more jets. Following this study, an additional correction to the efficiency of electrons with small p_T is found to be necessary. The corresponding correction factors are derived from the ratio of the p_T distribution of probe electrons in the Z sample in data and simulation. They are determined separately for 2015–2016, 2017, and 2018 data-taking periods. The systematic uncertainty due to the additional efficiency correction is evaluated using the comparison of the correction factors obtained with the baseline SHERPA MC generator and an alternative sample generated with MADGRAPH5_AMC@NLO. It is verified that the variation of the correction factors in events with different numbers of jets is within the assigned systematic uncertainty.

Muon reconstruction, identification, and isolation efficiencies, as well as muon momentum scale and resolution, are obtained using the prescriptions specified in Refs. [78, 93]. The size of the corresponding uncertainties are derived using $J/\psi \rightarrow \mu^+\mu^-$ events for muons with $p_T < 15$ GeV and $Z \rightarrow \mu^+\mu^-$ events for muons with $p_T > 15$ GeV.

The lepton trigger efficiencies are measured in $Z \rightarrow e^+e^-$ and $Z \rightarrow \mu^+\mu^-$ events using tag-and-probe techniques [80, 81], and are varied within the corresponding uncertainties.

The jet energy scale and resolution are evaluated using simulation and *in situ* measurements [85]. For the jet energy scale uncertainty, 35 independent nuisance parameters are used, and 13 nuisance parameters are taken into account for the jet energy resolution. The uncertainties in the jet b -tagging efficiency and rate of b -tagged background are estimated by using the semileptonic and dileptonic $t\bar{t}$ events, as well as Z +jets events [94–96]. The simulated pile-up events are weighted to reproduce the distribution of the average number of inelastic interactions per bunch crossing observed in the data. The associated uncertainty is included as a nuisance parameter in the measurement of $R_{\tau/e}$. The uncertainty associated with the use of the JVT algorithm is estimated by using the results of the study presented in Ref. [86].

The uncertainty in the integrated luminosity is 0.83% [97], obtained using the LUCID-2 detector for the primary luminosity measurements, complemented by measurements using the inner detector and calorimeters. This uncertainty has a negligible impact on $R_{\tau/e}$.

The measurement of $R_{\tau/e}$ depends on $B(\tau \rightarrow e\nu_e\nu_\tau)$, which has been measured to be $(17.82 \pm 0.04)\%$ [5]. The dependence on this branching fraction is included as an additional uncertainty. The limited size of the MC samples is treated as a separate contribution to the systematic uncertainty following the Barlow-Beeston approach [98].

8 Results

The numbers of observed events in the μe and ee channels and in different p_T bins, together with the fitted number of events from different sources, are given in Tables 1 and 2. The number of events in simulation agrees with that in data across different channels and p_T bins.

Figures 6 and 7 show the distribution in data and in simulation of $|d_0|$ in the six regions after the fit. Good agreement between data and simulation is observed, both in the total yield and differential shape. The p -value of the global goodness of the fit [91] is 87%. These figures also demonstrate the separation between

Table 1: Number of events in the μe channel from different sources, as estimated by the fit to the data, compared with the observed yield. Uncertainties include the statistical and systematic contributions. The uncertainty in the total expected number of events can be smaller than the uncertainties of the individual contributions because of correlations between them resulting from the fit.

	μe $7 < p_T < 10 \text{ GeV}$	μe $10 < p_T < 20 \text{ GeV}$	μe $20 < p_T < 250 \text{ GeV}$
Prompt $e(t\bar{t})$	1278 \pm 28	13370 \pm 150	178000 \pm 1000
e from $\tau(t\bar{t})$	1092 \pm 32	4490 \pm 100	11670 \pm 290
Prompt $e(Wt)$	34 \pm 6	340 \pm 60	5300 \pm 900
e from $\tau(Wt)$	28.0 \pm 2.5	119 \pm 16	380 \pm 110
Prompt e (not from $t\bar{t}$ or Wt)	5.2 \pm 1.5	23 \pm 7	180 \pm 50
e from $Z \rightarrow \tau^+\tau^-$	19.9 \pm 0.4	85.4 \pm 1.4	132.9 \pm 2.2
Fake e	317 \pm 22	380 \pm 33	840 \pm 60
Total predicted	2770 \pm 40	18880 \pm 120	196500 \pm 400
Data	2768	18783	196552

Table 2: Number of events in the ee channel from different sources, as estimated by the fit to the data, compared with the observed yield. Uncertainties include the statistical and systematic contributions. The uncertainty in the total expected number of events can be smaller than the uncertainties of the individual contributions because of correlations between them resulting from the fit.

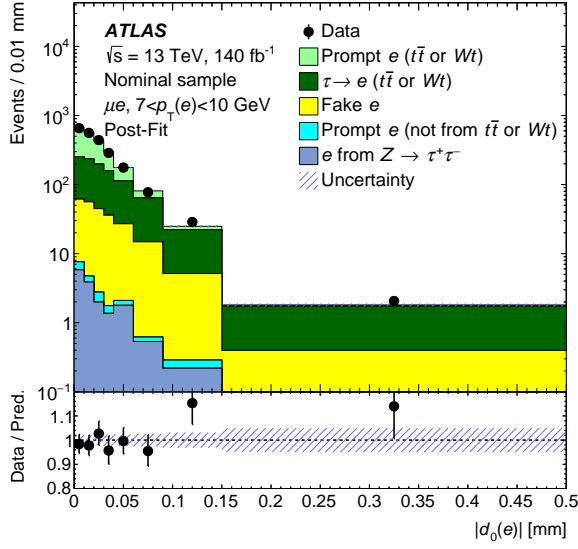
	ee $7 < p_T < 10 \text{ GeV}$	ee $10 < p_T < 20 \text{ GeV}$	ee $20 < p_T < 250 \text{ GeV}$
Prompt $e(t\bar{t})$	1238 \pm 35	12210 \pm 130	160300 \pm 900
e from $\tau(t\bar{t})$	1051 \pm 30	4060 \pm 100	10490 \pm 260
Prompt $e(Wt)$	35 \pm 7	320 \pm 50	5000 \pm 700
e from $\tau(Wt)$	30 \pm 4	116 \pm 13	340 \pm 100
e from $Z \rightarrow e^+e^-$	240 \pm 50	1770 \pm 120	12380 \pm 200
Prompt e (not from $t\bar{t}$ or Wt)	11.7 \pm 3.5	59 \pm 17	560 \pm 170
e from $Z \rightarrow \tau^+\tau^-$	19.7 \pm 0.4	69.7 \pm 0.9	105.3 \pm 1.3
Fake e	302 \pm 20	374 \pm 32	810 \pm 50
Total predicted	2930 \pm 50	18970 \pm 120	190000 \pm 400
Data	2928	19047	189945

the signal and background processes. The electrons from $W \rightarrow e$ dominate at high p_T and small $|d_0|$, while the electrons from $W \rightarrow \tau \rightarrow e$ dominate at high $|d_0|$. The fake electrons mainly contribute at small p_T .

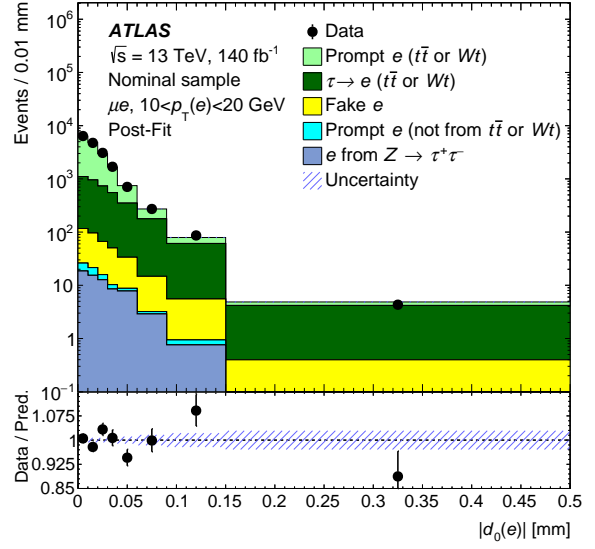
The measured value of $R_{\tau/e}$ is

$$R_{\tau/e} = 0.975 \pm 0.012 \text{ (stat.)} \pm 0.020 \text{ (syst.)}. \quad (5)$$

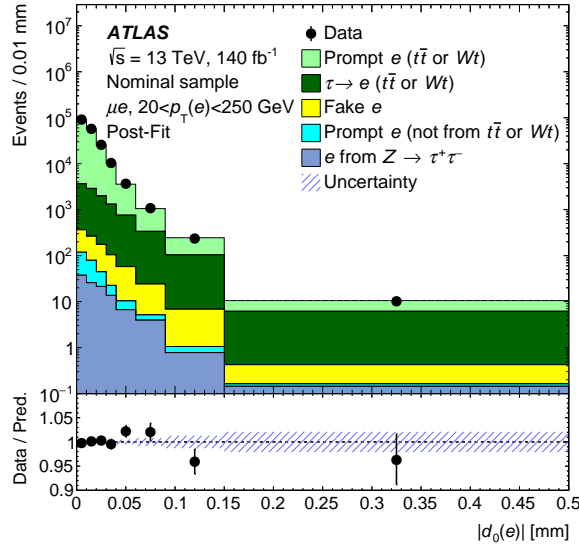
The values of k_{sig} and $k(\mu/e)$ obtained in the fit are $k_{\text{sig}} = 1.03 \pm 0.06$ and $k(\mu/e) = 0.986 \pm 0.010$ with uncertainties that include both statistical and systematic components. Both k_{sig} and $k(\mu/e)$ are consistent



(a)

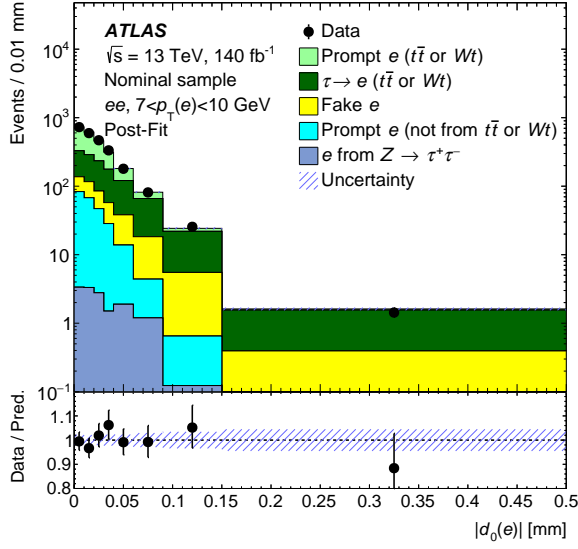


(b)

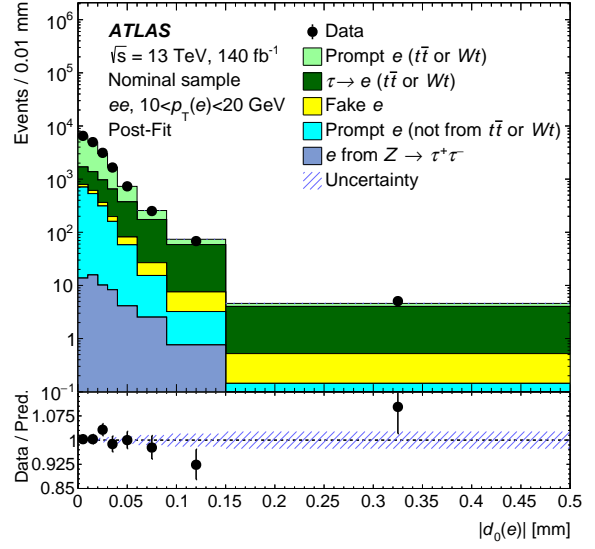


(c)

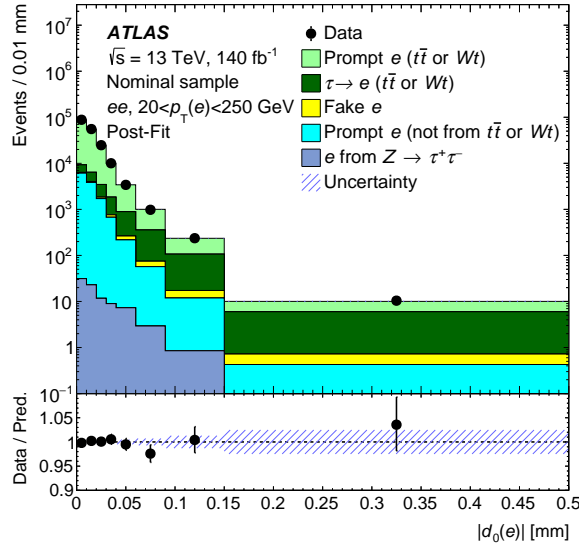
Figure 6: Distributions of $|d_0|$ for the μe channel of the nominal sample in different p_T bins. The data are represented by black markers. The different contributions to the nominal sample, taken from simulation after the fit ‘Post-Fit’, are shown by stacked histograms. The bottom panels show the ratio of the data to the simulation prediction after the fit. The systematic uncertainties in the prediction with the constraints from the fit and the correlation between the nuisance parameters applied are represented by the blue hatched bands.



(a)



(b)



(c)

Figure 7: Distributions of $|d_0|$ for the ee channel of the nominal sample in different p_T bins. The data are represented by black markers. The different contributions to the nominal sample, taken from simulation after the fit ('Post-Fit'), are shown by stacked histograms. The bottom panels show the ratio of the data to the simulation prediction after the fit. The systematic uncertainties in the prediction with the constraints from the fit and the correlation between the nuisance parameters applied are represented by the blue hatched bands.

Table 3: Measured values of $R_{\tau/e}$ in the different p_T bins.

p_T bin	$R_{\tau/e}$
$7 < p_T < 10$ GeV	1.13 ± 0.11 (stat) ± 0.07 (syst)
$10 < p_T < 20$ GeV	0.93 ± 0.04 (stat) ± 0.02 (syst)
$20 < p_T < 250$ GeV	0.98 ± 0.04 (stat) ± 0.02 (syst)

with unity within less than two standard deviations. Fixing $k(\mu/e)$ to unity in the fit has a negligible impact on the $R_{\tau/e}$ result, both central value and uncertainties.

Consistent results are found when performing the measurement separately for the 2015–2016, 2017 and 2018 data-taking periods, as well as for the individual channels and p_T bins. Table 3 shows the results for the different p_T bins.

A breakdown of uncertainties grouped into categories is shown in Table 4. Many systematic uncertainties are treated as correlated between the $W \rightarrow e$ and $W \rightarrow \tau \rightarrow e$ contributions. These include the uncertainties in the jet reconstruction, selection of b -jets, and trigger efficiencies. The impact of such correlated uncertainties on $R_{\tau/e}$ is reduced. The remaining dominant uncertainties are related to the modelling of $t\bar{t}$ production, the calibration of d_0 distributions (Section 5), the evaluation of the background (Section 6), and electron reconstruction, identification, and isolation. The largest impact on $R_{\tau/e}$ in the modelling group of uncertainties comes from NNLO re-weighting, the variation of PS and hadronisation model, the amount of parton radiation, and h_{damp} parameter.

Figure 8 provides a comparison of this result to other measurements of $R_{\tau/e}$. A similar precision is achieved to that of the CMS result [11]. This new measurement agrees with the SM expectation of lepton flavour universality and with the previous measurement of $R_{\tau/e}$ by the CMS Collaboration. It however differs from the combination of LEP measurements [9] by more than two standard deviations.

Table 4: Breakdown of statistical and systematic uncertainties in the fit to data. Different individual components used in the fit are combined into categories. The size of the impact each group of uncertainties has on $R_{\tau/e}$, which is denoted by $\sigma(R_{\tau/e})$ and shown in the second column, is assessed by subtracting in quadrature the uncertainty from the nominal fit and the fit with the relevant nuisance parameters fixed to their post-fit values. The group ‘Other sources’ includes the uncertainties due to trigger, JVT, luminosity, and pile-up.

Uncertainty group	$\sigma(R_{\tau/e})$
Modelling of $t\bar{t}$ and Wt	0.011
d_0 calibration	0.006
Background estimation	0.005
Electron reconstruction, identification, and isolation	0.005
Electron energy scale	0.003
Electron energy resolution	0.002
Jet energy resolution	0.004
Jet energy scale	0.003
Jet b -tagging	0.002
Muon reconstruction, identification, and isolation	0.001
Other sources	0.002
Variation of k_{sig} and $k(\mu/e)$	0.003
Finite size of simulated samples	0.003
$B(W \rightarrow \tau\nu_\tau \rightarrow e\nu_e\nu_\tau\nu_\tau)$	0.002
Total systematical uncertainty	0.020
Data statistical uncertainty	0.012
Total uncertainty	0.024

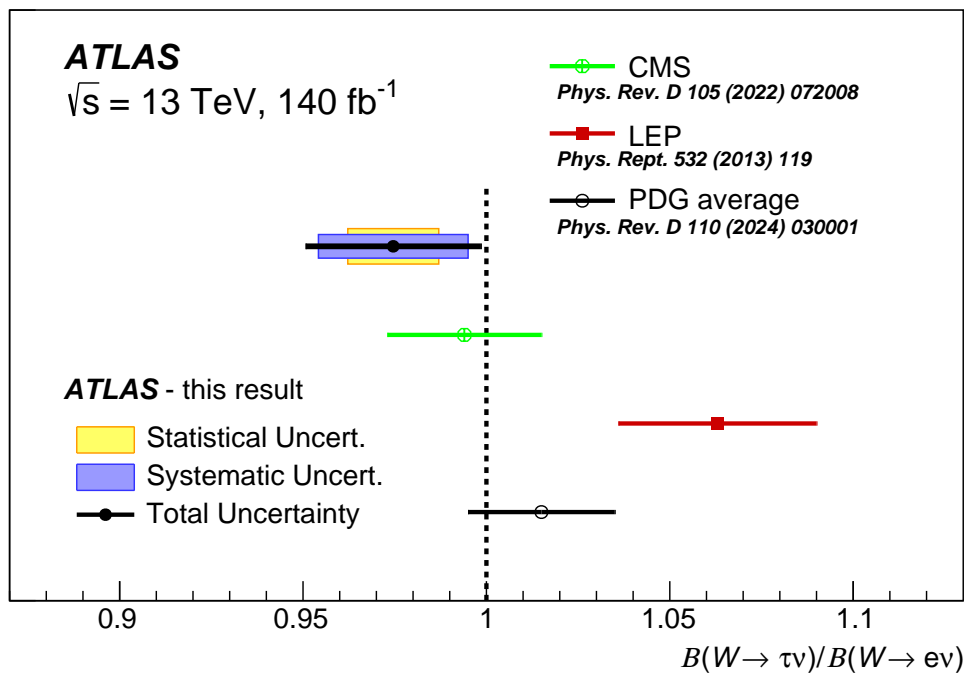


Figure 8: Summary of measurements of $R_{\tau/e} = B(W \rightarrow \tau\nu)/B(W \rightarrow e\nu)$. The $R_{\tau/e}$ value measured in this publication is shown together with the corresponding statistical and systematic uncertainties. It is compared with other measurements and the average value from the PDG [5]. The vertical dashed line at unity indicates the Standard Model assumption of equal branching fractions to all lepton flavours.

9 Conclusion

The value of $R_{\tau/e} = B(W \rightarrow \tau\nu_\tau)/B(W \rightarrow e\nu_e)$ has been measured using the decays of the top quark to final states containing τ -leptons or electrons. A sample of pp collisions at $\sqrt{s} = 13$ TeV collected by the ATLAS experiment in Run 2 and corresponding to 140 fb^{-1} was used in the analysis. The leptonic decay $\tau \rightarrow e\nu_e\nu_\tau$ was used for the τ -lepton selection. The decays $W \rightarrow \tau\nu_\tau \rightarrow e\nu_e\nu_\tau\nu_\tau$ and $W \rightarrow e\nu_e$ were distinguished by exploiting differences in the impact parameter and transverse momentum distributions of the electrons. The dominant systematic uncertainties are related to the modelling of $t\bar{t}$ and Wt production, the impact parameter calibration, the estimate of the background, and electron reconstruction, identification, and isolation requirements. The resulting value of $R_{\tau/e} = 0.975 \pm 0.012$ (stat) ± 0.020 (syst) is consistent with the Standard Model assumption of lepton flavour universality. The precision of this measurement is comparable to that of the LEP combination and that of the CMS Collaboration, and will further reduce the uncertainty in the world-average result for $R_{\tau/e}$.

Acknowledgements

We thank CERN for the very successful operation of the LHC and its injectors, as well as the support staff at CERN and at our institutions worldwide without whom ATLAS could not be operated efficiently.

The crucial computing support from all WLCG partners is acknowledged gratefully, in particular from CERN, the ATLAS Tier-1 facilities at TRIUMF/SFU (Canada), NDGF (Denmark, Norway, Sweden), CC-IN2P3 (France), KIT/GridKA (Germany), INFN-CNAF (Italy), NL-T1 (Netherlands), PIC (Spain), RAL (UK) and BNL (USA), the Tier-2 facilities worldwide and large non-WLCG resource providers. Major contributors of computing resources are listed in Ref. [99].

We gratefully acknowledge the support of ANPCyT, Argentina; YerPhI, Armenia; ARC, Australia; BMWFW and FWF, Austria; ANAS, Azerbaijan; CNPq and FAPESP, Brazil; NSERC, NRC and CFI, Canada; CERN; ANID, Chile; CAS, MOST and NSFC, China; Minciencias, Colombia; MEYS CR, Czech Republic; DNRf and DNSRC, Denmark; IN2P3-CNRS and CEA-DRF/IRFU, France; SRNSFG, Georgia; BMBF, HGF and MPG, Germany; GSRI, Greece; RGC and Hong Kong SAR, China; ICHEP and Academy of Sciences and Humanities, Israel; INFN, Italy; MEXT and JSPS, Japan; CNRST, Morocco; NWO, Netherlands; RCN, Norway; MNiSW, Poland; FCT, Portugal; MNE/IFA, Romania; MSTDI, Serbia; MSSR, Slovakia; ARIS and MVZI, Slovenia; DSI/NRF, South Africa; MICIU/AEI, Spain; SRC and Wallenberg Foundation, Sweden; SERI, SNSF and Cantons of Bern and Geneva, Switzerland; NSTC, Taipei; TENMAK, Türkiye; STFC/UKRI, United Kingdom; DOE and NSF, United States of America.

Individual groups and members have received support from BCKDF, CANARIE, CRC and DRAC, Canada; CERN-CZ, FORTE and PRIMUS, Czech Republic; COST, ERC, ERDF, Horizon 2020, ICSC-NextGenerationEU and Marie Skłodowska-Curie Actions, European Union; Investissements d’Avenir Labex, Investissements d’Avenir Idex and ANR, France; DFG and AvH Foundation, Germany; Herakleitos, Thales and Aristeia programmes co-financed by EU-ESF and the Greek NSRF, Greece; BSF-NSF and MINERVA, Israel; NCN and NAWA, Poland; La Caixa Banking Foundation, CERCA Programme Generalitat de Catalunya and PROMETEO and GenT Programmes Generalitat Valenciana, Spain; Göran Gustafssons Stiftelse, Sweden; The Royal Society and Leverhulme Trust, United Kingdom.

In addition, individual members wish to acknowledge support from Armenia: Yerevan Physics Institute (FAPERJ); CERN: European Organization for Nuclear Research (CERN PIAS); Chile: Agencia Nacional de

Investigación y Desarrollo (FONDECYT 1230812, FONDECYT 1230987, FONDECYT 1240864); China: Chinese Ministry of Science and Technology (MOST-2023YFA1605700, MOST-2023YFA1609300), National Natural Science Foundation of China (NSFC - 12175119, NSFC 12275265, NSFC-12075060); Czech Republic: Czech Science Foundation (GACR - 24-11373S), Ministry of Education Youth and Sports (FORTE CZ.02.01.01/00/22_008/0004632), PRIMUS Research Programme (PRIMUS/21/SCI/017); EU: H2020 European Research Council (ERC - 101002463); European Union: European Research Council (ERC - 948254, ERC 101089007), European Union, Future Artificial Intelligence Research (FAIR-NextGenerationEU PE00000013), Italian Center for High Performance Computing, Big Data and Quantum Computing (ICSC, NextGenerationEU); France: Agence Nationale de la Recherche (ANR-20-CE31-0013, ANR-21-CE31-0013, ANR-21-CE31-0022, ANR-22-EDIR-0002); Germany: Baden-Württemberg Stiftung (BW Stiftung-Postdoc Eliteprogramme), Deutsche Forschungsgemeinschaft (DFG - 469666862, DFG - CR 312/5-2); Italy: Istituto Nazionale di Fisica Nucleare (ICSC, NextGenerationEU), Ministero dell'Università e della Ricerca (PRIN - 20223N7F8K - PNRR M4.C2.1.1); Japan: Japan Society for the Promotion of Science (JSPS KAKENHI JP22H01227, JSPS KAKENHI JP22H04944, JSPS KAKENHI JP22KK0227, JSPS KAKENHI JP23KK0245); Netherlands: Netherlands Organisation for Scientific Research (NWO Veni 2020 - VI.Veni.202.179); Norway: Research Council of Norway (RCN-314472); Poland: Ministry of Science and Higher Education (IDUB AGH, POB8, D4 no 9722), Polish National Agency for Academic Exchange (PPN/PPO/2020/1/00002/U/00001), Polish National Science Centre (NCN 2021/42/E/ST2/00350, NCN OPUS 2023/51/B/ST2/02507, NCN OPUS nr 2022/47/B/ST2/03059, NCN UMO-2019/34/E/ST2/00393, NCN & H2020 MSCA 945339, UMO-2020/37/B/ST2/01043, UMO-2021/40/C/ST2/00187, UMO-2022/47/O/ST2/00148, UMO-2023/49/B/ST2/04085, UMO-2023/51/B/ST2/00920); Slovenia: Slovenian Research Agency (ARIS grant J1-3010); Spain: Generalitat Valenciana (Artemisa, FEDER, IDIFED-ER/2018/048), Ministry of Science and Innovation (MCIN & NextGenEU PCI2022-135018-2, MICIN & FEDER PID2021-125273NB, RYC2019-028510-I, RYC2020-030254-I, RYC2021-031273-I, RYC2022-038164-I); Sweden: Carl Trygger Foundation (Carl Trygger Foundation CTS 22:2312), Swedish Research Council (Swedish Research Council 2023-04654, VR 2018-00482, VR 2022-03845, VR 2022-04683, VR 2023-03403, VR grant 2021-03651), Knut and Alice Wallenberg Foundation (KAW 2018.0458, KAW 2019.0447, KAW 2022.0358); Switzerland: Swiss National Science Foundation (SNSF - PCEFP2_194658); United Kingdom: Leverhulme Trust (Leverhulme Trust RPG-2020-004), Royal Society (NIF-R1-231091); United States of America: U.S. Department of Energy (ECA DE-AC02-76SF00515), Neubauer Family Foundation.

References

- [1] S. L. Glashow, *Partial-symmetries of weak interactions*, *Nucl. Phys.* **22** (1961) 579.
- [2] S. Weinberg, *A Model of Leptons*, *Phys. Rev. Lett.* **19** (1967) 1264.
- [3] A. Salam, *Weak and Electromagnetic Interactions*, *Conf. Proc. C* **680519** (1968) 367.
- [4] A. Pich, *Precision Tau Physics*, *Prog. Part. Nucl. Phys.* **75** (2014) 41, arXiv: [1310.7922 \[hep-ph\]](#).
- [5] Particle Data Group, S. Navas et al., *Review of particle physics*, *Phys. Rev. D* **110** (2024) 030001.
- [6] A. Crivellin, M. Kirk, T. Kitahara and F. Mescia, *Global fit of modified quark couplings to EW gauge bosons and vector-like quarks in light of the Cabibbo angle anomaly*, *JHEP* **03** (2023) 234, arXiv: [2212.06862 \[hep-ph\]](#).
- [7] L. Allwicher, G. Isidori, J. M. Lizana, N. Selimović and B. A. Stefanek, *Third-family quark-lepton Unification and electroweak precision tests*, *JHEP* **05** (2023) 179, arXiv: [2302.11584 \[hep-ph\]](#).
- [8] A. Abada, J. Kriewald, E. Pinsard, S. Rosauero-Alcaraz and A. M. Teixeira, *Heavy neutral lepton corrections to SM boson decays: lepton flavour universality violation in low-scale seesaw realisations*, *Eur. Phys. J. C* **84** (2024) 149, arXiv: [2307.02558 \[hep-ph\]](#).
- [9] The ALEPH Collaboration, The DELPHI Collaboration, The L3 Collaboration, The OPAL Collaboration, The LEP Electroweak Working Group, *Electroweak Measurements in Electron-Positron Collisions at W-Boson-Pair Energies at LEP*, *Phys. Rept.* **532** (2013) 119, arXiv: [1302.3415 \[hep-ex\]](#).
- [10] ATLAS Collaboration, *Test of the universality of τ and μ lepton couplings in W-boson decays with the ATLAS detector*, *Nature Phys.* **17** (2021) 813, arXiv: [2007.14040 \[hep-ex\]](#).
- [11] CMS Collaboration, *Precision measurement of the W boson decay branching fractions in proton-proton collisions at $\sqrt{s} = 13$ TeV*, *Phys. Rev. D* **105** (2022) 072008, arXiv: [2201.07861 \[hep-ex\]](#).
- [12] ATLAS Collaboration, *Precise test of lepton flavour universality in W-boson decays into muons and electrons in pp collisions at $\sqrt{s} = 13$ TeV with the ATLAS detector*, *Eur. Phys. J. C* **84** (2024) 993, arXiv: [2403.02133 \[hep-ex\]](#).
- [13] ATLAS Collaboration, *The ATLAS Experiment at the CERN Large Hadron Collider*, *JINST* **3** (2008) S08003.
- [14] ATLAS Collaboration, *ATLAS Insertable B-Layer: Technical Design Report*, ATLAS-TDR-19; CERN-LHCC-2010-013, 2010, URL: <https://cds.cern.ch/record/1291633>, Addendum: ATLAS-TDR-19-ADD-1; CERN-LHCC-2012-009, 2012, URL: <https://cds.cern.ch/record/1451888>.
- [15] B. Abbott et al., *Production and integration of the ATLAS Insertable B-Layer*, *JINST* **13** (2018) T05008, arXiv: [1803.00844 \[physics.ins-det\]](#).
- [16] G. Avoni et al., *The new LUCID-2 detector for luminosity measurement and monitoring in ATLAS*, *JINST* **13** (2018) P07017.
- [17] ATLAS Collaboration, *Performance of the ATLAS trigger system in 2015*, *Eur. Phys. J. C* **77** (2017) 317, arXiv: [1611.09661 \[hep-ex\]](#).

- [18] ATLAS Collaboration, *Software and computing for Run 3 of the ATLAS experiment at the LHC*, 2024, arXiv: [2404.06335 \[hep-ex\]](#).
- [19] ATLAS Collaboration, *ATLAS data quality operations and performance for 2015–2018 data-taking*, *JINST* **15** (2020) P04003, arXiv: [1911.04632 \[physics.ins-det\]](#).
- [20] ATLAS Collaboration, *Luminosity determination in pp collisions at $\sqrt{s} = 13$ TeV using the ATLAS detector at the LHC*, *Eur. Phys. J. C* **83** (2023) 982, arXiv: [2212.09379 \[hep-ex\]](#).
- [21] S. Agostinelli et al., *GEANT4—a simulation toolkit*, *Nucl. Instrum. Meth. A* **506** (2003) 250.
- [22] ATLAS Collaboration, *The ATLAS Simulation Infrastructure*, *Eur. Phys. J. C* **70** (2010) 823, arXiv: [1005.4568 \[physics.ins-det\]](#).
- [23] T. Sjöstrand, S. Mrenna and P. Skands, *A brief introduction to PYTHIA 8.1*, *Comput. Phys. Commun.* **178** (2008) 852, arXiv: [0710.3820 \[hep-ph\]](#).
- [24] NNPDF Collaboration, R. D. Ball et al., *Parton distributions with LHC data*, *Nucl. Phys. B* **867** (2013) 244, arXiv: [1207.1303 \[hep-ph\]](#).
- [25] ATLAS Collaboration, *The Pythia 8 A3 tune description of ATLAS minimum bias and inelastic measurements incorporating the Donnachie–Landshoff diffractive model*, ATL-PHYS-PUB-2016-017, 2016, URL: <https://cds.cern.ch/record/2206965>.
- [26] ATLAS Collaboration, *ATLAS Pythia 8 tunes to 7 TeV data*, ATL-PHYS-PUB-2014-021, 2014, URL: <https://cds.cern.ch/record/1966419>.
- [27] M. Bähr et al., *Herwig++ physics and manual*, *Eur. Phys. J. C* **58** (2008) 639, arXiv: [0803.0883 \[hep-ph\]](#).
- [28] J. Bellm et al., *Herwig 7.1 Release Note*, 2017, arXiv: [1705.06919 \[hep-ph\]](#).
- [29] D. J. Lange, *The EvtGen particle decay simulation package*, *Nucl. Instrum. Meth. A* **462** (2001) 152.
- [30] S. Frixione, G. Ridolfi and P. Nason, *A positive-weight next-to-leading-order Monte Carlo for heavy flavour hadroproduction*, *JHEP* **09** (2007) 126, arXiv: [0707.3088 \[hep-ph\]](#).
- [31] P. Nason, *A new method for combining NLO QCD with shower Monte Carlo algorithms*, *JHEP* **11** (2004) 040, arXiv: [hep-ph/0409146](#).
- [32] S. Frixione, P. Nason and C. Oleari, *Matching NLO QCD computations with parton shower simulations: the POWHEG method*, *JHEP* **11** (2007) 070, arXiv: [0709.2092 \[hep-ph\]](#).
- [33] S. Alioli, P. Nason, C. Oleari and E. Re, *A general framework for implementing NLO calculations in shower Monte Carlo programs: the POWHEG BOX*, *JHEP* **06** (2010) 043, arXiv: [1002.2581 \[hep-ph\]](#).
- [34] NNPDF Collaboration, R. D. Ball et al., *Parton distributions for the LHC run II*, *JHEP* **04** (2015) 040, arXiv: [1410.8849 \[hep-ph\]](#).
- [35] ATLAS Collaboration, *Studies on top-quark Monte Carlo modelling for Top2016*, ATL-PHYS-PUB-2016-020, 2016, URL: <https://cds.cern.ch/record/2216168>.
- [36] T. Sjöstrand et al., *An introduction to PYTHIA 8.2*, *Comput. Phys. Commun.* **191** (2015) 159, arXiv: [1410.3012 \[hep-ph\]](#).

- [37] M. Czakon et al., *Top-pair production at the LHC through NNLO QCD and NLO EW*, *JHEP* **10** (2017) 186, arXiv: [1705.04105 \[hep-ph\]](#).
- [38] M. Beneke, P. Falgari, S. Klein and C. Schwinn, *Hadronic top-quark pair production with NNLL threshold resummation*, *Nucl. Phys. B* **855** (2012) 695, arXiv: [1109.1536 \[hep-ph\]](#).
- [39] M. Cacciari, M. Czakon, M. Mangano, A. Mitov and P. Nason, *Top-pair production at hadron colliders with next-to-next-to-leading logarithmic soft-gluon resummation*, *Phys. Lett. B* **710** (2012) 612, arXiv: [1111.5869 \[hep-ph\]](#).
- [40] P. Bärnreuther, M. Czakon and A. Mitov, *Percent-Level-Precision Physics at the Tevatron: Next-to-Next-to-Leading Order QCD Corrections to $q\bar{q} \rightarrow t\bar{t} + X$* , *Phys. Rev. Lett.* **109** (2012) 132001, arXiv: [1204.5201 \[hep-ph\]](#).
- [41] M. Czakon and A. Mitov, *NNLO corrections to top-pair production at hadron colliders: the all-fermionic scattering channels*, *JHEP* **12** (2012) 054, arXiv: [1207.0236 \[hep-ph\]](#).
- [42] M. Czakon and A. Mitov, *NNLO corrections to top pair production at hadron colliders: the quark-gluon reaction*, *JHEP* **01** (2013) 080, arXiv: [1210.6832 \[hep-ph\]](#).
- [43] M. Czakon, P. Fiedler and A. Mitov, *Total Top-Quark Pair-Production Cross Section at Hadron Colliders Through $O(\alpha_S^4)$* , *Phys. Rev. Lett.* **110** (2013) 252004, arXiv: [1303.6254 \[hep-ph\]](#).
- [44] M. Czakon and A. Mitov, *Top++: A program for the calculation of the top-pair cross-section at hadron colliders*, *Comput. Phys. Commun.* **185** (2014) 2930, arXiv: [1112.5675 \[hep-ph\]](#).
- [45] J. Butterworth et al., *PDF4LHC recommendations for LHC Run II*, *J. Phys. G* **43** (2016) 023001, arXiv: [1510.03865 \[hep-ph\]](#).
- [46] A. D. Martin, W. J. Stirling, R. S. Thorne and G. Watt, *Parton distributions for the LHC*, *Eur. Phys. J. C* **63** (2009) 189, arXiv: [0901.0002 \[hep-ph\]](#).
- [47] A. D. Martin, W. J. Stirling, R. S. Thorne and G. Watt, *Uncertainties on α_S in global PDF analyses and implications for predicted hadronic cross sections*, *Eur. Phys. J. C* **64** (2009) 653, arXiv: [0905.3531 \[hep-ph\]](#).
- [48] H.-L. Lai et al., *New parton distributions for collider physics*, *Phys. Rev. D* **82** (2010) 074024, arXiv: [1007.2241 \[hep-ph\]](#).
- [49] J. Gao et al., *CT10 next-to-next-to-leading order global analysis of QCD*, *Phys. Rev. D* **89** (2014) 033009, arXiv: [1302.6246 \[hep-ph\]](#).
- [50] S. Frixione, E. Laenen, P. Motylinski, C. White and B. R. Webber, *Single-top hadroproduction in association with a W boson*, *JHEP* **07** (2008) 029, arXiv: [0805.3067 \[hep-ph\]](#).
- [51] N. Kidonakis, *Two-loop soft anomalous dimensions for single top quark associated production with a W^- or H^-* , *Phys. Rev. D* **82** (2010) 054018, arXiv: [1005.4451 \[hep-ph\]](#).
- [52] N. Kidonakis, ‘Top Quark Production’, *Proceedings, Helmholtz International Summer School on Physics of Heavy Quarks and Hadrons (HQ 2013)* (JINR, Dubna, Russia, 15th–28th July 2013) 139, arXiv: [1311.0283 \[hep-ph\]](#).

- [53] J. Alwall et al., *The automated computation of tree-level and next-to-leading order differential cross sections, and their matching to parton shower simulations*, *JHEP* **07** (2014) 079, arXiv: [1405.0301 \[hep-ph\]](#).
- [54] S. Frixione, E. Laenen, P. Motylinski and B. R. Webber, *Angular correlations of lepton pairs from vector boson and top quark decays in Monte Carlo simulations*, *JHEP* **04** (2007) 081, arXiv: [hep-ph/0702198](#).
- [55] P. Artoisenet, R. Frederix, O. Mattelaer and R. Rietkerk, *Automatic spin-entangled decays of heavy resonances in Monte Carlo simulations*, *JHEP* **03** (2013) 015, arXiv: [1212.3460 \[hep-ph\]](#).
- [56] D. de Florian et al., *Handbook of LHC Higgs Cross Sections: 4. Deciphering the Nature of the Higgs Sector*, 2017, arXiv: [1610.07922 \[hep-ph\]](#).
- [57] H. B. Hartanto, B. Jäger, L. Reina and D. Wackerroth, *Higgs boson production in association with top quarks in the POWHEG BOX*, *Phys. Rev. D* **91** (2015) 094003, arXiv: [1501.04498 \[hep-ph\]](#).
- [58] E. Bothmann et al., *Event generation with Sherpa 2.2*, *SciPost Phys.* **7** (2019) 034, arXiv: [1905.09127 \[hep-ph\]](#).
- [59] T. Gleisberg and S. Höche, *Comix, a new matrix element generator*, *JHEP* **12** (2008) 039, arXiv: [0808.3674 \[hep-ph\]](#).
- [60] F. Buccioni et al., *OpenLoops 2*, *Eur. Phys. J. C* **79** (2019) 866, arXiv: [1907.13071 \[hep-ph\]](#).
- [61] F. Cascioli, P. Maierhöfer and S. Pozzorini, *Scattering Amplitudes with Open Loops*, *Phys. Rev. Lett.* **108** (2012) 111601, arXiv: [1111.5206 \[hep-ph\]](#).
- [62] A. Denner, S. Dittmaier and L. Hofer, *COLLIER: A fortran-based complex one-loop library in extended regularizations*, *Comput. Phys. Commun.* **212** (2017) 220, arXiv: [1604.06792 \[hep-ph\]](#).
- [63] S. Schumann and F. Krauss, *A parton shower algorithm based on Catani–Seymour dipole factorisation*, *JHEP* **03** (2008) 038, arXiv: [0709.1027 \[hep-ph\]](#).
- [64] J.-C. Winter, F. Krauss and G. Soff, *A modified cluster-hadronisation model*, *Eur. Phys. J. C* **36** (2004) 381, arXiv: [hep-ph/0311085](#).
- [65] S. Höche, F. Krauss, M. Schönherr and F. Siegert, *A critical appraisal of NLO+PS matching methods*, *JHEP* **09** (2012) 049, arXiv: [1111.1220 \[hep-ph\]](#).
- [66] S. Catani, F. Krauss, B. R. Webber and R. Kuhn, *QCD Matrix Elements + Parton Showers*, *JHEP* **11** (2001) 063, arXiv: [hep-ph/0109231](#).
- [67] S. Höche, F. Krauss, S. Schumann and F. Siegert, *QCD matrix elements and truncated showers*, *JHEP* **05** (2009) 053, arXiv: [0903.1219 \[hep-ph\]](#).
- [68] S. Höche, F. Krauss, M. Schönherr and F. Siegert, *QCD matrix elements + parton showers. The NLO case*, *JHEP* **04** (2013) 027, arXiv: [1207.5030 \[hep-ph\]](#).

- [69] R. Frederix, E. Re and P. Torrielli, *Single-top t -channel hadroproduction in the four-flavour scheme with POWHEG and aMC@NLO*, *JHEP* **09** (2012) 130, arXiv: [1207.5391 \[hep-ph\]](#).
- [70] L. A. Harland-Lang, A. D. Martin, P. Motylinski and R. S. Thorne, *Parton distributions in the LHC era: MMHT 2014 PDFs*, *Eur. Phys. J. C* **75** (2015) 204, arXiv: [1412.3989 \[hep-ph\]](#).
- [71] S. Höche, S. Mrenna, S. Payne, C. T. Preuss and P. Skands, *A Study of QCD Radiation in VBF Higgs Production with Vincia and Pythia*, *SciPost Phys.* **12** (2022) 010, arXiv: [2106.10987 \[hep-ph\]](#).
- [72] ATLAS Collaboration, *Studies on the improvement of the matching uncertainty definition in top-quark processes simulated with POWHEG+PYTHIA8*, ATL-PHYS-PUB-2023-029, 2013, URL: <https://cds.cern.ch/record/2872787>.
- [73] L. Lönnblad, *Correcting the Colour-Dipole Cascade Model with Fixed Order Matrix Elements*, *JHEP* **05** (2002) 046, arXiv: [hep-ph/0112284](#).
- [74] L. Lönnblad and S. Prestel, *Matching tree-level matrix elements with interleaved showers*, *JHEP* **03** (2012) 019, arXiv: [1109.4829 \[hep-ph\]](#).
- [75] C. Anastasiou, L. Dixon, K. Melnikov and F. Petriello, *High-precision QCD at hadron colliders: Electroweak gauge boson rapidity distributions at next-to-next-to leading order*, *Phys. Rev. D* **69** (2004) 094008, arXiv: [hep-ph/0312266](#).
- [76] ATLAS Collaboration, *Electron and photon performance measurements with the ATLAS detector using the 2015–2017 LHC proton-proton collision data*, *JINST* **14** (2019) P12006, arXiv: [1908.00005 \[hep-ex\]](#).
- [77] ATLAS Collaboration, *Electron and photon efficiencies in LHC Run 2 with the ATLAS experiment*, *JHEP* **05** (2024) 162, arXiv: [2308.13362 \[hep-ex\]](#).
- [78] ATLAS Collaboration, *Muon reconstruction and identification efficiency in ATLAS using the full Run 2 pp collision data set at $\sqrt{s} = 13$ TeV*, *Eur. Phys. J. C* **81** (2021) 578, arXiv: [2012.00578 \[hep-ex\]](#).
- [79] ATLAS Collaboration, *The ATLAS inner detector trigger performance in pp collisions at 13 TeV during LHC Run 2*, *Eur. Phys. J. C* **82** (2022) 206, arXiv: [2107.02485 \[hep-ex\]](#).
- [80] ATLAS Collaboration, *Performance of electron and photon triggers in ATLAS during LHC Run 2*, *Eur. Phys. J. C* **80** (2020) 47, arXiv: [1909.00761 \[hep-ex\]](#).
- [81] ATLAS Collaboration, *Performance of the ATLAS muon triggers in Run 2*, *JINST* **15** (2020) P09015, arXiv: [2004.13447 \[physics.ins-det\]](#).
- [82] M. Cacciari, G. P. Salam and G. Soyez, *The anti- k_t jet clustering algorithm*, *JHEP* **04** (2008) 063, arXiv: [0802.1189 \[hep-ph\]](#).
- [83] M. Cacciari, G. P. Salam and G. Soyez, *FastJet User Manual*, *Eur. Phys. J. C* **72** (2012) 1896, arXiv: [1111.6097 \[hep-ph\]](#).
- [84] ATLAS Collaboration, *Jet reconstruction and performance using particle flow with the ATLAS Detector*, *Eur. Phys. J. C* **77** (2017) 466, arXiv: [1703.10485 \[hep-ex\]](#).

- [85] ATLAS Collaboration, *Jet energy scale and resolution measured in proton–proton collisions at $\sqrt{s} = 13$ TeV with the ATLAS detector*, *Eur. Phys. J. C* **81** (2021) 689, arXiv: [2007.02645 \[hep-ex\]](#).
- [86] ATLAS Collaboration, *Performance of pile-up mitigation techniques for jets in pp collisions at $\sqrt{s} = 8$ TeV using the ATLAS detector*, *Eur. Phys. J. C* **76** (2016) 581, arXiv: [1510.03823 \[hep-ex\]](#).
- [87] ATLAS Collaboration, *ATLAS flavour-tagging algorithms for the LHC Run 2 pp collision dataset*, *Eur. Phys. J. C* **83** (2023) 681, arXiv: [2211.16345 \[physics.data-an\]](#).
- [88] Belle Collaboration, K. Belous et al., *Measurement of the τ -lepton lifetime at Belle*, *Phys. Rev. Lett.* **112** (2014) 031801, arXiv: [1310.8503 \[hep-ex\]](#).
- [89] R. Barlow, *Extended maximum likelihood*, *Nucl. Instrum. Meth. A* **297** (1990) 496.
- [90] W. Voigt, *On the law of intensity distribution within the lines of a gas spectrum*, vol. 1912,25, Meeting reports, Munich, 1912, URL: <https://publikationen.badw.de/de/003395768>.
- [91] R. D. Cousins, *Generalization of Chisquare Goodness-of-Fit Test for Binned Data Using Saturated Models, with Application to Histograms*, URL: http://www.physics.ucla.edu/~cousins/stats/cousins_saturated.pdf.
- [92] ATLAS Collaboration, *Electron and photon energy calibration with the ATLAS detector using LHC Run 2 data*, *JINST* **19** (2023) P02009, arXiv: [2309.05471 \[hep-ex\]](#).
- [93] ATLAS Collaboration, *Studies of the muon momentum calibration and performance of the ATLAS detector with pp collisions at $\sqrt{s} = 13$ TeV*, *Eur. Phys. J. C* **83** (2023) 686, arXiv: [2212.07338 \[hep-ex\]](#).
- [94] ATLAS Collaboration, *ATLAS b-jet identification performance and efficiency measurement with $t\bar{t}$ events in pp collisions at $\sqrt{s} = 13$ TeV*, *Eur. Phys. J. C* **79** (2019) 970, arXiv: [1907.05120 \[hep-ex\]](#).
- [95] ATLAS Collaboration, *Measurement of the c-jet mistagging efficiency in $t\bar{t}$ events using pp collision data at $\sqrt{s} = 13$ TeV collected with the ATLAS detector*, *Eur. Phys. J. C* **82** (2022) 95, arXiv: [2109.10627 \[hep-ex\]](#).
- [96] ATLAS Collaboration, *Calibration of the light-flavour jet mistagging efficiency of the b-tagging algorithms with Z+jets events using 139 fb^{-1} of ATLAS proton–proton collision data at $\sqrt{s} = 13$ TeV*, *Eur. Phys. J. C* **83** (2023) 728, arXiv: [2301.06319 \[hep-ex\]](#).
- [97] ATLAS Collaboration, *Luminosity determination in pp collisions at $\sqrt{s} = 13$ TeV using the ATLAS detector at the LHC*, *Eur. Phys. J. C* **83** (2023) 982, arXiv: [2212.09379 \[hep-ex\]](#).
- [98] R. Barlow and C. Beeston, *Fitting using finite Monte Carlo samples*, *Comput. Phys. Commun.* **77** (1993) 219.
- [99] ATLAS Collaboration, *ATLAS Computing Acknowledgements*, ATL-SOFT-PUB-2023-001, 2023, URL: <https://cds.cern.ch/record/2869272>.

The ATLAS Collaboration

G. Aad ¹⁰⁵, E. Aakvaag ¹⁷, B. Abbott ¹²⁴, S. Abdelhameed ^{120a}, K. Abeling ⁵⁷, N.J. Abicht ⁵¹, S.H. Abidi ³⁰, M. Aboeela ⁴⁶, A. Aboulhorma ^{36e}, H. Abramowicz ¹⁵⁶, Y. Abulaiti ¹²¹, B.S. Acharya ^{71a,71b,m}, A. Ackermann ^{65a}, C. Adam Bourdarios ⁴, L. Adamczyk ^{88a}, S.V. Addepalli ¹⁴⁸, M.J. Addison ¹⁰⁴, J. Adelman ¹¹⁹, A. Adiguzel ^{22c}, T. Adye ¹³⁸, A.A. Affolder ¹⁴⁰, Y. Afik ⁴¹, M.N. Agaras ¹³, A. Aggarwal ¹⁰³, C. Agheorghiesei ^{28c}, F. Ahmadov ^{40,ab}, S. Ahuja ⁹⁸, X. Ai ^{64e}, G. Aielli ^{78a,78b}, A. Aikot ¹⁶⁸, M. Ait Tamlihat ^{36e}, B. Aitbenkikh ^{36a}, M. Akbiyik ¹⁰³, T.P.A. Åkesson ¹⁰¹, A.V. Akimov ¹⁵⁰, D. Akiyama ¹⁷³, N.N. Akolkar ²⁵, S. Aktas ^{22a}, K. Al Houry ⁴³, G.L. Alberghi ^{24b}, J. Albert ¹⁷⁰, P. Albicocco ⁵⁵, G.L. Albouy ⁶², S. Alderweireldt ⁵⁴, Z.L. Alegria ¹²⁵, M. Aleksa ³⁷, I.N. Aleksandrov ⁴⁰, C. Alexa ^{28b}, T. Alexopoulos ¹⁰, F. Alfonsi ^{24b}, M. Algren ⁵⁸, M. Alhroob ¹⁷², B. Ali ¹³⁶, H.M.J. Ali ^{94,v}, S. Ali ³², S.W. Alibocus ⁹⁵, M. Aliev ^{34c}, G. Alimonti ^{73a}, W. Alkakhi ⁵⁷, C. Allaire ⁶⁸, B.M.M. Allbrooke ¹⁵¹, J.S. Allen ¹⁰⁴, J.F. Allen ⁵⁴, C.A. Allendes Flores ^{141f}, P.P. Allport ²¹, A. Aloisio ^{74a,74b}, F. Alonso ⁹³, C. Alpigiani ¹⁴³, Z.M.K. Alsolami ⁹⁴, M. Alvarez Estevez ¹⁰², A. Alvarez Fernandez ¹⁰³, M. Alves Cardoso ⁵⁸, M.G. Alviggi ^{74a,74b}, M. Aly ¹⁰⁴, Y. Amaral Coutinho ^{85b}, A. Ambler ¹⁰⁷, C. Amelung ³⁷, M. Amerl ¹⁰⁴, C.G. Ames ¹¹², D. Amidei ¹⁰⁹, B. Amini ⁵⁶, K.J. Amirie ¹⁵⁹, S.P. Amor Dos Santos ^{134a}, K.R. Amos ¹⁶⁸, D. Amperiadou ¹⁵⁷, S. An ⁸⁶, V. Ananiev ¹²⁹, C. Anastopoulos ¹⁴⁴, T. Andeen ¹¹, J.K. Anders ³⁷, A.C. Anderson ⁶¹, A. Andreatza ^{73a,73b}, S. Angelidakis ⁹, A. Angerami ⁴³, A.V. Anisenkov ³⁹, A. Annovi ^{76a}, C. Antel ⁵⁸, E. Antipov ¹⁵⁰, M. Antonelli ⁵⁵, F. Anulli ^{77a}, M. Aoki ⁸⁶, T. Aoki ¹⁵⁸, M.A. Aparo ¹⁵¹, L. Aperio Bella ⁵⁰, C. Appelt ¹⁵⁶, A. Apyan ²⁷, S.J. Arbiol Val ⁸⁹, C. Arcangeletti ⁵⁵, A.T.H. Arce ⁵³, J-F. Arguin ¹¹¹, S. Argyropoulos ¹⁵⁷, J.-H. Arling ⁵⁰, O. Arnaez ⁴, H. Arnold ¹⁵⁰, G. Artoni ^{77a,77b}, H. Asada ¹¹⁴, K. Asai ¹²², S. Asai ¹⁵⁸, N.A. Asbah ³⁷, R.A. Ashby Pickering ¹⁷², K. Assamagan ³⁰, R. Astalos ^{29a}, K.S.V. Astrand ¹⁰¹, S. Atashi ¹⁶³, R.J. Atkin ^{34a}, H. Atmani ^{36f}, P.A. Atlasiddha ¹³², K. Augsten ¹³⁶, A.D. Auriol ²¹, V.A. Austrup ¹⁰⁴, G. Avolio ³⁷, K. Axiotis ⁵⁸, G. Azuelos ^{111,af}, D. Babal ^{29b}, H. Bachacou ¹³⁹, K. Bachas ^{157,q}, A. Bachiu ³⁵, E. Bachmann ⁵², A. Badea ⁴¹, T.M. Baer ¹⁰⁹, P. Bagnaia ^{77a,77b}, M. Bahmani ¹⁹, D. Bahner ⁵⁶, K. Bai ¹²⁷, J.T. Baines ¹³⁸, L. Baines ⁹⁷, O.K. Baker ¹⁷⁷, E. Bakos ¹⁶, D. Bakshi Gupta ⁸, L.E. Balabram Filho ^{85b}, V. Balakrishnan ¹²⁴, R. Balasubramanian ⁴, E.M. Baldin ³⁹, P. Balek ^{88a}, E. Ballabene ^{24b,24a}, F. Balli ¹³⁹, L.M. Baltes ^{65a}, W.K. Balunas ³³, J. Balz ¹⁰³, I. Bamwidhi ^{120b}, E. Banas ⁸⁹, M. Bandieramonte ¹³³, A. Bandyopadhyay ²⁵, S. Bansal ²⁵, L. Barak ¹⁵⁶, M. Barakat ⁵⁰, E.L. Barberio ¹⁰⁸, D. Barberis ^{59b,59a}, M. Barbero ¹⁰⁵, M.Z. Barel ¹¹⁸, T. Barillari ¹¹³, M-S. Barisits ³⁷, T. Barklow ¹⁴⁸, P. Baron ¹²⁶, D.A. Baron Moreno ¹⁰⁴, A. Baroncelli ^{64a}, A.J. Barr ¹³⁰, J.D. Barr ⁹⁹, F. Barreiro ¹⁰², J. Barreiro Guimarões da Costa ¹⁴, M.G. Barros Teixeira ^{134a}, S. Barsov ³⁹, F. Bartels ^{65a}, R. Bartoldus ¹⁴⁸, A.E. Barton ⁹⁴, P. Bartos ^{29a}, A. Basan ¹⁰³, M. Baselga ⁵¹, A. Bassalat ^{68,b}, M.J. Basso ^{160a}, S. Bataju ⁴⁶, R. Bate ¹⁶⁹, R.L. Bates ⁶¹, S. Batlamous ¹⁰², B. Batool ¹⁴⁶, M. Battaglia ¹⁴⁰, D. Battulga ¹⁹, M. Bauge ^{77a,77b}, M. Bauer ⁸¹, P. Bauer ²⁵, L.T. Bazzano Hurrell ³¹, J.B. Beacham ⁵³, T. Beau ¹³¹, J.Y. Beaucamp ⁹³, P.H. Beauchemin ¹⁶², P. Bechtel ²⁵, H.P. Beck ^{20,p}, K. Becker ¹⁷², A.J. Beddall ⁸⁴, V.A. Bednyakov ⁴⁰, C.P. Bee ¹⁵⁰, L.J. Beemster ¹⁶, T.A. Beermann ³⁷, M. Begalli ^{85d}, M. Begel ³⁰, J.K. Behr ⁵⁰, J.F. Beirer ³⁷, F. Beisiegel ²⁵, M. Belfkir ^{120b}, G. Bella ¹⁵⁶, L. Bellagamba ^{24b}, A. Bellerive ³⁵, P. Bellos ²¹, K. Beloborodov ³⁹, D. Benchekroun ^{36a}, F. Bendebba ^{36a}, Y. Benhammou ¹⁵⁶,

K.C. Benkendorfer [ID⁶³](#), L. Beresford [ID⁵⁰](#), M. Beretta [ID⁵⁵](#), E. Bergeaas Kuutmann [ID¹⁶⁶](#), N. Berger [ID⁴](#),
 B. Bergmann [ID¹³⁶](#), J. Beringer [ID^{18a}](#), G. Bernardi [ID⁵](#), C. Bernius [ID¹⁴⁸](#), F.U. Bernlochner [ID²⁵](#),
 F. Bernon [ID³⁷](#), A. Berrocal Guardia [ID¹³](#), T. Berry [ID⁹⁸](#), P. Berta [ID¹³⁷](#), A. Berthold [ID⁵²](#), S. Bethke [ID¹¹³](#),
 A. Betti [ID^{77a,77b}](#), A.J. Bevan [ID⁹⁷](#), N.K. Bhalla [ID⁵⁶](#), S. Bharthuar [ID¹¹³](#), S. Bhatta [ID¹⁵⁰](#),
 D.S. Bhattacharya [ID¹⁷¹](#), P. Bhattarai [ID¹⁴⁸](#), Z.M. Bhatti [ID¹²¹](#), K.D. Bhide [ID⁵⁶](#), V.S. Bhopatkar [ID¹²⁵](#),
 R.M. Bianchi [ID¹³³](#), G. Bianco [ID^{24b,24a}](#), O. Biebel [ID¹¹²](#), M. Biglietti [ID^{79a}](#), C.S. Billingsley [ID⁴⁶](#),
 Y. Bimgdi [ID^{36f}](#), M. Bindi [ID⁵⁷](#), A. Bingham [ID¹⁷⁶](#), A. Bingul [ID^{22b}](#), C. Bini [ID^{77a,77b}](#), G.A. Bird [ID³³](#),
 M. Birman [ID¹⁷⁴](#), M. Biros [ID¹³⁷](#), S. Biryukov [ID¹⁵¹](#), T. Bisanz [ID⁵¹](#), E. Bisceglie [ID^{45b,45a}](#), J.P. Biswal [ID¹³⁸](#),
 D. Biswas [ID¹⁴⁶](#), I. Bloch [ID⁵⁰](#), A. Blue [ID⁶¹](#), U. Blumenschein [ID⁹⁷](#), J. Blumenthal [ID¹⁰³](#),
 V.S. Bobrovnikov [ID³⁹](#), M. Boehler [ID⁵⁶](#), B. Boehm [ID¹⁷¹](#), D. Bogavac [ID³⁷](#), A.G. Bogdanchikov [ID³⁹](#),
 L.S. Boggia [ID¹³¹](#), C. Bohm [ID^{49a}](#), V. Boisvert [ID⁹⁸](#), P. Bokan [ID³⁷](#), T. Bold [ID^{88a}](#), M. Bomben [ID⁵](#),
 M. Bona [ID⁹⁷](#), M. Boonekamp [ID¹³⁹](#), A.G. Borbély [ID⁶¹](#), I.S. Bordulev [ID³⁹](#), G. Borissov [ID⁹⁴](#),
 D. Bortoletto [ID¹³⁰](#), D. Boscherini [ID^{24b}](#), M. Bosman [ID¹³](#), K. Bouaouda [ID^{36a}](#), N. Bouchhar [ID¹⁶⁸](#),
 L. Boudet [ID⁴](#), J. Boudreau [ID¹³³](#), E.V. Bouhova-Thacker [ID⁹⁴](#), D. Boumediene [ID⁴²](#), R. Bouquet [ID^{59b,59a}](#),
 A. Boveia [ID¹²³](#), J. Boyd [ID³⁷](#), D. Boye [ID³⁰](#), I.R. Boyko [ID⁴⁰](#), L. Bozianu [ID⁵⁸](#), J. Bracnik [ID²¹](#),
 N. Brahimí [ID⁴](#), G. Brandt [ID¹⁷⁶](#), O. Brandt [ID³³](#), B. Brau [ID¹⁰⁶](#), J.E. Brau [ID¹²⁷](#), R. Brenner [ID¹⁷⁴](#),
 L. Brenner [ID¹¹⁸](#), R. Brenner [ID¹⁶⁶](#), S. Bressler [ID¹⁷⁴](#), G. Brianti [ID^{80a,80b}](#), D. Britton [ID⁶¹](#), D. Britzger [ID¹¹³](#),
 I. Brock [ID²⁵](#), R. Brock [ID¹¹⁰](#), G. Brooijmans [ID⁴³](#), A.J. Brooks [ID⁷⁰](#), E.M. Brooks [ID^{160b}](#), E. Brost [ID³⁰](#),
 L.M. Brown [ID¹⁷⁰](#), L.E. Bruce [ID⁶³](#), T.L. Bruckler [ID¹³⁰](#), P.A. Bruckman de Renstrom [ID⁸⁹](#), B. Brüers [ID⁵⁰](#),
 A. Bruni [ID^{24b}](#), G. Bruni [ID^{24b}](#), D. Brunner [ID^{49a,49b}](#), M. Bruschi [ID^{24b}](#), N. Bruscinò [ID^{77a,77b}](#), T. Buanes [ID¹⁷](#),
 Q. Buat [ID¹⁴³](#), D. Buchin [ID¹¹³](#), A.G. Buckley [ID⁶¹](#), O. Bulekov [ID³⁹](#), B.A. Bullard [ID¹⁴⁸](#), S. Burdin [ID⁹⁵](#),
 C.D. Burgard [ID⁵¹](#), A.M. Burger [ID³⁷](#), B. Burghgrave [ID⁸](#), O. Burlayenko [ID⁵⁶](#), J. Burleson [ID¹⁶⁷](#),
 J.T.P. Burr [ID³³](#), J.C. Burzynski [ID¹⁴⁷](#), E.L. Busch [ID⁴³](#), V. Büscher [ID¹⁰³](#), P.J. Bussey [ID⁶¹](#), J.M. Butler [ID²⁶](#),
 C.M. Buttar [ID⁶¹](#), J.M. Butterworth [ID⁹⁹](#), W. Buttinger [ID¹³⁸](#), C.J. Buxo Vazquez [ID¹¹⁰](#), A.R. Buzykaev [ID³⁹](#),
 S. Cabrera Urbán [ID¹⁶⁸](#), L. Cadamuro [ID⁶⁸](#), D. Caforio [ID⁶⁰](#), H. Cai [ID¹³³](#), Y. Cai [ID^{14,115c}](#), Y. Cai [ID^{115a}](#),
 V.M.M. Cairo [ID³⁷](#), O. Cakir [ID^{3a}](#), N. Calace [ID³⁷](#), P. Calafiura [ID^{18a}](#), G. Calderini [ID¹³¹](#), P. Calfayan [ID³⁵](#),
 G. Callea [ID⁶¹](#), L.P. Caloba [ID^{85b}](#), D. Calvet [ID⁴²](#), S. Calvet [ID⁴²](#), R. Camacho Toro [ID¹³¹](#), S. Camarda [ID³⁷](#),
 D. Camarero Munoz [ID²⁷](#), P. Camarri [ID^{78a,78b}](#), M.T. Camerlingo [ID^{74a,74b}](#), D. Cameron [ID³⁷](#),
 C. Camincher [ID¹⁷⁰](#), M. Campanelli [ID⁹⁹](#), A. Camplani [ID⁴⁴](#), V. Canale [ID^{74a,74b}](#), A.C. Canbay [ID^{3a}](#),
 E. Canonero [ID⁹⁸](#), J. Cantero [ID¹⁶⁸](#), Y. Cao [ID¹⁶⁷](#), F. Capocasa [ID²⁷](#), M. Capua [ID^{45b,45a}](#), A. Carbone [ID^{73a,73b}](#),
 R. Cardarelli [ID^{78a}](#), J.C.J. Cardenas [ID⁸](#), M.P. Cardiff [ID²⁷](#), G. Carducci [ID^{45b,45a}](#), T. Carli [ID³⁷](#),
 G. Carlino [ID^{74a}](#), J.I. Carlotto [ID¹³](#), B.T. Carlson [ID^{133,r}](#), E.M. Carlson [ID^{170,160a}](#), J. Carmignani [ID⁹⁵](#),
 L. Carminati [ID^{73a,73b}](#), A. Carnelli [ID¹³⁹](#), M. Carnesale [ID³⁷](#), S. Caron [ID¹¹⁷](#), E. Carquin [ID^{141f}](#),
 I.B. Carr [ID¹⁰⁸](#), S. Carrá [ID^{73a}](#), G. Carratta [ID^{24b,24a}](#), A.M. Carroll [ID¹²⁷](#), M.P. Casado [ID^{13,i}](#), M. Caspar [ID⁵⁰](#),
 F.L. Castillo [ID⁴](#), L. Castillo Garcia [ID¹³](#), V. Castillo Gimenez [ID¹⁶⁸](#), N.F. Castro [ID^{134a,134e}](#),
 A. Catinaccio [ID³⁷](#), J.R. Catmore [ID¹²⁹](#), T. Cavaliere [ID⁴](#), V. Cavaliere [ID³⁰](#), L.J. Caviedes Betancourt [ID^{23b}](#),
 Y.C. Cekmecelioglu [ID⁵⁰](#), E. Celebi [ID⁸⁴](#), S. Cella [ID³⁷](#), V. Cepaitis [ID⁵⁸](#), K. Cerny [ID¹²⁶](#),
 A.S. Cerqueira [ID^{85a}](#), A. Cerri [ID¹⁵¹](#), L. Cerrito [ID^{78a,78b}](#), F. Cerutti [ID^{18a}](#), B. Cervato [ID¹⁴⁶](#), A. Cervelli [ID^{24b}](#),
 G. Cesarini [ID⁵⁵](#), S.A. Cetin [ID⁸⁴](#), P.M. Chabrilat [ID¹³¹](#), D. Chakraborty [ID¹¹⁹](#), J. Chan [ID^{18a}](#),
 W.Y. Chan [ID¹⁵⁸](#), J.D. Chapman [ID³³](#), E. Chapon [ID¹³⁹](#), B. Chargeishvili [ID^{154b}](#), D.G. Charlton [ID²¹](#),
 M. Chatterjee [ID²⁰](#), C. Chauhan [ID¹³⁷](#), Y. Che [ID^{115a}](#), S. Chekanov [ID⁶](#), S.V. Chekulav [ID^{160a}](#),
 G.A. Chelkov [ID^{40,a}](#), A. Chen [ID¹⁰⁹](#), B. Chen [ID¹⁵⁶](#), B. Chen [ID¹⁷⁰](#), H. Chen [ID^{115a}](#), H. Chen [ID³⁰](#),
 J. Chen [ID^{64c}](#), J. Chen [ID¹⁴⁷](#), M. Chen [ID¹³⁰](#), S. Chen [ID⁹⁰](#), S.J. Chen [ID^{115a}](#), X. Chen [ID^{64c}](#), X. Chen [ID^{15,ae}](#),
 Y. Chen [ID^{64a}](#), C.L. Cheng [ID¹⁷⁵](#), H.C. Cheng [ID^{66a}](#), S. Cheong [ID¹⁴⁸](#), A. Cheplakov [ID⁴⁰](#),
 E. Cheremushkina [ID⁵⁰](#), E. Cherepanova [ID¹¹⁸](#), R. Cherkaoui El Moursli [ID^{36e}](#), E. Cheu [ID⁷](#), K. Cheung [ID⁶⁷](#),
 L. Chevalier [ID¹³⁹](#), V. Chiarella [ID⁵⁵](#), G. Chiarelli [ID^{76a}](#), N. Chiedde [ID¹⁰⁵](#), G. Chiodini [ID^{72a}](#),
 A.S. Chisholm [ID²¹](#), A. Chitan [ID^{28b}](#), M. Chitishvili [ID¹⁶⁸](#), M.V. Chizhov [ID^{40,s}](#), K. Choi [ID¹¹](#), Y. Chou [ID¹⁴³](#),

E.Y.S. Chow ¹¹⁷, K.L. Chu ¹⁷⁴, M.C. Chu ^{66a}, X. Chu ^{14,115c}, Z. Chubinidze ⁵⁵, J. Chudoba ¹³⁵,
 J.J. Chwastowski ⁸⁹, D. Cieri ¹¹³, K.M. Ciesla ^{88a}, V. Cindro ⁹⁶, A. Ciocio ^{18a}, F. Ciroto ^{74a,74b},
 Z.H. Citron ¹⁷⁴, M. Citterio ^{73a}, D.A. Ciubotaru ^{28b}, A. Clark ⁵⁸, P.J. Clark ⁵⁴, N. Clarke Hall ⁹⁹,
 C. Clarry ¹⁵⁹, J.M. Clavijo Columbie ⁵⁰, S.E. Clawson ⁵⁰, C. Clement ^{49a,49b}, Y. Coadou ¹⁰⁵,
 M. Cobal ^{71a,71c}, A. Coccaro ^{59b}, R.F. Coelho Barrue ^{134a}, R. Coelho Lopes De Sa ¹⁰⁶,
 S. Coelli ^{73a}, L.S. Colangeli ¹⁵⁹, B. Cole ⁴³, J. Collot ⁶², P. Conde Muiño ^{134a,134g},
 M.P. Connell ^{34c}, S.H. Connell ^{34c}, E.I. Conroy ¹³⁰, F. Conventi ^{74a,ag}, H.G. Cooke ²¹,
 A.M. Cooper-Sarkar ¹³⁰, F.A. Corchia ^{24b,24a}, A. Cordeiro Oudot Choi ¹³¹, L.D. Corpe ⁴²,
 M. Corradi ^{77a,77b}, F. Corriveau ^{107,aa}, A. Cortes-Gonzalez ¹⁹, M.J. Costa ¹⁶⁸, F. Costanza ⁴,
 D. Costanzo ¹⁴⁴, B.M. Cote ¹²³, J. Couthures ⁴, G. Cowan ⁹⁸, K. Cranmer ¹⁷⁵, L. Cremer ⁵¹,
 D. Cremonini ^{24b,24a}, S. Crépe-Renaudin ⁶², F. Crescioli ¹³¹, M. Cristinziani ¹⁴⁶,
 M. Cristoforetti ^{80a,80b}, V. Croft ¹¹⁸, J.E. Crosby ¹²⁵, G. Crosetti ^{45b,45a}, A. Cueto ¹⁰², H. Cui ⁹⁹,
 Z. Cui ⁷, W.R. Cunningham ⁶¹, F. Curcio ¹⁶⁸, J.R. Curran ⁵⁴, P. Czodrowski ³⁷,
 M.J. Da Cunha Sargedas De Sousa ^{59b,59a}, J.V. Da Fonseca Pinto ^{85b}, C. Da Via ¹⁰⁴,
 W. Dabrowski ^{88a}, T. Dado ³⁷, S. Dahbi ¹⁵³, T. Dai ¹⁰⁹, D. Dal Santo ²⁰, C. Dallapiccola ¹⁰⁶,
 M. Dam ⁴⁴, G. D'amen ³⁰, V. D'Amico ¹¹², J. Damp ¹⁰³, J.R. Dandoy ³⁵, D. Dannheim ³⁷,
 M. Danninger ¹⁴⁷, V. Dao ¹⁵⁰, G. Darbo ^{59b}, S.J. Das ³⁰, F. Dattola ⁵⁰, S. D'Auria ^{73a,73b},
 A. D'Avanzo ^{74a,74b}, C. David ^{34a}, T. Davidek ¹³⁷, I. Dawson ⁹⁷, H.A. Day-hall ¹³⁶, K. De ⁸,
 C. De Almeida Rossi ¹⁵⁹, R. De Asmundis ^{74a}, N. De Biase ⁵⁰, S. De Castro ^{24b,24a},
 N. De Groot ¹¹⁷, P. de Jong ¹¹⁸, H. De la Torre ¹¹⁹, A. De Maria ^{115a}, A. De Salvo ^{77a},
 U. De Sanctis ^{78a,78b}, F. De Santis ^{72a,72b}, A. De Santo ¹⁵¹, J.B. De Vivie De Regie ⁶²,
 J. Debevc ⁹⁶, D.V. Dedovich ⁴⁰, J. Degens ⁹⁵, A.M. Deiana ⁴⁶, F. Del Corso ^{24b,24a},
 J. Del Peso ¹⁰², L. Delagrangé ¹³¹, F. Deliot ¹³⁹, C.M. Delitzsch ⁵¹, M. Della Pietra ^{74a,74b},
 D. Della Volpe ⁵⁸, A. Dell'Acqua ³⁷, L. Dell'Asta ^{73a,73b}, M. Delmastro ⁴, C.C. Delogu ¹⁰³,
 P.A. Delsart ⁶², S. Demers ¹⁷⁷, M. Demichev ⁴⁰, S.P. Denisov ³⁹, H. Denizli ^{22a}, L. D'Eramo ⁴²,
 D. Derendarz ⁸⁹, F. Derue ¹³¹, P. Dervan ⁹⁵, K. Desch ²⁵, C. Deutsch ²⁵, F.A. Di Bello ^{59b,59a},
 A. Di Ciaccio ^{78a,78b}, L. Di Ciaccio ⁴, A. Di Domenico ^{77a,77b}, C. Di Donato ^{74a,74b},
 A. Di Girolamo ³⁷, G. Di Gregorio ³⁷, A. Di Luca ^{80a,80b}, B. Di Micco ^{79a,79b}, R. Di Nardo ^{79a,79b},
 K.F. Di Petrillo ⁴¹, M. Diamantopoulou ³⁵, F.A. Dias ¹¹⁸, T. Dias Do Vale ¹⁴⁷,
 M.A. Diaz ^{141a,141b}, A.R. Didenko ⁴⁰, M. Didenko ¹⁶⁸, E.B. Diehl ¹⁰⁹, S. Díez Cornell ⁵⁰,
 C. Díez Pardos ¹⁴⁶, C. Dimitriadi ¹⁶⁶, A. Dimitrievska ²¹, J. Dingfelder ²⁵, T. Dingley ¹³⁰,
 I-M. Dinu ^{28b}, S.J. Dittmeier ^{65b}, F. Dittus ³⁷, M. Divisek ¹³⁷, B. Dixit ⁹⁵, F. Djama ¹⁰⁵,
 T. Djobava ^{154b}, C. Doglioni ^{104,101}, A. Dohnalova ^{29a}, Z. Dolezal ¹³⁷, K. Domijan ^{88a},
 K.M. Dona ⁴¹, M. Donadelli ^{85d}, B. Dong ¹¹⁰, J. Donini ⁴², A. D'Onofrio ^{74a,74b},
 M. D'Onofrio ⁹⁵, J. Dopke ¹³⁸, A. Doria ^{74a}, N. Dos Santos Fernandes ^{134a}, P. Dougan ¹⁰⁴,
 M.T. Dova ⁹³, A.T. Doyle ⁶¹, M.A. Dragnet ¹³⁰, M.P. Drescher ⁵⁷, E. Dreyer ¹⁷⁴,
 I. Drivas-koulouris ¹⁰, M. Drnevich ¹²¹, M. Drozdova ⁵⁸, D. Du ^{64a}, T.A. du Pree ¹¹⁸,
 F. Dubinin ³⁹, M. Dubovsky ^{29a}, E. Duchovni ¹⁷⁴, G. Duckeck ¹¹², O.A. Ducu ^{28b}, D. Duda ⁵⁴,
 A. Dudarev ³⁷, E.R. Duden ²⁷, M. D'uffizi ¹⁰⁴, L. Duflot ⁶⁸, M. Dührssen ³⁷, I. Duminica ^{28g},
 A.E. Dumitriu ^{28b}, M. Dunford ^{65a}, S. Dungs ⁵¹, K. Dunne ^{49a,49b}, A. Duperrin ¹⁰⁵,
 H. Duran Yildiz ^{3a}, M. Düren ⁶⁰, A. Durglishvili ^{154b}, D. Duvnjak ³⁵, B.L. Dwyer ¹¹⁹,
 G.I. Dyckes ^{18a}, M. Dyndal ^{88a}, B.S. Dziedzic ³⁷, Z.O. Earnshaw ¹⁵¹, G.H. Eberwein ¹³⁰,
 B. Eckerova ^{29a}, S. Eggebrecht ⁵⁷, E. Egidio Purcino De Souza ^{85e}, L.F. Ehrke ⁵⁸, G. Eigen ¹⁷,
 K. Einsweiler ^{18a}, T. Ekelof ¹⁶⁶, P.A. Ekman ¹⁰¹, S. El Farkh ^{36b}, Y. El Ghazali ^{64a},
 H. El Jarrari ³⁷, A. El Moussaouy ^{36a}, V. Ellajosyula ¹⁶⁶, M. Ellert ¹⁶⁶, F. Ellinghaus ¹⁷⁶,
 N. Ellis ³⁷, J. Elmsheuser ³⁰, M. Elsayy ^{120a}, M. Elsing ³⁷, D. Emeliyanov ¹³⁸, Y. Enari ⁸⁶,
 I. Ene ^{18a}, S. Epari ¹³, P.A. Erland ⁸⁹, D. Ernani Martins Neto ⁸⁹, M. Errenst ¹⁷⁶, M. Escalier ⁶⁸,

C. Escobar [ID168](#), E. Etzion [ID156](#), G. Evans [ID134a,134b](#), H. Evans [ID70](#), L.S. Evans [ID98](#), A. Ezhilov [ID39](#),
 S. Ezzarqtouni [ID36a](#), F. Fabbri [ID24b,24a](#), L. Fabbri [ID24b,24a](#), G. Facini [ID99](#), V. Fadeyev [ID140](#),
 R.M. Fakhrutdinov [ID39](#), D. Fakoudis [ID103](#), S. Falciano [ID77a](#), L.F. Falda Ulhoa Coelho [ID134a](#),
 F. Fallavollita [ID113](#), G. Falsetti [ID45b,45a](#), J. Faltova [ID137](#), C. Fan [ID167](#), K.Y. Fan [ID66b](#), Y. Fan [ID14](#),
 Y. Fang [ID14,115c](#), M. Fanti [ID73a,73b](#), M. Faraj [ID71a,71b](#), Z. Farazpay [ID100](#), A. Farbin [ID8](#), A. Farilla [ID79a](#),
 T. Farooque [ID110](#), J.N. Farr [ID177](#), S.M. Farrington [ID138,54](#), F. Fassi [ID36e](#), D. Fassouliotis [ID9](#),
 M. Faucci Giannelli [ID78a,78b](#), W.J. Fawcett [ID33](#), L. Fayard [ID68](#), P. Federic [ID137](#), P. Federicova [ID135](#),
 O.L. Fedin [ID39,a](#), M. Feickert [ID175](#), L. Feligioni [ID105](#), D.E. Fellers [ID127](#), C. Feng [ID64b](#), Z. Feng [ID118](#),
 M.J. Fenton [ID163](#), L. Ferencz [ID50](#), R.A.M. Ferguson [ID94](#), P. Fernandez Martinez [ID69](#),
 M.J.V. Fernoux [ID105](#), J. Ferrando [ID94](#), A. Ferrari [ID166](#), P. Ferrari [ID118,117](#), R. Ferrari [ID75a](#), D. Ferrere [ID58](#),
 C. Ferretti [ID109](#), M.P. Fewell [ID1](#), D. Fiacco [ID77a,77b](#), F. Fiedler [ID103](#), P. Fiedler [ID136](#), S. Filimonov [ID39](#),
 A. Filipčič [ID96](#), E.K. Filmer [ID160a](#), F. Filthaut [ID117](#), M.C.N. Fiolhais [ID134a,134c,c](#), L. Fiorini [ID168](#),
 W.C. Fisher [ID110](#), T. Fitschen [ID104](#), P.M. Fitzhugh [ID139](#), I. Fleck [ID146](#), P. Fleischmann [ID109](#), T. Flick [ID176](#),
 M. Flores [ID34d,ac](#), L.R. Flores Castillo [ID66a](#), L. Flores Sanz De Acedo [ID37](#), F.M. Follega [ID80a,80b](#),
 N. Fomin [ID33](#), J.H. Foo [ID159](#), A. Formica [ID139](#), A.C. Forti [ID104](#), E. Fortin [ID37](#), A.W. Fortman [ID18a](#),
 M.G. Foti [ID18a](#), L. Fountas [ID9,j](#), D. Fournier [ID68](#), H. Fox [ID94](#), P. Francavilla [ID76a,76b](#), S. Francescato [ID63](#),
 S. Franchellucci [ID58](#), M. Franchini [ID24b,24a](#), S. Franchino [ID65a](#), D. Francis [ID37](#), L. Franco [ID117](#),
 V. Franco Lima [ID37](#), L. Franconi [ID50](#), M. Franklin [ID63](#), G. Frattari [ID27](#), Y.Y. Frid [ID156](#), J. Friend [ID61](#),
 N. Fritzsche [ID37](#), A. Froch [ID58](#), D. Froidevaux [ID37](#), J.A. Frost [ID130](#), Y. Fu [ID64a](#),
 S. Fuenzalida Garrido [ID141f](#), M. Fujimoto [ID105](#), K.Y. Fung [ID66a](#), E. Furtado De Simas Filho [ID85e](#),
 M. Furukawa [ID158](#), J. Fuster [ID168](#), A. Gaa [ID57](#), A. Gabrielli [ID24b,24a](#), A. Gabrielli [ID159](#), P. Gadow [ID37](#),
 G. Gagliardi [ID59b,59a](#), L.G. Gagnon [ID18a](#), S. Gaid [ID165](#), S. Galantzan [ID156](#), J. Gallagher [ID1](#),
 E.J. Gallas [ID130](#), A.L. Gallen [ID166](#), B.J. Gallop [ID138](#), K.K. Gan [ID123](#), S. Ganguly [ID158](#), Y. Gao [ID54](#),
 F.M. Garay Walls [ID141a,141b](#), B. Garcia [ID30](#), C. García [ID168](#), A. Garcia Alonso [ID118](#),
 A.G. Garcia Caffaro [ID177](#), J.E. García Navarro [ID168](#), M. Garcia-Sciveres [ID18a](#), G.L. Gardner [ID132](#),
 R.W. Gardner [ID41](#), N. Garelli [ID162](#), R.B. Garg [ID148](#), J.M. Gargan [ID54](#), C.A. Garner [ID159](#), C.M. Garvey [ID34a](#),
 V.K. Gassmann [ID162](#), G. Gaudio [ID75a](#), V. Gautam [ID13](#), P. Gauzzi [ID77a,77b](#), J. Gavranovic [ID96](#),
 I.L. Gavrilenko [ID39](#), A. Gavriluk [ID39](#), C. Gay [ID169](#), G. Gaycken [ID127](#), E.N. Gazis [ID10](#), A.A. Geanta [ID28b](#),
 A. Gekow [ID123](#), C. Gemme [ID59b](#), M.H. Genest [ID62](#), A.D. Gentry [ID116](#), S. George [ID98](#), W.F. George [ID21](#),
 T. Geralis [ID48](#), A.A. Gerwin [ID124](#), P. Gessinger-Befurt [ID37](#), M.E. Geyik [ID176](#), M. Ghani [ID172](#),
 K. Ghorbanian [ID97](#), A. Ghosal [ID146](#), A. Ghosh [ID163](#), A. Ghosh [ID7](#), B. Giacobbe [ID24b](#), S. Giagu [ID77a,77b](#),
 T. Giani [ID118](#), A. Giannini [ID64a](#), S.M. Gibson [ID98](#), M. Gignac [ID140](#), D.T. Gil [ID88b](#), A.K. Gilbert [ID88a](#),
 B.J. Gilbert [ID43](#), D. Gillberg [ID35](#), G. Gilles [ID118](#), L. Ginabat [ID131](#), D.M. Gingrich [ID2,af](#),
 M.P. Giordani [ID71a,71c](#), P.F. Giraud [ID139](#), G. Giugliarelli [ID71a,71c](#), D. Giugni [ID73a](#), F. Giuli [ID78a,78b](#),
 I. Gkialas [ID9,j](#), L.K. Gladilin [ID39](#), C. Glasman [ID102](#), G.R. Gledhill [ID127](#), G. Glemža [ID50](#), M. Glisic [ID127](#),
 I. Gnesi [ID45b](#), Y. Go [ID30](#), M. Goblirsch-Kolb [ID37](#), B. Gocke [ID51](#), D. Godin [ID111](#), B. Gokturk [ID22a](#),
 S. Goldfarb [ID108](#), T. Golling [ID58](#), M.G.D. Gololo [ID34g](#), D. Golubkov [ID39](#), J.P. Gombas [ID110](#),
 A. Gomes [ID134a,134b](#), G. Gomes Da Silva [ID146](#), A.J. Gomez Delegido [ID168](#), R. Gonçalves [ID134a](#),
 L. Gonella [ID21](#), A. Gongadze [ID154c](#), F. Gonnella [ID21](#), J.L. Gonski [ID148](#), R.Y. González Andana [ID54](#),
 S. González de la Hoz [ID168](#), R. Gonzalez Lopez [ID95](#), C. Gonzalez Renteria [ID18a](#),
 M.V. Gonzalez Rodrigues [ID50](#), R. Gonzalez Suarez [ID166](#), S. Gonzalez-Sevilla [ID58](#), L. Goossens [ID37](#),
 B. Gorini [ID37](#), E. Gorini [ID72a,72b](#), A. Gorišek [ID96](#), T.C. Gosart [ID132](#), A.T. Goshaw [ID53](#), M.I. Gostkin [ID40](#),
 S. Goswami [ID125](#), C.A. Gottardo [ID37](#), S.A. Gotz [ID112](#), M. Goughri [ID36b](#), V. Goumarre [ID50](#),
 A.G. Goussiou [ID143](#), N. Govender [ID34c](#), R.P. Grabarczyk [ID130](#), I. Grabowska-Bold [ID88a](#), K. Graham [ID35](#),
 E. Gramstad [ID129](#), S. Grancagnolo [ID72a,72b](#), C.M. Grant [ID1,139](#), P.M. Gravila [ID28f](#), F.G. Gravili [ID72a,72b](#),
 H.M. Gray [ID18a](#), M. Greco [ID72a,72b](#), M.J. Green [ID1](#), C. Grefe [ID25](#), A.S. Grefsrud [ID17](#), I.M. Gregor [ID50](#),
 K.T. Greif [ID163](#), P. Grenier [ID148](#), S.G. Grewe [ID113](#), A.A. Grillo [ID140](#), K. Grimm [ID32](#), S. Grinstein [ID13,w](#),

J.-F. Grivaz ⁶⁸, E. Gross ¹⁷⁴, J. Grosse-Knetter ⁵⁷, L. Guan ¹⁰⁹, J.G.R. Guerrero Rojas ¹⁶⁸,
 G. Guerrieri ³⁷, R. Gugel ¹⁰³, J.A.M. Guhit ¹⁰⁹, A. Guida ¹⁹, E. Guilloton ¹⁷², S. Guindon ³⁷,
 F. Guo ^{14,115c}, J. Guo ^{64c}, L. Guo ⁵⁰, L. Guo ^{14,u}, Y. Guo ¹⁰⁹, A. Gupta ⁵¹, R. Gupta ¹³³,
 S. Gurbuz ²⁵, S.S. Gurdasani ⁵⁶, G. Gustavino ^{77a,77b}, P. Gutierrez ¹²⁴,
 L.F. Gutierrez Zagazeta ¹³², M. Gutsche ⁵², C. Gutschow ⁹⁹, C. Gwenlan ¹³⁰, C.B. Gwilliam ⁹⁵,
 E.S. Haaland ¹²⁹, A. Haas ¹²¹, M. Habedank ⁶¹, C. Haber ^{18a}, H.K. Hadavand ⁸, A. Hadeef ⁵²,
 A.I. Hagan ⁹⁴, J.J. Hahn ¹⁴⁶, E.H. Haines ⁹⁹, M. Haleem ¹⁷¹, J. Haley ¹²⁵, G.D. Hallowell ¹⁰⁵,
 L. Halser ²⁰, K. Hamano ¹⁷⁰, M. Hamer ²⁵, E.J. Hampshire ⁹⁸, J. Han ^{64b}, L. Han ^{115a},
 L. Han ^{64a}, S. Han ^{18a}, Y.F. Han ¹⁵⁹, K. Hanagaki ⁸⁶, M. Hance ¹⁴⁰, D.A. Hangal ⁴³,
 H. Hanif ¹⁴⁷, M.D. Hank ¹³², J.B. Hansen ⁴⁴, P.H. Hansen ⁴⁴, D. Harada ⁵⁸, T. Harenberg ¹⁷⁶,
 S. Harkusha ¹⁷⁸, M.L. Harris ¹⁰⁶, Y.T. Harris ²⁵, J. Harrison ¹³, N.M. Harrison ¹²³,
 P.F. Harrison ¹⁷², N.M. Hartman ¹¹³, N.M. Hartmann ¹¹², R.Z. Hasan ^{98,138}, Y. Hasegawa ¹⁴⁵,
 F. Haslbeck ¹³⁰, S. Hassan ¹⁷, R. Hauser ¹¹⁰, C.M. Hawkes ²¹, R.J. Hawkings ³⁷,
 Y. Hayashi ¹⁵⁸, D. Hayden ¹¹⁰, C. Hayes ¹⁰⁹, R.L. Hayes ¹¹⁸, C.P. Hays ¹³⁰, J.M. Hays ⁹⁷,
 H.S. Hayward ⁹⁵, F. He ^{64a}, M. He ^{14,115c}, Y. He ⁵⁰, Y. He ⁹⁹, N.B. Heatley ⁹⁷, V. Hedberg ¹⁰¹,
 A.L. Heggelund ¹²⁹, C. Heidegger ⁵⁶, K.K. Heidegger ⁵⁶, J. Heilman ³⁵, S. Heim ⁵⁰,
 T. Heim ^{18a}, J.G. Heinlein ¹³², J.J. Heinrich ¹²⁷, L. Heinrich ^{113,ad}, J. Hejbal ¹³⁵, A. Held ¹⁷⁵,
 S. Hellesund ¹⁷, C.M. Helling ¹⁶⁹, S. Hellman ^{49a,49b}, R.C.W. Henderson ⁹⁴, L. Henkelmann ³³,
 A.M. Henriques Correia ³⁷, H. Herde ¹⁰¹, Y. Hernández Jiménez ¹⁵⁰, L.M. Herrmann ²⁵,
 T. Herrmann ⁵², G. Herten ⁵⁶, R. Hertenberger ¹¹², L. Hervas ³⁷, M.E. Hespings ¹⁰³,
 N.P. Hessey ^{160a}, J. Hessler ¹¹³, M. Hidaoui ^{36b}, N. Hidic ¹³⁷, E. Hill ¹⁵⁹, S.J. Hillier ²¹,
 J.R. Hinds ¹¹⁰, F. Hinterkeuser ²⁵, M. Hirose ¹²⁸, S. Hirose ¹⁶¹, D. Hirschbuehl ¹⁷⁶,
 T.G. Hitchings ¹⁰⁴, B. Hiti ⁹⁶, J. Hobbs ¹⁵⁰, R. Hobincu ^{28e}, N. Hod ¹⁷⁴, M.C. Hodgkinson ¹⁴⁴,
 B.H. Hodgkinson ¹³⁰, A. Hoecker ³⁷, D.D. Hofer ¹⁰⁹, J. Hofer ¹⁶⁸, T. Holm ²⁵, M. Holzbock ³⁷,
 L.B.A.H. Hommels ³³, B.P. Honan ¹⁰⁴, J.J. Hong ⁷⁰, J. Hong ^{64c}, T.M. Hong ¹³³,
 B.H. Hooberman ¹⁶⁷, W.H. Hopkins ⁶, M.C. Hoppesch ¹⁶⁷, Y. Horii ¹¹⁴, M.E. Horstmann ¹¹³,
 S. Hou ¹⁵³, M.R. Housenga ¹⁶⁷, A.S. Howard ⁹⁶, J. Howarth ⁶¹, J. Hoya ⁶, M. Hrabovsky ¹²⁶,
 A. Hrynevich ⁵⁰, T. Hryn'ova ⁴, P.J. Hsu ⁶⁷, S.-C. Hsu ¹⁴³, T. Hsu ⁶⁸, M. Hu ^{18a}, Q. Hu ^{64a},
 S. Huang ³³, X. Huang ^{14,115c}, Y. Huang ¹⁴⁴, Y. Huang ¹⁰³, Y. Huang ¹⁴, Z. Huang ¹⁰⁴,
 Z. Hubacek ¹³⁶, M. Huebner ²⁵, F. Huegging ²⁵, T.B. Huffman ¹³⁰,
 M. Hufnagel Maranha De Faria ^{85a}, C.A. Hugli ⁵⁰, M. Huhtinen ³⁷, S.K. Huiberts ¹⁷,
 R. Hulsken ¹⁰⁷, N. Huseynov ^{12,g}, J. Huston ¹¹⁰, J. Huth ⁶³, R. Hyneman ⁷, G. Iacobucci ⁵⁸,
 G. Iakovidis ³⁰, L. Iconomidou-Fayard ⁶⁸, J.P. Iddon ³⁷, P. Iengo ^{74a,74b}, R. Iguchi ¹⁵⁸,
 Y. Iiyama ¹⁵⁸, T. Iizawa ¹³⁰, Y. Ikegami ⁸⁶, D. Iliadis ¹⁵⁷, N. Ilic ¹⁵⁹, H. Imam ^{85c},
 G. Inacio Goncalves ^{85d}, T. Ingebretsen Carlson ^{49a,49b}, J.M. Inglis ⁹⁷, G. Introzzi ^{75a,75b},
 M. Iodice ^{79a}, V. Ippolito ^{77a,77b}, R.K. Irwin ⁹⁵, M. Ishino ¹⁵⁸, W. Islam ¹⁷⁵, C. Issever ¹⁹,
 S. Istin ^{22a,ak}, H. Ito ¹⁷³, R. Iuppa ^{80a,80b}, A. Ivina ¹⁷⁴, J.M. Izen ⁴⁷, V. Izzo ^{74a}, P. Jacka ¹³⁵,
 P. Jackson ¹, C.S. Jagfeld ¹¹², G. Jain ^{160a}, P. Jain ⁵⁰, K. Jakobs ⁵⁶, T. Jakoubek ¹⁷⁴,
 J. Jamieson ⁶¹, W. Jang ¹⁵⁸, M. Javurkova ¹⁰⁶, P. Jawahar ¹⁰⁴, L. Jeanty ¹²⁷, J. Jejelava ^{154a},
 P. Jenni ^{56,f}, C.E. Jessiman ³⁵, C. Jia ^{64b}, H. Jia ¹⁶⁹, J. Jia ¹⁵⁰, X. Jia ^{14,115c}, Z. Jia ^{115a},
 C. Jiang ⁵⁴, S. Jiggins ⁵⁰, J. Jimenez Pena ¹³, S. Jin ^{115a}, A. Jinaru ^{28b}, O. Jinnouchi ¹⁴²,
 P. Johansson ¹⁴⁴, K.A. Johns ⁷, J.W. Johnson ¹⁴⁰, F.A. Jolly ⁵⁰, D.M. Jones ¹⁵¹, E. Jones ⁵⁰,
 K.S. Jones ⁸, P. Jones ³³, R.W.L. Jones ⁹⁴, T.J. Jones ⁹⁵, H.L. Joos ^{57,37}, R. Joshi ¹²³,
 J. Jovicevic ¹⁶, X. Ju ^{18a}, J.J. Junggeburth ³⁷, T. Junkermann ^{65a}, A. Juste Rozas ^{13,w},
 M.K. Juzek ⁸⁹, S. Kabana ^{141e}, A. Kaczmarska ⁸⁹, M. Kado ¹¹³, H. Kagan ¹²³, M. Kagan ¹⁴⁸,
 A. Kahn ¹³², C. Kahra ¹⁰³, T. Kaji ¹⁵⁸, E. Kajomovitz ¹⁵⁵, N. Kakati ¹⁷⁴, I. Kalaitzidou ⁵⁶,
 C.W. Kalderon ³⁰, N.J. Kang ¹⁴⁰, D. Kar ^{34g}, K. Karava ¹³⁰, M.J. Kareem ^{160b}, E. Karentzos ²⁵,

O. Karkout ¹¹⁸, S.N. Karpov ⁴⁰, Z.M. Karpova ⁴⁰, V. Kartvelishvili ⁹⁴, A.N. Karyukhin ³⁹, E. Kasimi ¹⁵⁷, J. Katzy ⁵⁰, S. Kaur ³⁵, K. Kawade ¹⁴⁵, M.P. Kawale ¹²⁴, C. Kawamoto ⁹⁰, T. Kawamoto ^{64a}, E.F. Kay ³⁷, F.I. Kaya ¹⁶², S. Kazakos ¹¹⁰, V.F. Kazanin ³⁹, Y. Ke ¹⁵⁰, J.M. Keaveney ^{34a}, R. Keeler ¹⁷⁰, G.V. Kehris ⁶³, J.S. Keller ³⁵, J.J. Kempster ¹⁵¹, O. Kepka ¹³⁵, J. Kerr ^{160b}, B.P. Kerridge ¹³⁸, S. Kersten ¹⁷⁶, B.P. Kerševan ⁹⁶, L. Keszezhova ^{29a}, S. Ketabchi Haghghat ¹⁵⁹, R.A. Khan ¹³³, A. Khanov ¹²⁵, A.G. Kharlamov ³⁹, T. Kharlamova ³⁹, E.E. Khoda ¹⁴³, M. Kholodenko ^{134a}, T.J. Khoo ¹⁹, G. Khoriauli ¹⁷¹, J. Khubua ^{154b,*}, Y.A.R. Khwaira ¹³¹, B. Kibirige^{34g}, D. Kim ⁶, D.W. Kim ^{49a,49b}, Y.K. Kim ⁴¹, N. Kimura ⁹⁹, M.K. Kingston ⁵⁷, A. Kirchhoff ⁵⁷, C. Kirfel ²⁵, F. Kirfel ²⁵, J. Kirk ¹³⁸, A.E. Kiryunin ¹¹³, S. Kita ¹⁶¹, C. Kitsaki ¹⁰, O. Kivernyk ²⁵, M. Klassen ¹⁶², C. Klein ³⁵, L. Klein ¹⁷¹, M.H. Klein ⁴⁶, S.B. Klein ⁵⁸, U. Klein ⁹⁵, A. Klimentov ³⁰, T. Klioutchnikova ³⁷, P. Kluit ¹¹⁸, S. Kluth ¹¹³, E. Kneringer ⁸¹, T.M. Knight ¹⁵⁹, A. Knue ⁵¹, D. Kobylanskii ¹⁷⁴, S.F. Koch ¹³⁰, M. Kocian ¹⁴⁸, P. Kodyš ¹³⁷, D.M. Koeck ¹²⁷, P.T. Koenig ²⁵, T. Koffas ³⁵, O. Kolay ⁵², I. Koletsou ⁴, T. Komarek ⁸⁹, K. Köneke ⁵⁷, A.X.Y. Kong ¹, T. Kono ¹²², N. Konstantinidis ⁹⁹, P. Kontaxakis ⁵⁸, B. Konya ¹⁰¹, R. Kopeliansky ⁴³, S. Koperny ^{88a}, K. Korcyl ⁸⁹, K. Kordas ^{157,e}, A. Korn ⁹⁹, S. Korn ⁵⁷, I. Korolkov ¹³, N. Korotkova ³⁹, B. Kortman ¹¹⁸, O. Kortner ¹¹³, S. Kortner ¹¹³, W.H. Kostecka ¹¹⁹, V.V. Kostyukhin ¹⁴⁶, A. Kotsokechagia ³⁷, A. Kotwal ⁵³, A. Koulouris ³⁷, A. Kourkoumeli-Charalampidi ^{75a,75b}, C. Kourkoumelis ⁹, E. Kourlitis ^{113,ad}, O. Kovanda ¹²⁷, R. Kowalewski ¹⁷⁰, W. Kozanecki ¹²⁷, A.S. Kozhin ³⁹, V.A. Kramarenko ³⁹, G. Kramberger ⁹⁶, P. Kramer ²⁵, M.W. Krasny ¹³¹, A. Krasznahorkay ³⁷, A.C. Kraus ¹¹⁹, J.W. Kraus ¹⁷⁶, J.A. Kremer ⁵⁰, T. Kresse ⁵², L. Kretschmann ¹⁷⁶, J. Kretschmar ⁹⁵, K. Kreul ¹⁹, P. Krieger ¹⁵⁹, K. Krizka ²¹, K. Kroeninger ⁵¹, H. Kroha ¹¹³, J. Kroll ¹³⁵, J. Kroll ¹³², K.S. Krowpman ¹¹⁰, U. Kruchonak ⁴⁰, H. Krüger ²⁵, N. Krumnack⁸³, M.C. Kruse ⁵³, O. Kuchinskaja ³⁹, S. Kuday ^{3a}, S. Kuehn ³⁷, R. Kuesters ⁵⁶, T. Kuhl ⁵⁰, V. Kukhtin ⁴⁰, Y. Kulchitsky ⁴⁰, S. Kuleshov ^{141d,141b}, M. Kumar ^{34g}, N. Kumari ⁵⁰, P. Kumari ^{160b}, A. Kupco ¹³⁵, T. Kupfer⁵¹, A. Kupich ³⁹, O. Kuprash ⁵⁶, H. Kurashige ⁸⁷, L.L. Kurchaninov ^{160a}, O. Kurdysh ⁶⁸, Y.A. Kurochkin ³⁸, A. Kurova ³⁹, M. Kuze ¹⁴², A.K. Kvam ¹⁰⁶, J. Kvita ¹²⁶, T. Kwan ¹⁰⁷, N.G. Kyriacou ¹⁰⁹, L.A.O. Laatu ¹⁰⁵, C. Lacasta ¹⁶⁸, F. Lacava ^{77a,77b}, H. Lacker ¹⁹, D. Lacour ¹³¹, N.N. Lad ⁹⁹, E. Ladygin ⁴⁰, A. Lafarge ⁴², B. Laforge ¹³¹, T. Lagouri ¹⁷⁷, F.Z. Lahbabi ^{36a}, S. Lai ⁵⁷, J.E. Lambert ¹⁷⁰, S. Lammers ⁷⁰, W. Lampl ⁷, C. Lampoudis ^{157,e}, G. Lamprinoudis ¹⁰³, A.N. Lancaster ¹¹⁹, E. Lançon ³⁰, U. Landgraf ⁵⁶, M.P.J. Landon ⁹⁷, V.S. Lang ⁵⁶, O.K.B. Langrekken ¹²⁹, A.J. Lankford ¹⁶³, F. Lanni ³⁷, K. Lantzsch ²⁵, A. Lanza ^{75a}, M. Lanzac Berrocal ¹⁶⁸, J.F. Laporte ¹³⁹, T. Lari ^{73a}, F. Lasagni Manghi ^{24b}, M. Lassnig ³⁷, V. Latonova ¹³⁵, S.D. Lawlor ¹⁴⁴, Z. Lawrence ¹⁰⁴, R. Lazaridou¹⁷², M. Lazzaroni ^{73a,73b}, H.D.M. Le ¹¹⁰, E.M. Le Boulicaut ¹⁷⁷, L.T. Le Pottier ^{18a}, B. Leban ^{24b,24a}, A. Lebedev ⁸³, M. LeBlanc ¹⁰⁴, F. Ledroit-Guillon ⁶², S.C. Lee ¹⁵³, S. Lee ^{49a,49b}, T.F. Lee ⁹⁵, L.L. Leeuw ^{34c,ai}, M. Lefebvre ¹⁷⁰, C. Leggett ^{18a}, G. Lehmann Miotto ³⁷, M. Leigh ⁵⁸, W.A. Leight ¹⁰⁶, W. Leinonen ¹¹⁷, A. Leisos ^{157,t}, M.A.L. Leite ^{85c}, C.E. Leitgeb ¹⁹, R. Leitner ¹³⁷, K.J.C. Leney ⁴⁶, T. Lenz ²⁵, S. Leone ^{76a}, C. Leonidopoulos ⁵⁴, A. Leopold ¹⁴⁹, R. Les ¹¹⁰, C.G. Lester ³³, M. Levchenko ³⁹, J. Levêque ⁴, L.J. Levinson ¹⁷⁴, G. Levrini ^{24b,24a}, M.P. Lewicki ⁸⁹, C. Lewis ¹⁴³, D.J. Lewis ⁴, L. Lewitt ¹⁴⁴, A. Li ³⁰, B. Li ^{64b}, C. Li¹⁰⁹, C-Q. Li ¹¹³, H. Li ^{64a}, H. Li ^{64b}, H. Li ^{115a}, H. Li ¹⁵, H. Li ^{64b}, J. Li ^{64c}, K. Li ¹⁴, L. Li ^{64c}, M. Li ^{14,115c}, R. Li ¹⁷⁷, S. Li ^{14,115c}, S. Li ^{64d,64c,d}, T. Li ⁵, X. Li ¹⁰⁷, Z. Li ¹⁵⁸, Z. Li ^{14,115c}, Z. Li ^{64a}, S. Liang ^{14,115c}, Z. Liang ¹⁴, M. Liberatore ¹³⁹, B. Liberti ^{78a}, K. Lie ^{66c}, J. Lieber Marin ^{85e}, H. Lien ⁷⁰, H. Lin ¹⁰⁹, K. Lin ¹¹⁰, L. Linden ¹¹², R.E. Lindley ⁷, J.H. Lindon ², J. Ling ⁶³, E. Lipeles ¹³², A. Lipniacka ¹⁷, A. Lister ¹⁶⁹, J.D. Little ⁷⁰, B. Liu ¹⁴, B.X. Liu ^{115b}, D. Liu ^{64d,64c},




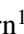

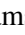
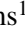

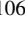
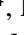
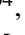



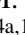


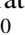

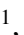






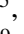
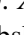

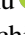
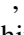

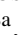
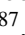




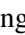



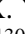
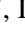
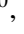

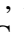

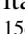

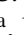

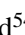
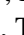



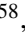

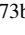
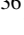
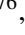


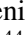
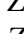
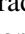



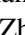

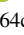


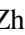

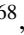

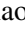



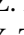


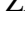

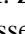
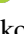
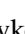
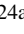









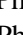
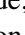


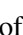
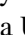
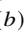

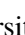
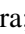







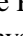
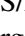



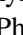
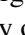

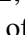

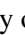
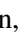


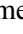
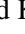
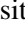

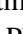

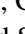

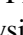





E.H.L. Liu ²¹, J.B. Liu ^{64a}, J.K.K. Liu ³³, K. Liu ^{64d}, K. Liu ^{64d,64c}, M. Liu ^{64a}, M.Y. Liu ^{64a}, P. Liu ¹⁴, Q. Liu ^{64d,143,64c}, X. Liu ^{64a}, X. Liu ^{64b}, Y. Liu ^{115b,115c}, Y.L. Liu ^{64b}, Y.W. Liu ^{64a}, S.L. Lloyd ⁹⁷, E.M. Lobodzinska ⁵⁰, P. Loch ⁷, E. Lodhi ¹⁵⁹, T. Lohse ¹⁹, K. Lohwasser ¹⁴⁴, E. Loiacono ⁵⁰, J.D. Lomas ²¹, J.D. Long ⁴³, I. Longarini ¹⁶³, R. Longo ¹⁶⁷, I. Lopez Paz ⁶⁹, A. Lopez Solis ⁵⁰, N.A. Lopez-canelas ⁷, N. Lorenzo Martinez ⁴, A.M. Lory ¹¹², M. Losada ^{120a}, G. Lösckce Centeno ¹⁵¹, O. Loseva ³⁹, X. Lou ^{49a,49b}, X. Lou ^{14,115c}, A. Lounis ⁶⁸, P.A. Love ⁹⁴, G. Lu ^{14,115c}, M. Lu ⁶⁸, S. Lu ¹³², Y.J. Lu ¹⁵³, H.J. Lubatti ¹⁴³, C. Luci ^{77a,77b}, F.L. Lucio Alves ^{115a}, F. Luehring ⁷⁰, O. Lukianchuk ⁶⁸, B.S. Lunday ¹³², O. Lundberg ¹⁴⁹, B. Lund-Jensen ^{149,*}, N.A. Luongo ⁶, M.S. Lutz ³⁷, A.B. Lux ²⁶, D. Lynn ³⁰, R. Lysak ¹³⁵, E. Lytken ¹⁰¹, V. Lyubushkin ⁴⁰, T. Lyubushkina ⁴⁰, M.M. Lyukova ¹⁵⁰, M.Firdaus M. Soberi ⁵⁴, H. Ma ³⁰, K. Ma ^{64a}, L.L. Ma ^{64b}, W. Ma ^{64a}, Y. Ma ¹²⁵, J.C. MacDonald ¹⁰³, P.C. Machado De Abreu Farias ^{85e}, R. Madar ⁴², T. Madula ⁹⁹, J. Maeda ⁸⁷, T. Maeno ³⁰, P.T. Mafa ^{34c,k}, H. Maguire ¹⁴⁴, V. Maiboroda ¹³⁹, A. Maio ^{134a,134b,134d}, K. Maj ^{88a}, O. Majersky ⁵⁰, S. Majewski ¹²⁷, N. Makovec ⁶⁸, V. Maksimovic ¹⁶, B. Malaescu ¹³¹, Pa. Malecki ⁸⁹, V.P. Maleev ³⁹, F. Malek ^{62,o}, M. Mali ⁹⁶, D. Malito ⁹⁸, U. Mallik ^{82,*}, S. Maltezos ¹⁰, S. Malyukov ⁴⁰, J. Mamuzic ¹³, G. Mancini ⁵⁵, M.N. Mancini ²⁷, G. Manco ^{75a,75b}, J.P. Mandalia ⁹⁷, S.S. Mandarray ¹⁵¹, I. Mandić ⁹⁶, L. Manhaes de Andrade Filho ^{85a}, I.M. Maniatis ¹⁷⁴, J. Manjarres Ramos ⁹², D.C. Mankad ¹⁷⁴, A. Mann ¹¹², S. Manzoni ³⁷, L. Mao ^{64c}, X. Mapekula ^{34c}, A. Marantis ^{157,t}, G. Marchiori ⁵, M. Marcisovsky ¹³⁵, C. Marcon ^{73a}, M. Marinescu ²¹, S. Marium ⁵⁰, M. Marjanovic ¹²⁴, A. Markhoos ⁵⁶, M. Markovitch ⁶⁸, M.K. Maroun ¹⁰⁶, E.J. Marshall ⁹⁴, Z. Marshall ^{18a}, S. Marti-Garcia ¹⁶⁸, J. Martin ⁹⁹, T.A. Martin ¹³⁸, V.J. Martin ⁵⁴, B. Martin dit Latour ¹⁷, L. Martinelli ^{77a,77b}, M. Martinez ^{13,w}, P. Martinez Agullo ¹⁶⁸, V.I. Martinez Outschoorn ¹⁰⁶, P. Martinez Suarez ¹³, S. Martin-Haugh ¹³⁸, G. Martinovicova ¹³⁷, V.S. Martoiu ^{28b}, A.C. Martyniuk ⁹⁹, A. Marzin ³⁷, D. Mascione ^{80a,80b}, L. Masetti ¹⁰³, J. Masik ¹⁰⁴, A.L. Maslennikov ³⁹, S.L. Mason ⁴³, P. Massarotti ^{74a,74b}, P. Mastrandrea ^{76a,76b}, A. Mastroberardino ^{45b,45a}, T. Masubuchi ¹²⁸, T.T. Mathew ¹²⁷, T. Mathisen ¹⁶⁶, J. Matousek ¹³⁷, D.M. Mattern ⁵¹, J. Maurer ^{28b}, T. Maurin ⁶¹, A.J. Maury ⁶⁸, B. Maček ⁹⁶, D.A. Maximov ³⁹, A.E. May ¹⁰⁴, R. Mazini ^{34g}, I. Maznas ¹¹⁹, M. Mazza ¹¹⁰, S.M. Mazza ¹⁴⁰, E. Mazzeo ^{73a,73b}, J.P. Mc Gowan ¹⁷⁰, S.P. Mc Kee ¹⁰⁹, C.A. Mc Lean ⁶, C.C. McCracken ¹⁶⁹, E.F. McDonald ¹⁰⁸, A.E. McDougall ¹¹⁸, L.F. Mcelhinney ⁹⁴, J.A. Mcfayden ¹⁵¹, R.P. McGovern ¹³², R.P. Mckenzie ^{34g}, T.C. Mclachlan ⁵⁰, D.J. McLaughlin ⁹⁹, S.J. McMahon ¹³⁸, C.M. Mcpartland ⁹⁵, R.A. McPherson ^{170,aa}, S. Mehlhase ¹¹², A. Mehta ⁹⁵, D. Melini ¹⁶⁸, B.R. Mellado Garcia ^{34g}, A.H. Melo ⁵⁷, F. Meloni ⁵⁰, A.M. Mendes Jacques Da Costa ¹⁰⁴, H.Y. Meng ¹⁵⁹, L. Meng ⁹⁴, S. Menke ¹¹³, M. Mentink ³⁷, E. Meoni ^{45b,45a}, G. Mercado ¹¹⁹, S. Merianos ¹⁵⁷, C. Merlassino ^{71a,71c}, L. Merola ^{74a,74b}, C. Meroni ^{73a,73b}, J. Metcalfe ⁶, A.S. Mete ⁶, E. Meuser ¹⁰³, C. Meyer ⁷⁰, J-P. Meyer ¹³⁹, R.P. Middleton ¹³⁸, L. Mijović ⁵⁴, G. Mikenberg ¹⁷⁴, M. Mikestikova ¹³⁵, M. Mikuž ⁹⁶, H. Mildner ¹⁰³, A. Milic ³⁷, D.W. Miller ⁴¹, E.H. Miller ¹⁴⁸, L.S. Miller ³⁵, A. Milov ¹⁷⁴, D.A. Milstead ^{49a,49b}, T. Min ^{115a}, A.A. Minaenko ³⁹, I.A. Minashvili ^{154b}, A.I. Mincer ¹²¹, B. Mindur ^{88a}, M. Mineev ⁴⁰, Y. Mino ⁹⁰, L.M. Mir ¹³, M. Miralles Lopez ⁶¹, M. Mironova ^{18a}, M.C. Missio ¹¹⁷, A. Mitra ¹⁷², V.A. Mitsou ¹⁶⁸, Y. Mitsumori ¹¹⁴, O. Miu ¹⁵⁹, P.S. Miyagawa ⁹⁷, T. Mkrtchyan ^{65a}, M. Mlinarevic ⁹⁹, T. Mlinarevic ⁹⁹, M. Mlynarikova ³⁷, S. Mobius ²⁰, P. Mogg ¹¹², M.H. Mohamed Farook ¹¹⁶, A.F. Mohammed ^{14,115c}, S. Mohapatra ⁴³, G. Mokgatitwane ^{34g}, L. Moleri ¹⁷⁴, B. Mondal ¹⁴⁶, S. Mondal ¹³⁶, K. Mönig ⁵⁰, E. Monnier ¹⁰⁵, L. Monsonis Romero ¹⁶⁸, J. Montejo Berlingen ¹³, A. Montella ^{49a,49b}, M. Montella ¹²³, F. Montekali ^{79a,79b}, F. Monticelli ⁹³, S. Monzani ^{71a,71c}, A. Morancho Tarda ⁴⁴, N. Morange ⁶⁸, A.L. Moreira De Carvalho ⁵⁰, M. Moreno Llácer ¹⁶⁸, C. Moreno Martinez ⁵⁸,

J.M. Moreno Perez^{23b}, P. Morettini^{59b}, S. Morgenstern³⁷, M. Morii⁶³, M. Morinaga¹⁵⁸, M. Moritsu⁹¹, F. Morodei^{77a,77b}, P. Moschovakos³⁷, B. Moser¹³⁰, M. Mosidze^{154b}, T. Moskalets⁴⁶, P. Moskvitina¹¹⁷, J. Moss^{32,1}, P. Moszkowicz^{88a}, A. Moussa^{36d}, Y. Moyal¹⁷⁴, E.J.W. Moyse¹⁰⁶, O. Mtintsilana^{34g}, S. Muanza¹⁰⁵, J. Mueller¹³³, D. Muenstermann⁹⁴, R. Müller³⁷, G.A. Mullier¹⁶⁶, A.J. Mullin³³, J.J. Mullin¹³², A.E. Mulski⁶³, D.P. Mungo¹⁵⁹, D. Munoz Perez¹⁶⁸, F.J. Munoz Sanchez¹⁰⁴, M. Murin¹⁰⁴, W.J. Murray^{172,138}, M. Muškinja⁹⁶, C. Mwewa³⁰, A.G. Myagkov^{39,a}, A.J. Myers⁸, G. Myers¹⁰⁹, M. Myska¹³⁶, B.P. Nachman^{18a}, K. Nagai¹³⁰, K. Nagano⁸⁶, R. Nagasaka¹⁵⁸, J.L. Nagle^{30,ah}, E. Nagy¹⁰⁵, A.M. Nairz³⁷, Y. Nakahama⁸⁶, K. Nakamura⁸⁶, K. Nakkalil⁵, H. Nanjo¹²⁸, E.A. Narayanan⁴⁶, Y. Narukawa¹⁵⁸, I. Naryshkin³⁹, L. Nasella^{73a,73b}, S. Nasri^{120b}, C. Nass²⁵, G. Navarro^{23a}, J. Navarro-Gonzalez¹⁶⁸, A. Nayaz¹⁹, P.Y. Nechaeva³⁹, S. Nechaeva^{24b,24a}, F. Nechansky¹³⁵, L. Nedic¹³⁰, T.J. Neep²¹, A. Negri^{75a,75b}, M. Negrini^{24b}, C. Nellist¹¹⁸, C. Nelson¹⁰⁷, K. Nelson¹⁰⁹, S. Nemecek¹³⁵, M. Nessi^{37,h}, M.S. Neubauer¹⁶⁷, F. Neuhaus¹⁰³, J. Neundorff⁵⁰, J. Newell⁹⁵, P.R. Newman²¹, C.W. Ng¹³³, Y.W.Y. Ng⁵⁰, B. Ngair^{120a}, H.D.N. Nguyen¹¹¹, R.B. Nickerson¹³⁰, R. Nicolaidou¹³⁹, J. Nielsen¹⁴⁰, M. Niemeyer⁵⁷, J. Niermann³⁷, N. Nikiforou³⁷, V. Nikolaenko^{39,a}, I. Nikolic-Audit¹³¹, K. Nikolopoulos²¹, P. Nilsson³⁰, I. Ninca⁵⁰, G. Ninio¹⁵⁶, A. Nisati^{77a}, N. Nishu², R. Nisius¹¹³, N. Nitika^{71a,71c}, J-E. Nitschke⁵², E.K. Nkadimeng^{34g}, T. Nobe¹⁵⁸, T. Nommensen¹⁵², M.B. Norfolk¹⁴⁴, B.J. Norman³⁵, M. Noury^{36a}, J. Novak⁹⁶, T. Novak⁹⁶, L. Novotny¹³⁶, R. Novotny¹¹⁶, L. Nozka¹²⁶, K. Ntekas¹⁶³, N.M.J. Nunes De Moura Junior^{85b}, J. Ocariz¹³¹, A. Ochi⁸⁷, I. Ochoa^{134a}, S. Oerdek^{50,x}, J.T. Offermann⁴¹, A. Ogrodnik¹³⁷, A. Oh¹⁰⁴, C.C. Ohm¹⁴⁹, H. Oide⁸⁶, R. Oishi¹⁵⁸, M.L. Ojeda³⁷, Y. Okumura¹⁵⁸, L.F. Oleiro Seabra^{134a}, I. Oleksiyuk⁵⁸, S.A. Olivares Pino^{141d}, G. Oliveira Correa¹³, D. Oliveira Damazio³⁰, J.L. Oliver¹⁶³, Ö.O. Öncel⁵⁶, A.P. O'Neill²⁰, A. Onofre^{134a,134e}, P.U.E. Onyisi¹¹, M.J. Oreglia⁴¹, D. Orestano^{79a,79b}, N. Orlando¹³, R.S. Orr¹⁵⁹, L.M. Osojnak¹³², Y. Osumi¹¹⁴, G. Otero y Garzon³¹, H. Otono⁹¹, P.S. Ott^{65a}, G.J. Ottino^{18a}, M. Ouchrif^{36d}, F. Ould-Saada¹²⁹, T. Ovsiannikova¹⁴³, M. Owen⁶¹, R.E. Owen¹³⁸, V.E. Ozcan^{22a}, F. Ozturk⁸⁹, N. Ozturk⁸, S. Ozturk⁸⁴, H.A. Pacey¹³⁰, A. Pacheco Pages¹³, C. Padilla Aranda¹³, G. Padovano^{77a,77b}, S. Pagan Griso^{18a}, G. Palacino⁷⁰, A. Palazzo^{72a,72b}, J. Pampel²⁵, J. Pan¹⁷⁷, T. Pan^{66a}, D.K. Panchal¹¹, C.E. Pandini¹¹⁸, J.G. Panduro Vazquez¹³⁸, H.D. Pandya¹, H. Pang¹⁵, P. Pani⁵⁰, G. Panizzo^{71a,71c}, L. Panwar¹³¹, L. Paolozzi⁵⁸, S. Parajuli¹⁶⁷, A. Paramonov⁶, C. Paraskevopoulos⁵⁵, D. Paredes Hernandez^{66b}, A. Pareti^{75a,75b}, K.R. Park⁴³, T.H. Park¹⁵⁹, M.A. Parker³³, F. Parodi^{59b,59a}, V.A. Parrish⁵⁴, J.A. Parsons⁴³, U. Parzefall⁵⁶, B. Pascual Dias¹¹¹, L. Pascual Dominguez¹⁰², E. Pasqualucci^{77a}, S. Passaggio^{59b}, F. Pastore⁹⁸, P. Patel⁸⁹, U.M. Patel⁵³, J.R. Pater¹⁰⁴, T. Pauly³⁷, F. Pauwels¹³⁷, C.I. Pazos¹⁶², M. Pedersen¹²⁹, R. Pedro^{134a}, S.V. Peleganchuk³⁹, O. Penc³⁷, E.A. Pender⁵⁴, S. Peng¹⁵, G.D. Penn¹⁷⁷, K.E. Pensi¹¹², M. Penzin³⁹, B.S. Peralva^{85d}, A.P. Pereira Peixoto¹⁴³, L. Pereira Sanchez¹⁴⁸, D.V. Perepelitsa^{30,ah}, G. Perera¹⁰⁶, E. Perez Codina^{160a}, M. Perganti¹⁰, H. Pernegger³⁷, S. Perrella^{77a,77b}, O. Perrin⁴², K. Peters⁵⁰, R.F.Y. Peters¹⁰⁴, B.A. Petersen³⁷, T.C. Petersen⁴⁴, E. Petit¹⁰⁵, V. Petousis¹³⁶, C. Petridou^{157,e}, T. Petru¹³⁷, A. Petrukhin¹⁴⁶, M. Pettee^{18a}, A. Petukhov⁸⁴, K. Petukhova³⁷, R. Pezoa^{141f}, L. Pezzotti³⁷, G. Pezzullo¹⁷⁷, A.J. Pflieger³⁷, T.M. Pham¹⁷⁵, T. Pham¹⁰⁸, P.W. Phillips¹³⁸, G. Piacquadio¹⁵⁰, E. Pianori^{18a}, F. Piazza¹²⁷, R. Piegaia³¹, D. Pietreanu^{28b}, A.D. Pilkington¹⁰⁴, M. Pinamonti^{71a,71c}, J.L. Pinfold², B.C. Pinheiro Pereira^{134a}, J. Pinol Bel¹³, A.E. Pinto Pinoargote^{139,139}, L. Pintucci^{71a,71c}, K.M. Piper¹⁵¹, A. Pirttikoski⁵⁸, D.A. Pizzi³⁵, L. Pizzimento^{66b}, A. Pizzini¹¹⁸, M.-A. Pleier³⁰, V. Pleskot¹³⁷, E. Plotnikova⁴⁰, G. Poddar⁹⁷, R. Poettgen¹⁰¹,

L. Poggioli ¹³¹, S. Polacek ¹³⁷, G. Polesello ^{75a}, A. Poley ^{147,160a}, A. Polini ^{24b}, C.S. Pollard ¹⁷²,
 Z.B. Pollock ¹²³, E. Pompa Pacchi ¹²⁴, N.I. Pond ⁹⁹, D. Ponomarenko ⁷⁰, L. Pontecorvo ³⁷,
 S. Popa ^{28a}, G.A. Popeneciu ^{28d}, A. Poreba ³⁷, D.M. Portillo Quintero ^{160a}, S. Pospisil ¹³⁶,
 M.A. Postill ¹⁴⁴, P. Postolache ^{28c}, K. Potamianos ¹⁷², P.A. Potepa ^{88a}, I.N. Potrap ⁴⁰,
 C.J. Potter ³³, H. Potti ¹⁵², J. Poveda ¹⁶⁸, M.E. Pozo Astigarraga ³⁷, A. Prades Ibanez ^{78a,78b},
 J. Pretel ¹⁷⁰, D. Price ¹⁰⁴, M. Primavera ^{72a}, L. Primomo ^{71a,71c}, M.A. Principe Martin ¹⁰²,
 R. Privara ¹²⁶, T. Procter ⁶¹, M.L. Proffitt ¹⁴³, N. Proklova ¹³², K. Prokofiev ^{66c}, G. Proto ¹¹³,
 J. Proudfoot ⁶, M. Przybycien ^{88a}, W.W. Przygoda ^{88b}, A. Psallidas ⁴⁸, J.E. Puddefoot ¹⁴⁴,
 D. Pudzha ⁵⁶, D. Pyatiizbyantseva ³⁹, J. Qian ¹⁰⁹, R. Qian ¹¹⁰, D. Qichen ¹⁰⁴, Y. Qin ¹³,
 T. Qiu ⁵⁴, A. Quadt ⁵⁷, M. Queitsch-Maitland ¹⁰⁴, G. Quetant ⁵⁸, R.P. Quinn ¹⁶⁹,
 G. Rabanal Bolanos ⁶³, D. Rafanoharana ⁵⁶, F. Raffaelli ^{78a,78b}, F. Ragusa ^{73a,73b}, J.L. Rainbolt ⁴¹,
 J.A. Raine ⁵⁸, S. Rajagopalan ³⁰, E. Ramakoti ³⁹, L. Rambelli ^{59b,59a}, I.A. Ramirez-Berend ³⁵,
 K. Ran ^{50,115c}, D.S. Rankin ¹³², N.P. Rapheeha ^{34g}, H. Rasheed ^{28b}, V. Raskina ¹³¹,
 D.F. Rassloff ^{65a}, A. Rastogi ^{18a}, S. Rave ¹⁰³, S. Ravera ^{59b,59a}, B. Ravina ⁵⁷, I. Ravinovich ¹⁷⁴,
 M. Raymond ³⁷, A.L. Read ¹²⁹, N.P. Readioff ¹⁴⁴, D.M. Rebuzzi ^{75a,75b}, G. Redlinger ³⁰,
 A.S. Reed ¹¹³, K. Reeves ²⁷, J.A. Reidelsturz ¹⁷⁶, D. Reikher ¹²⁷, A. Rej ⁵¹, C. Rembser ³⁷,
 H. Ren ^{64a}, M. Renda ^{28b}, F. Renner ⁵⁰, A.G. Rennie ¹⁶³, A.L. Rescia ⁵⁰, S. Resconi ^{73a},
 M. Ressegotti ^{59b,59a}, S. Rettie ³⁷, W.F. Rettie ³⁵, J.G. Reyes Rivera ¹¹⁰, E. Reynolds ^{18a},
 O.L. Rezanova ³⁹, P. Reznicek ¹³⁷, H. Riani ^{36d}, N. Ribaric ⁵³, E. Ricci ^{80a,80b}, R. Richter ¹¹³,
 S. Richter ^{49a,49b}, E. Richter-Was ^{88b}, M. Ridel ¹³¹, S. Ridouani ^{36d}, P. Rieck ¹²¹, P. Riedler ³⁷,
 E.M. Riefel ^{49a,49b}, J.O. Rieger ¹¹⁸, M. Rijssenbeek ¹⁵⁰, M. Rimoldi ³⁷, L. Rinaldi ^{24b,24a},
 P. Rincke ^{57,166}, T.T. Rinn ³⁰, M.P. Rinnagel ¹¹², G. Ripellino ¹⁶⁶, I. Riu ¹³,
 J.C. Rivera Vergara ¹⁷⁰, F. Rizatdinova ¹²⁵, E. Rizvi ⁹⁷, B.R. Roberts ^{18a}, S.S. Roberts ¹⁴⁰,
 S.H. Robertson ^{107,aa}, D. Robinson ³³, M. Robles Manzano ¹⁰³, A. Robson ⁶¹, A. Rocchi ^{78a,78b},
 C. Roda ^{76a,76b}, S. Rodriguez Bosca ³⁷, Y. Rodriguez Garcia ^{23a}, A.M. Rodríguez Vera ¹¹⁹,
 S. Roe ³⁷, J.T. Roemer ³⁷, O. Røhne ¹²⁹, R.A. Rojas ¹⁰⁶, C.P.A. Roland ¹³¹, J. Roloff ³⁰,
 A. Romaniouk ⁸¹, E. Romano ^{75a,75b}, M. Romano ^{24b}, A.C. Romero Hernandez ¹⁶⁷,
 N. Rompotis ⁹⁵, L. Roos ¹³¹, S. Rosati ^{77a}, B.J. Rosser ⁴¹, E. Rossi ¹³⁰, E. Rossi ^{74a,74b},
 L.P. Rossi ⁶³, L. Rossini ⁵⁶, R. Rosten ¹²³, M. Rotaru ^{28b}, B. Rottler ⁵⁶, C. Rougier ⁹²,
 D. Rousseau ⁶⁸, D. Rouso ⁵⁰, A. Roy ¹⁶⁷, S. Roy-Garand ¹⁵⁹, A. Rozanov ¹⁰⁵,
 Z.M.A. Rozario ⁶¹, Y. Rozen ¹⁵⁵, A. Rubio Jimenez ¹⁶⁸, V.H. Ruelas Rivera ¹⁹, T.A. Ruggeri ¹,
 A. Ruggiero ¹³⁰, A. Ruiz-Martinez ¹⁶⁸, A. Rummler ³⁷, Z. Rurikova ⁵⁶, N.A. Rusakovich ⁴⁰,
 H.L. Russell ¹⁷⁰, G. Russo ^{77a,77b}, J.P. Rutherford ⁷, S. Rutherford Colmenares ³³, M. Rybar ¹³⁷,
 E.B. Rye ¹²⁹, A. Ryzhov ⁴⁶, J.A. Sabater Iglesias ⁵⁸, H.F.W. Sadrozinski ¹⁴⁰, F. Safai Tehrani ^{77a},
 B. Safarzadeh Samani ¹³⁸, S. Saha ¹, M. Sahinsoy ⁸⁴, A. Saibel ¹⁶⁸, M. Saimpert ¹³⁹,
 M. Saito ¹⁵⁸, T. Saito ¹⁵⁸, A. Sala ^{73a,73b}, D. Salamani ³⁷, A. Salnikov ¹⁴⁸, J. Salt ¹⁶⁸,
 A. Salvador Salas ¹⁵⁶, D. Salvatore ^{45b,45a}, F. Salvatore ¹⁵¹, A. Salzburger ³⁷, D. Sammel ⁵⁶,
 E. Sampson ⁹⁴, D. Sampsonidis ^{157,e}, D. Sampsonidou ¹²⁷, J. Sánchez ¹⁶⁸,
 V. Sanchez Sebastian ¹⁶⁸, H. Sandaker ¹²⁹, C.O. Sander ⁵⁰, J.A. Sandesara ¹⁰⁶, M. Sandhoff ¹⁷⁶,
 C. Sandoval ^{23b}, L. Sanfilippo ^{65a}, D.P.C. Sankey ¹³⁸, T. Sano ⁹⁰, A. Sansoni ⁵⁵, L. Santi ^{37,77b},
 C. Santoni ⁴², H. Santos ^{134a,134b}, A. Santra ¹⁷⁴, E. Sanzani ^{24b,24a}, K.A. Saoucha ¹⁶⁵,
 J.G. Saraiva ^{134a,134d}, J. Sardain ⁷, O. Sasaki ⁸⁶, K. Sato ¹⁶¹, C. Sauer ³⁷, E. Sauvan ⁴,
 P. Savard ^{159,af}, R. Sawada ¹⁵⁸, C. Sawyer ¹³⁸, L. Sawyer ¹⁰⁰, C. Sbarra ^{24b}, A. Sbrizzi ^{24b,24a},
 T. Scanlon ⁹⁹, J. Schaarschmidt ¹⁴³, U. Schäfer ¹⁰³, A.C. Schaffer ^{68,46}, D. Schaile ¹¹²,
 R.D. Schamberger ¹⁵⁰, C. Scharf ¹⁹, M.M. Schefer ²⁰, V.A. Schegelsky ³⁹, D. Scheirich ¹³⁷,
 M. Schernau ^{141e}, C. Scheulen ⁵⁸, C. Schiavi ^{59b,59a}, M. Schioppa ^{45b,45a}, B. Schlag ¹⁴⁸,
 S. Schlenker ³⁷, J. Schmeing ¹⁷⁶, M.A. Schmidt ¹⁷⁶, K. Schmieden ¹⁰³, C. Schmitt ¹⁰³,

N. Schmitt ¹⁰³, S. Schmitt ⁵⁰, L. Schoeffel ¹³⁹, A. Schoening ^{65b}, P.G. Scholer ³⁵, E. Schopf ¹³⁰,
 M. Schott ²⁵, J. Schovancova ³⁷, S. Schramm ⁵⁸, T. Schroer ⁵⁸, H-C. Schultz-Coulon ^{65a},
 M. Schumacher ⁵⁶, B.A. Schumm ¹⁴⁰, Ph. Schune ¹³⁹, H.R. Schwartz ¹⁴⁰, A. Schwartzman ¹⁴⁸,
 T.A. Schwarz ¹⁰⁹, Ph. Schwemling ¹³⁹, R. Schwienhorst ¹¹⁰, F.G. Sciacca ²⁰, A. Sciandra ³⁰,
 G. Sciolla ²⁷, F. Scuri ^{76a}, C.D. Sebastiani ⁹⁵, K. Sedlaczek ¹¹⁹, S.C. Seidel ¹¹⁶, A. Seiden ¹⁴⁰,
 B.D. Seidlitz ⁴³, C. Seitz ⁵⁰, J.M. Seixas ^{85b}, G. Sekhniaidze ^{74a}, L. Selem ⁶²,
 N. Semprini-Cesari ^{24b,24a}, A. Semushin ^{178,39}, D. Sengupta ⁵⁸, V. Senthilkumar ¹⁶⁸, L. Serin ⁶⁸,
 M. Sessa ^{78a,78b}, H. Severini ¹²⁴, F. Sforza ^{59b,59a}, A. Sfyrla ⁵⁸, Q. Sha ¹⁴, E. Shabalina ⁵⁷,
 A.H. Shah ³³, R. Shaheen ¹⁴⁹, J.D. Shahinian ¹³², D. Shaked Renous ¹⁷⁴, L.Y. Shan ¹⁴,
 M. Shapiro ^{18a}, A. Sharma ³⁷, A.S. Sharma ¹⁶⁹, P. Sharma ³⁰, P.B. Shatalov ³⁹, K. Shaw ¹⁵¹,
 S.M. Shaw ¹⁰⁴, Q. Shen ^{64c}, D.J. Sheppard ¹⁴⁷, P. Sherwood ⁹⁹, L. Shi ⁹⁹, X. Shi ¹⁴,
 S. Shimizu ⁸⁶, C.O. Shimmin ¹⁷⁷, I.P.J. Shipsey ^{130,*}, S. Shirabe ⁹¹, M. Shiyakova ^{40,y},
 M.J. Shochet ⁴¹, D.R. Shope ¹²⁹, B. Shrestha ¹²⁴, S. Shrestha ^{123,aj}, I. Shreyber ³⁹,
 M.J. Shroff ¹⁷⁰, P. Sicho ¹³⁵, A.M. Sickles ¹⁶⁷, E. Sideras Haddad ^{34g,164}, A.C. Sidley ¹¹⁸,
 A. Sidoti ^{24b}, F. Siegert ⁵², Dj. Sijacki ¹⁶, F. Sili ⁹³, J.M. Silva ⁵⁴, I. Silva Ferreira ^{85b},
 M.V. Silva Oliveira ³⁰, S.B. Silverstein ^{49a}, S. Simion ⁶⁸, R. Simoniello ³⁷, E.L. Simpson ¹⁰⁴,
 H. Simpson ¹⁵¹, L.R. Simpson ¹⁰⁹, S. Simsek ⁸⁴, S. Sindhu ⁵⁷, P. Sinervo ¹⁵⁹, S. Singh ³⁰,
 S. Sinha ⁵⁰, S. Sinha ¹⁰⁴, M. Sioli ^{24b,24a}, I. Siral ³⁷, E. Sitnikova ⁵⁰, J. Sjölin ^{49a,49b},
 A. Skaf ⁵⁷, E. Skorda ²¹, P. Skubic ¹²⁴, M. Slawinska ⁸⁹, I. Slazyk ¹⁷, V. Smakhtin ¹⁷⁴,
 B.H. Smart ¹³⁸, S. Yu. Smirnov ³⁹, Y. Smirnov ³⁹, L.N. Smirnova ^{39,a}, O. Smirnova ¹⁰¹,
 A.C. Smith ⁴³, D.R. Smith ¹⁶³, E.A. Smith ⁴¹, J.L. Smith ¹⁰⁴, R. Smith ¹⁴⁸, H. Smitmanns ¹⁰³,
 M. Smizanska ⁹⁴, K. Smolek ¹³⁶, A.A. Snesarev ³⁹, H.L. Snoek ¹¹⁸, S. Snyder ³⁰,
 R. Sobie ^{170,aa}, A. Soffer ¹⁵⁶, C.A. Solans Sanchez ³⁷, E.Yu. Soldatov ³⁹, U. Soldevila ¹⁶⁸,
 A.A. Solodkov ³⁹, S. Solomon ²⁷, A. Soloshenko ⁴⁰, K. Solovieva ⁵⁶, O.V. Solovyanov ⁴²,
 P. Sommer ⁵², A. Sonay ¹³, W.Y. Song ^{160b}, A. Sopczak ¹³⁶, A.L. Sopio ⁵⁴, F. Sopkova ^{29b},
 J.D. Sorenson ¹¹⁶, I.R. Sotarriva Alvarez ¹⁴², V. Sothilingam ^{65a}, O.J. Soto Sandoval ^{141c,141b},
 S. Sottocornola ⁷⁰, R. Soualah ¹⁶⁵, Z. Soumami ^{36e}, D. South ⁵⁰, N. Soybelman ¹⁷⁴,
 S. Spagnolo ^{72a,72b}, M. Spalla ¹¹³, D. Sperlich ⁵⁶, G. Spigo ³⁷, B. Spisso ^{74a,74b}, D.P. Spiteri ⁶¹,
 M. Spousta ¹³⁷, E.J. Staats ³⁵, R. Stamen ^{65a}, A. Stampekis ²¹, E. Stanecka ⁸⁹,
 W. Stanek-Maslouska ⁵⁰, M.V. Stange ⁵², B. Stanislaus ^{18a}, M.M. Stanitzki ⁵⁰, B. Stapf ⁵⁰,
 E.A. Starchenko ³⁹, G.H. Stark ¹⁴⁰, J. Stark ⁹², P. Staroba ¹³⁵, P. Starovoitov ¹⁶⁵, S. Stärz ¹⁰⁷,
 R. Staszewski ⁸⁹, G. Stavropoulos ⁴⁸, A. Steff ³⁷, P. Steinberg ³⁰, B. Stelzer ^{147,160a},
 H.J. Stelzer ¹³³, O. Stelzer-Chilton ^{160a}, H. Stenzel ⁶⁰, T.J. Stevenson ¹⁵¹, G.A. Stewart ³⁷,
 J.R. Stewart ¹²⁵, M.C. Stockton ³⁷, G. Stoicea ^{28b}, M. Stolarski ^{134a}, S. Stonjek ¹¹³,
 A. Straessner ⁵², J. Strandberg ¹⁴⁹, S. Strandberg ^{49a,49b}, M. Stratmann ¹⁷⁶, M. Strauss ¹²⁴,
 T. Streblner ¹⁰⁵, P. Strizenec ^{29b}, R. Ströhmer ¹⁷¹, D.M. Strom ¹²⁷, R. Stroynowski ⁴⁶,
 A. Strubig ^{49a,49b}, S.A. Stucci ³⁰, B. Stugu ¹⁷, J. Stupak ¹²⁴, N.A. Styles ⁵⁰, D. Su ¹⁴⁸,
 S. Su ^{64a}, W. Su ^{64d}, X. Su ^{64a}, D. Suchy ^{29a}, K. Sugizaki ¹⁵⁸, V.V. Sulim ³⁹, M.J. Sullivan ⁹⁵,
 D.M.S. Sultan ¹³⁰, L. Sultanaliyeva ³⁹, S. Sultansoy ^{3b}, S. Sun ¹⁷⁵, W. Sun ¹⁴,
 O. Sunneborn Gudnadottir ¹⁶⁶, N. Sur ¹⁰⁵, M.R. Sutton ¹⁵¹, H. Suzuki ¹⁶¹, M. Svatos ¹³⁵,
 M. Swiatlowski ^{160a}, T. Swirski ¹⁷¹, I. Sykora ^{29a}, M. Sykora ¹³⁷, T. Sykora ¹³⁷, D. Ta ¹⁰³,
 K. Tackmann ^{50,x}, A. Taffard ¹⁶³, R. Tafirout ^{160a}, J.S. Tafoya Vargas ⁵⁸, Y. Takubo ⁸⁶,
 M. Talby ¹⁰⁵, A.A. Talyshev ³⁹, K.C. Tam ^{66b}, N.M. Tamir ¹⁵⁶, A. Tanaka ¹⁵⁸, J. Tanaka ¹⁵⁸,
 R. Tanaka ⁶⁸, M. Tanasini ¹⁵⁰, Z. Tao ¹⁶⁹, S. Tapia Araya ^{141f}, S. Tapprogge ¹⁰³,
 A. Tarek Abouelfadl Mohamed ¹¹⁰, S. Tarem ¹⁵⁵, K. Tariq ¹⁴, G. Tarna ^{28b}, G.F. Tartarelli ^{73a},
 M.J. Tartarin ⁹², P. Tas ¹³⁷, M. Tasevsky ¹³⁵, E. Tassi ^{45b,45a}, A.C. Tate ¹⁶⁷, G. Tateno ¹⁵⁸,
 Y. Tayalati ^{36e,z}, G.N. Taylor ¹⁰⁸, W. Taylor ^{160b}, P. Teixeira-Dias ⁹⁸, J.J. Teoh ¹⁵⁹,

K. Terashi ¹⁵⁸, J. Terron ¹⁰², S. Terzo ¹³, M. Testa ⁵⁵, R.J. Teuscher ^{159,aa}, A. Thaler ⁸¹,
 O. Theiner ⁵⁸, T. Thevenaux-Pelzer ¹⁰⁵, O. Thielmann ¹⁷⁶, D.W. Thomas ⁹⁸, J.P. Thomas ²¹,
 E.A. Thompson ^{18a}, P.D. Thompson ²¹, E. Thomson ¹³², R.E. Thornberry ⁴⁶, C. Tian ^{64a},
 Y. Tian ⁵⁸, V. Tikhomirov ^{39,a}, Yu.A. Tikhonov ³⁹, S. Timoshenko ³⁹, D. Timoshyn ¹³⁷,
 E.X.L. Ting ¹, P. Tipton ¹⁷⁷, A. Tishelman-Charny ³⁰, S.H. Tlou ^{34g}, K. Todome ¹⁴²,
 S. Todorova-Nova ¹³⁷, S. Todt ⁵², L. Toffolin ^{71a,71c}, M. Togawa ⁸⁶, J. Tojo ⁹¹, S. Tokár ^{29a},
 K. Tokushuku ⁸⁶, O. Toldaiev ⁷⁰, G. Tolkachev ¹⁰⁵, M. Tomoto ^{86,114}, L. Tompkins ^{148,n},
 E. Torrence ¹²⁷, H. Torres ⁹², E. Torró Pastor ¹⁶⁸, M. Toscani ³¹, C. Toscirri ⁴¹, M. Tost ¹¹,
 D.R. Tovey ¹⁴⁴, I.S. Trandafir ^{28b}, T. Trefzger ¹⁷¹, A. Tricoli ³⁰, I.M. Trigger ^{160a},
 S. Trincaz-Duvoid ¹³¹, D.A. Trischuk ²⁷, B. Trocmé ⁶², A. Tropina ⁴⁰, L. Truong ^{34c},
 M. Trzebinski ⁸⁹, A. Trzuppek ⁸⁹, F. Tsai ¹⁵⁰, M. Tsai ¹⁰⁹, A. Tsiamis ¹⁵⁷, P.V. Tsiarehka ⁴⁰,
 S. Tsigaridas ^{160a}, A. Tsigotis ^{157,t}, V. Tsiskaridze ¹⁵⁹, E.G. Tskhadadze ^{154a}, M. Tsopoulou ¹⁵⁷,
 Y. Tsujikawa ⁹⁰, I.I. Tsukerman ³⁹, V. Tsulaia ^{18a}, S. Tsuno ⁸⁶, K. Tsuru ¹²², D. Tsybychev ¹⁵⁰,
 Y. Tu ^{66b}, A. Tudorache ^{28b}, V. Tudorache ^{28b}, A.N. Tuna ⁶³, S. Turchikhin ^{59b,59a},
 I. Turk Cakir ^{3a}, R. Turra ^{73a}, T. Turtuvshin ⁴⁰, P.M. Tuts ⁴³, S. Tzamarias ^{157,e}, E. Tzovara ¹⁰³,
 F. Ukegawa ¹⁶¹, P.A. Ulloa Poblete ^{141c,141b}, E.N. Umaka ³⁰, G. Unal ³⁷, A. Undrus ³⁰,
 G. Unel ¹⁶³, J. Urban ^{29b}, P. Urrejola ^{141a}, G. Usai ⁸, R. Ushioda ¹⁴², M. Usman ¹¹¹,
 F. Ustuner ⁵⁴, Z. Uysal ⁸⁴, V. Vacek ¹³⁶, B. Vachon ¹⁰⁷, T. Vafeiadis ³⁷, A. Vaitkus ⁹⁹,
 C. Valderanis ¹¹², E. Valdes Santurio ^{49a,49b}, M. Valente ^{160a}, S. Valentinetti ^{24b,24a}, A. Valero ¹⁶⁸,
 E. Valiente Moreno ¹⁶⁸, A. Vallier ⁹², J.A. Valls Ferrer ¹⁶⁸, D.R. Van Arneman ¹¹⁸,
 T.R. Van Daalen ¹⁴³, A. Van Der Graaf ⁵¹, P. Van Gemmeren ⁶, M. Van Rijnbach ³⁷,
 S. Van Stroud ⁹⁹, I. Van Vulpen ¹¹⁸, P. Vana ¹³⁷, M. Vanadia ^{78a,78b}, U.M. Vande Voorde ¹⁴⁹,
 W. Vandelli ³⁷, E.R. Vandewall ¹²⁵, D. Vannicola ¹⁵⁶, L. Vannoli ⁵⁵, R. Vari ^{77a}, E.W. Varnes ⁷,
 C. Varni ^{18b}, D. Varouchas ⁶⁸, L. Varriale ¹⁶⁸, K.E. Varvell ¹⁵², M.E. Vasile ^{28b}, L. Vaslin ⁸⁶,
 A. Vasyukov ⁴⁰, L.M. Vaughan ¹²⁵, R. Vavricka ¹⁰³, T. Vazquez Schroeder ³⁷, J. Veatch ³²,
 V. Vecchio ¹⁰⁴, M.J. Veen ¹⁰⁶, I. Veliscek ³⁰, L.M. Veloce ¹⁵⁹, F. Veloso ^{134a,134c},
 S. Veneziano ^{77a}, A. Ventura ^{72a,72b}, S. Ventura Gonzalez ¹³⁹, A. Verbytskyi ¹¹³,
 M. Verducci ^{76a,76b}, C. Vergis ⁹⁷, M. Verissimo De Araujo ^{85b}, W. Verkerke ¹¹⁸,
 J.C. Vermeulen ¹¹⁸, C. Vernieri ¹⁴⁸, M. Vessella ¹⁶³, M.C. Vetterli ^{147,af}, A. Vgenopoulos ¹⁰³,
 N. Viaux Maira ^{141f}, T. Vickey ¹⁴⁴, O.E. Vickey Boeriu ¹⁴⁴, G.H.A. Viehhauser ¹³⁰, L. Vignani ^{65b},
 M. Vigl ¹¹³, M. Villa ^{24b,24a}, M. Villaplana Perez ¹⁶⁸, E.M. Villhauer ⁵⁴, E. Vilucchi ⁵⁵,
 M.G. Vincter ³⁵, A. Visibile ¹¹⁸, C. Vittori ³⁷, I. Vivarelli ^{24b,24a}, E. Voevodina ¹¹³, F. Vogel ¹¹²,
 J.C. Voigt ⁵², P. Vokac ¹³⁶, Yu. Volkotrub ^{88b}, E. Von Toerne ²⁵, B. Vormwald ³⁷,
 V. Vorobel ¹³⁷, K. Vorobev ³⁹, M. Vos ¹⁶⁸, K. Voss ¹⁴⁶, M. Vozak ¹¹⁸, L. Vozdecky ¹²⁴,
 N. Vranjes ¹⁶, M. Vranjes Milosavljevic ¹⁶, M. Vreeswijk ¹¹⁸, N.K. Vu ^{64d,64c}, R. Vuillermet ³⁷,
 O. Vujanovic ¹⁰³, I. Vukotic ⁴¹, I.K. Vyas ³⁵, S. Wada ¹⁶¹, C. Wagner ¹⁴⁸, J.M. Wagner ^{18a},
 W. Wagner ¹⁷⁶, S. Wahdan ¹⁷⁶, H. Wahlberg ⁹³, C.H. Waits ¹²⁴, J. Walder ¹³⁸, R. Walker ¹¹²,
 W. Walkowiak ¹⁴⁶, A. Wall ¹³², E.J. Wallin ¹⁰¹, T. Wamorkar ^{18a}, A.Z. Wang ¹⁴⁰, C. Wang ¹⁰³,
 C. Wang ¹¹, H. Wang ^{18a}, J. Wang ^{66c}, P. Wang ¹⁰⁴, P. Wang ⁹⁹, R. Wang ⁶³, R. Wang ⁶,
 S.M. Wang ¹⁵³, S. Wang ¹⁴, T. Wang ^{64a}, W.T. Wang ⁸², W. Wang ¹⁴, X. Wang ¹⁶⁷,
 X. Wang ^{64c}, Y. Wang ^{64d}, Y. Wang ^{115a}, Y. Wang ^{64a}, Z. Wang ¹⁰⁹, Z. Wang ^{64d,53,64c},
 Z. Wang ¹⁰⁹, A. Warburton ¹⁰⁷, R.J. Ward ²¹, N. Warrack ⁶¹, S. Waterhouse ⁹⁸, A.T. Watson ²¹,
 H. Watson ⁵⁴, M.F. Watson ²¹, E. Watton ^{61,138}, G. Watts ¹⁴³, B.M. Waugh ⁹⁹, J.M. Webb ⁵⁶,
 C. Weber ³⁰, H.A. Weber ¹⁹, M.S. Weber ²⁰, S.M. Weber ^{65a}, C. Wei ^{64a}, Y. Wei ⁵⁶,
 A.R. Weidberg ¹³⁰, E.J. Weik ¹²¹, J. Weingarten ⁵¹, C. Weiser ⁵⁶, C.J. Wells ⁵⁰, T. Wenaus ³⁰,
 B. Wendland ⁵¹, T. Wengler ³⁷, N.S. Wenke ¹¹³, N. Wermes ²⁵, M. Wessels ^{65a}, A.M. Wharton ⁹⁴,
 A.S. White ⁶³, A. White ⁸, M.J. White ¹, D. Whiteson ¹⁶³, L. Wickremasinghe ¹²⁸,

W. Wiedenmann , M. Wielers , C. Wigglesworth , D.J. Wilbern , H.G. Wilkens , J.J.H. Wilkinson , D.M. Williams , H.H. Williams , S. Williams , S. Willocq , B.J. Wilson , D.J. Wilson , P.J. Windischhofer , F.I. Winkel , F. Winklmeier , B.T. Winter , M. Wittgen , M. Wobisch , T. Wojtkowski , Z. Wolffs , J. Wollrath , M.W. Wolter , H. Wolters , M.C. Wong , E.L. Woodward , S.D. Worm , B.K. Wosiek , K.W. Woźniak , S. Wozniowski , K. Wraight , C. Wu , M. Wu , M. Wu , S.L. Wu , X. Wu , X. Wu , Y. Wu , Z. Wu , J. Wuerzinger , T.R. Wyatt , B.M. Wynne , S. Xella , L. Xia , M. Xia , M. Xie , A. Xiong , J. Xiong , D. Xu , H. Xu , L. Xu , R. Xu , T. Xu , Y. Xu , Z. Xu , Z. Xu , B. Yabsley , S. Yacoob , Y. Yamaguchi , E. Yamashita , H. Yamauchi , T. Yamazaki , Y. Yamazaki , S. Yan , Z. Yan , H.J. Yang , H.T. Yang , S. Yang , T. Yang , X. Yang , X. Yang , Y. Yang , Y. Yang , W-M. Yao , H. Ye , J. Ye , S. Ye , X. Ye , Y. Yeh , I. Yeletsikh , B. Yeo , M.R. Yexley , T.P. Yildirim , P. Yin , K. Yorita , S. Younas , C.J.S. Young , C. Young , C. Yu , Y. Yu , J. Yuan , M. Yuan , R. Yuan , L. Yue , M. Zaazoua , B. Zabinski , I. Zahir , E. Zaid , Z.K. Zak , T. Zakareishvili , S. Zambito , J.A. Zamora Saa , J. Zang , D. Zanzi , R. Zanzottera , O. Zaplatilek , C. Zeitnitz , H. Zeng , J.C. Zeng , D.T. Zenger Jr , O. Zenin , T. Ženiš , S. Zenz , S. Zerradi , D. Zerwas , M. Zhai , D.F. Zhang , J. Zhang , J. Zhang , K. Zhang , L. Zhang , L. Zhang , P. Zhang , R. Zhang , S. Zhang , S. Zhang , T. Zhang , X. Zhang , Y. Zhang , Y. Zhang , Y. Zhang , Z. Zhang , Z. Zhang , Z. Zhang , H. Zhao , T. Zhao , Y. Zhao , Z. Zhao , Z. Zhao , A. Zhemchugov , J. Zheng , K. Zheng , X. Zheng , Z. Zheng , D. Zhong , B. Zhou , H. Zhou , N. Zhou , Y. Zhou , Y. Zhou , C.G. Zhu , J. Zhu , X. Zhu , Y. Zhu , Y. Zhu , X. Zhuang , K. Zhukov , N.I. Zimine , J. Zinsser , M. Ziolkowski , L. Živković , A. Zoccoli , K. Zoch , T.G. Zorbas , O. Zormpa , W. Zou , L. Zwalinski .

¹Department of Physics, University of Adelaide, Adelaide; Australia.

²Department of Physics, University of Alberta, Edmonton AB; Canada.

³(^a)Department of Physics, Ankara University, Ankara; (^b)Division of Physics, TOBB University of Economics and Technology, Ankara; Türkiye.

⁴LAPP, Université Savoie Mont Blanc, CNRS/IN2P3, Annecy; France.

⁵APC, Université Paris Cité, CNRS/IN2P3, Paris; France.

⁶High Energy Physics Division, Argonne National Laboratory, Argonne IL; United States of America.

⁷Department of Physics, University of Arizona, Tucson AZ; United States of America.

⁸Department of Physics, University of Texas at Arlington, Arlington TX; United States of America.

⁹Physics Department, National and Kapodistrian University of Athens, Athens; Greece.

¹⁰Physics Department, National Technical University of Athens, Zografou; Greece.

¹¹Department of Physics, University of Texas at Austin, Austin TX; United States of America.

¹²Institute of Physics, Azerbaijan Academy of Sciences, Baku; Azerbaijan.

¹³Institut de Física d'Altes Energies (IFAE), Barcelona Institute of Science and Technology, Barcelona; Spain.

¹⁴Institute of High Energy Physics, Chinese Academy of Sciences, Beijing; China.

¹⁵Physics Department, Tsinghua University, Beijing; China.

¹⁶Institute of Physics, University of Belgrade, Belgrade; Serbia.

¹⁷Department for Physics and Technology, University of Bergen, Bergen; Norway.

- ¹⁸(*a*) Physics Division, Lawrence Berkeley National Laboratory, Berkeley CA; (*b*) University of California, Berkeley CA; United States of America.
- ¹⁹Institut für Physik, Humboldt Universität zu Berlin, Berlin; Germany.
- ²⁰Albert Einstein Center for Fundamental Physics and Laboratory for High Energy Physics, University of Bern, Bern; Switzerland.
- ²¹School of Physics and Astronomy, University of Birmingham, Birmingham; United Kingdom.
- ²²(*a*) Department of Physics, Bogazici University, Istanbul; (*b*) Department of Physics Engineering, Gaziantep University, Gaziantep; (*c*) Department of Physics, Istanbul University, Istanbul; Türkiye.
- ²³(*a*) Facultad de Ciencias y Centro de Investigaciones, Universidad Antonio Nariño, Bogotá; (*b*) Departamento de Física, Universidad Nacional de Colombia, Bogotá; Colombia.
- ²⁴(*a*) Dipartimento di Fisica e Astronomia A. Righi, Università di Bologna, Bologna; (*b*) INFN Sezione di Bologna; Italy.
- ²⁵Physikalisches Institut, Universität Bonn, Bonn; Germany.
- ²⁶Department of Physics, Boston University, Boston MA; United States of America.
- ²⁷Department of Physics, Brandeis University, Waltham MA; United States of America.
- ²⁸(*a*) Transilvania University of Brasov, Brasov; (*b*) Horia Hulubei National Institute of Physics and Nuclear Engineering, Bucharest; (*c*) Department of Physics, Alexandru Ioan Cuza University of Iasi, Iasi; (*d*) National Institute for Research and Development of Isotopic and Molecular Technologies, Physics Department, Cluj-Napoca; (*e*) National University of Science and Technology Politehnica, Bucharest; (*f*) West University in Timisoara, Timisoara; (*g*) Faculty of Physics, University of Bucharest, Bucharest; Romania.
- ²⁹(*a*) Faculty of Mathematics, Physics and Informatics, Comenius University, Bratislava; (*b*) Department of Subnuclear Physics, Institute of Experimental Physics of the Slovak Academy of Sciences, Kosice; Slovak Republic.
- ³⁰Physics Department, Brookhaven National Laboratory, Upton NY; United States of America.
- ³¹Universidad de Buenos Aires, Facultad de Ciencias Exactas y Naturales, Departamento de Física, y CONICET, Instituto de Física de Buenos Aires (IFIBA), Buenos Aires; Argentina.
- ³²California State University, CA; United States of America.
- ³³Cavendish Laboratory, University of Cambridge, Cambridge; United Kingdom.
- ³⁴(*a*) Department of Physics, University of Cape Town, Cape Town; (*b*) iThemba Labs, Western Cape; (*c*) Department of Mechanical Engineering Science, University of Johannesburg, Johannesburg; (*d*) National Institute of Physics, University of the Philippines Diliman (Philippines); (*e*) University of South Africa, Department of Physics, Pretoria; (*f*) University of Zululand, KwaDlangezwa; (*g*) School of Physics, University of the Witwatersrand, Johannesburg; South Africa.
- ³⁵Department of Physics, Carleton University, Ottawa ON; Canada.
- ³⁶(*a*) Faculté des Sciences Ain Chock, Université Hassan II de Casablanca; (*b*) Faculté des Sciences, Université Ibn-Tofail, Kénitra; (*c*) Faculté des Sciences Semlalia, Université Cadi Ayyad, LPHEA-Marrakech; (*d*) LPMR, Faculté des Sciences, Université Mohamed Premier, Oujda; (*e*) Faculté des sciences, Université Mohammed V, Rabat; (*f*) Institute of Applied Physics, Mohammed VI Polytechnic University, Ben Guerir; Morocco.
- ³⁷CERN, Geneva; Switzerland.
- ³⁸Affiliated with an institute formerly covered by a cooperation agreement with CERN.
- ³⁹Affiliated with an institute covered by a cooperation agreement with CERN.
- ⁴⁰Affiliated with an international laboratory covered by a cooperation agreement with CERN.
- ⁴¹Enrico Fermi Institute, University of Chicago, Chicago IL; United States of America.
- ⁴²LPC, Université Clermont Auvergne, CNRS/IN2P3, Clermont-Ferrand; France.
- ⁴³Nevis Laboratory, Columbia University, Irvington NY; United States of America.
- ⁴⁴Niels Bohr Institute, University of Copenhagen, Copenhagen; Denmark.

- ^{45(a)}Dipartimento di Fisica, Università della Calabria, Rende; ^(b)INFN Gruppo Collegato di Cosenza, Laboratori Nazionali di Frascati; Italy.
- ⁴⁶Physics Department, Southern Methodist University, Dallas TX; United States of America.
- ⁴⁷Physics Department, University of Texas at Dallas, Richardson TX; United States of America.
- ⁴⁸National Centre for Scientific Research "Demokritos", Agia Paraskevi; Greece.
- ^{49(a)}Department of Physics, Stockholm University; ^(b)Oskar Klein Centre, Stockholm; Sweden.
- ⁵⁰Deutsches Elektronen-Synchrotron DESY, Hamburg and Zeuthen; Germany.
- ⁵¹Fakultät Physik, Technische Universität Dortmund, Dortmund; Germany.
- ⁵²Institut für Kern- und Teilchenphysik, Technische Universität Dresden, Dresden; Germany.
- ⁵³Department of Physics, Duke University, Durham NC; United States of America.
- ⁵⁴SUPA - School of Physics and Astronomy, University of Edinburgh, Edinburgh; United Kingdom.
- ⁵⁵INFN e Laboratori Nazionali di Frascati, Frascati; Italy.
- ⁵⁶Physikalisches Institut, Albert-Ludwigs-Universität Freiburg, Freiburg; Germany.
- ⁵⁷II. Physikalisches Institut, Georg-August-Universität Göttingen, Göttingen; Germany.
- ⁵⁸Département de Physique Nucléaire et Corpusculaire, Université de Genève, Genève; Switzerland.
- ^{59(a)}Dipartimento di Fisica, Università di Genova, Genova; ^(b)INFN Sezione di Genova; Italy.
- ⁶⁰II. Physikalisches Institut, Justus-Liebig-Universität Giessen, Giessen; Germany.
- ⁶¹SUPA - School of Physics and Astronomy, University of Glasgow, Glasgow; United Kingdom.
- ⁶²LPSC, Université Grenoble Alpes, CNRS/IN2P3, Grenoble INP, Grenoble; France.
- ⁶³Laboratory for Particle Physics and Cosmology, Harvard University, Cambridge MA; United States of America.
- ^{64(a)}Department of Modern Physics and State Key Laboratory of Particle Detection and Electronics, University of Science and Technology of China, Hefei; ^(b)Institute of Frontier and Interdisciplinary Science and Key Laboratory of Particle Physics and Particle Irradiation (MOE), Shandong University, Qingdao; ^(c)School of Physics and Astronomy, Shanghai Jiao Tong University, Key Laboratory for Particle Astrophysics and Cosmology (MOE), SKLPPC, Shanghai; ^(d)Tsung-Dao Lee Institute, Shanghai; ^(e)School of Physics, Zhengzhou University; China.
- ^{65(a)}Kirchhoff-Institut für Physik, Ruprecht-Karls-Universität Heidelberg, Heidelberg; ^(b)Physikalisches Institut, Ruprecht-Karls-Universität Heidelberg, Heidelberg; Germany.
- ^{66(a)}Department of Physics, Chinese University of Hong Kong, Shatin, N.T., Hong Kong; ^(b)Department of Physics, University of Hong Kong, Hong Kong; ^(c)Department of Physics and Institute for Advanced Study, Hong Kong University of Science and Technology, Clear Water Bay, Kowloon, Hong Kong; China.
- ⁶⁷Department of Physics, National Tsing Hua University, Hsinchu; Taiwan.
- ⁶⁸IJCLab, Université Paris-Saclay, CNRS/IN2P3, 91405, Orsay; France.
- ⁶⁹Centro Nacional de Microelectrónica (IMB-CNM-CSIC), Barcelona; Spain.
- ⁷⁰Department of Physics, Indiana University, Bloomington IN; United States of America.
- ^{71(a)}INFN Gruppo Collegato di Udine, Sezione di Trieste, Udine; ^(b)ICTP, Trieste; ^(c)Dipartimento Politecnico di Ingegneria e Architettura, Università di Udine, Udine; Italy.
- ^{72(a)}INFN Sezione di Lecce; ^(b)Dipartimento di Matematica e Fisica, Università del Salento, Lecce; Italy.
- ^{73(a)}INFN Sezione di Milano; ^(b)Dipartimento di Fisica, Università di Milano, Milano; Italy.
- ^{74(a)}INFN Sezione di Napoli; ^(b)Dipartimento di Fisica, Università di Napoli, Napoli; Italy.
- ^{75(a)}INFN Sezione di Pavia; ^(b)Dipartimento di Fisica, Università di Pavia, Pavia; Italy.
- ^{76(a)}INFN Sezione di Pisa; ^(b)Dipartimento di Fisica E. Fermi, Università di Pisa, Pisa; Italy.
- ^{77(a)}INFN Sezione di Roma; ^(b)Dipartimento di Fisica, Sapienza Università di Roma, Roma; Italy.
- ^{78(a)}INFN Sezione di Roma Tor Vergata; ^(b)Dipartimento di Fisica, Università di Roma Tor Vergata, Roma; Italy.
- ^{79(a)}INFN Sezione di Roma Tre; ^(b)Dipartimento di Matematica e Fisica, Università Roma Tre, Roma;

Italy.

^{80(a)}INFN-TIFPA;^(b)Università degli Studi di Trento, Trento; Italy.

⁸¹Universität Innsbruck, Department of Astro and Particle Physics, Innsbruck; Austria.

⁸²University of Iowa, Iowa City IA; United States of America.

⁸³Department of Physics and Astronomy, Iowa State University, Ames IA; United States of America.

⁸⁴Istinye University, Sariyer, Istanbul; Türkiye.

^{85(a)}Departamento de Engenharia Elétrica, Universidade Federal de Juiz de Fora (UFJF), Juiz de Fora;^(b)Universidade Federal do Rio De Janeiro COPPE/EE/IF, Rio de Janeiro;^(c)Instituto de Física, Universidade de São Paulo, São Paulo;^(d)Rio de Janeiro State University, Rio de Janeiro;^(e)Federal University of Bahia, Bahia; Brazil.

⁸⁶KEK, High Energy Accelerator Research Organization, Tsukuba; Japan.

⁸⁷Graduate School of Science, Kobe University, Kobe; Japan.

^{88(a)}AGH University of Krakow, Faculty of Physics and Applied Computer Science, Krakow;^(b)Marian Smoluchowski Institute of Physics, Jagiellonian University, Krakow; Poland.

⁸⁹Institute of Nuclear Physics Polish Academy of Sciences, Krakow; Poland.

⁹⁰Faculty of Science, Kyoto University, Kyoto; Japan.

⁹¹Research Center for Advanced Particle Physics and Department of Physics, Kyushu University, Fukuoka ; Japan.

⁹²L2IT, Université de Toulouse, CNRS/IN2P3, UPS, Toulouse; France.

⁹³Instituto de Física La Plata, Universidad Nacional de La Plata and CONICET, La Plata; Argentina.

⁹⁴Physics Department, Lancaster University, Lancaster; United Kingdom.

⁹⁵Oliver Lodge Laboratory, University of Liverpool, Liverpool; United Kingdom.

⁹⁶Department of Experimental Particle Physics, Jožef Stefan Institute and Department of Physics, University of Ljubljana, Ljubljana; Slovenia.

⁹⁷School of Physics and Astronomy, Queen Mary University of London, London; United Kingdom.

⁹⁸Department of Physics, Royal Holloway University of London, Egham; United Kingdom.

⁹⁹Department of Physics and Astronomy, University College London, London; United Kingdom.

¹⁰⁰Louisiana Tech University, Ruston LA; United States of America.

¹⁰¹Fysiska institutionen, Lunds universitet, Lund; Sweden.

¹⁰²Departamento de Física Teórica C-15 and CIAFF, Universidad Autónoma de Madrid, Madrid; Spain.

¹⁰³Institut für Physik, Universität Mainz, Mainz; Germany.

¹⁰⁴School of Physics and Astronomy, University of Manchester, Manchester; United Kingdom.

¹⁰⁵CPPM, Aix-Marseille Université, CNRS/IN2P3, Marseille; France.

¹⁰⁶Department of Physics, University of Massachusetts, Amherst MA; United States of America.

¹⁰⁷Department of Physics, McGill University, Montreal QC; Canada.

¹⁰⁸School of Physics, University of Melbourne, Victoria; Australia.

¹⁰⁹Department of Physics, University of Michigan, Ann Arbor MI; United States of America.

¹¹⁰Department of Physics and Astronomy, Michigan State University, East Lansing MI; United States of America.

¹¹¹Group of Particle Physics, University of Montreal, Montreal QC; Canada.

¹¹²Fakultät für Physik, Ludwig-Maximilians-Universität München, München; Germany.

¹¹³Max-Planck-Institut für Physik (Werner-Heisenberg-Institut), München; Germany.

¹¹⁴Graduate School of Science and Kobayashi-Maskawa Institute, Nagoya University, Nagoya; Japan.

^{115(a)}Department of Physics, Nanjing University, Nanjing;^(b)School of Science, Shenzhen Campus of Sun Yat-sen University;^(c)University of Chinese Academy of Science (UCAS), Beijing; China.

¹¹⁶Department of Physics and Astronomy, University of New Mexico, Albuquerque NM; United States of America.

- ¹¹⁷Institute for Mathematics, Astrophysics and Particle Physics, Radboud University/Nikhef, Nijmegen; Netherlands.
- ¹¹⁸Nikhef National Institute for Subatomic Physics and University of Amsterdam, Amsterdam; Netherlands.
- ¹¹⁹Department of Physics, Northern Illinois University, DeKalb IL; United States of America.
- ¹²⁰^(a)New York University Abu Dhabi, Abu Dhabi;^(b)United Arab Emirates University, Al Ain; United Arab Emirates.
- ¹²¹Department of Physics, New York University, New York NY; United States of America.
- ¹²²Ochanomizu University, Otsuka, Bunkyo-ku, Tokyo; Japan.
- ¹²³Ohio State University, Columbus OH; United States of America.
- ¹²⁴Homer L. Dodge Department of Physics and Astronomy, University of Oklahoma, Norman OK; United States of America.
- ¹²⁵Department of Physics, Oklahoma State University, Stillwater OK; United States of America.
- ¹²⁶Palacký University, Joint Laboratory of Optics, Olomouc; Czech Republic.
- ¹²⁷Institute for Fundamental Science, University of Oregon, Eugene, OR; United States of America.
- ¹²⁸Graduate School of Science, Osaka University, Osaka; Japan.
- ¹²⁹Department of Physics, University of Oslo, Oslo; Norway.
- ¹³⁰Department of Physics, Oxford University, Oxford; United Kingdom.
- ¹³¹LPNHE, Sorbonne Université, Université Paris Cité, CNRS/IN2P3, Paris; France.
- ¹³²Department of Physics, University of Pennsylvania, Philadelphia PA; United States of America.
- ¹³³Department of Physics and Astronomy, University of Pittsburgh, Pittsburgh PA; United States of America.
- ¹³⁴^(a)Laboratório de Instrumentação e Física Experimental de Partículas - LIP, Lisboa;^(b)Departamento de Física, Faculdade de Ciências, Universidade de Lisboa, Lisboa;^(c)Departamento de Física, Universidade de Coimbra, Coimbra;^(d)Centro de Física Nuclear da Universidade de Lisboa, Lisboa;^(e)Departamento de Física, Universidade do Minho, Braga;^(f)Departamento de Física Teórica y del Cosmos, Universidad de Granada, Granada (Spain);^(g)Departamento de Física, Instituto Superior Técnico, Universidade de Lisboa, Lisboa; Portugal.
- ¹³⁵Institute of Physics of the Czech Academy of Sciences, Prague; Czech Republic.
- ¹³⁶Czech Technical University in Prague, Prague; Czech Republic.
- ¹³⁷Charles University, Faculty of Mathematics and Physics, Prague; Czech Republic.
- ¹³⁸Particle Physics Department, Rutherford Appleton Laboratory, Didcot; United Kingdom.
- ¹³⁹IRFU, CEA, Université Paris-Saclay, Gif-sur-Yvette; France.
- ¹⁴⁰Santa Cruz Institute for Particle Physics, University of California Santa Cruz, Santa Cruz CA; United States of America.
- ¹⁴¹^(a)Departamento de Física, Pontificia Universidad Católica de Chile, Santiago;^(b)Millennium Institute for Subatomic physics at high energy frontier (SAPHIR), Santiago;^(c)Instituto de Investigación Multidisciplinario en Ciencia y Tecnología, y Departamento de Física, Universidad de La Serena;^(d)Universidad Andres Bello, Department of Physics, Santiago;^(e)Instituto de Alta Investigación, Universidad de Tarapacá, Arica;^(f)Departamento de Física, Universidad Técnica Federico Santa María, Valparaíso; Chile.
- ¹⁴²Department of Physics, Institute of Science, Tokyo; Japan.
- ¹⁴³Department of Physics, University of Washington, Seattle WA; United States of America.
- ¹⁴⁴Department of Physics and Astronomy, University of Sheffield, Sheffield; United Kingdom.
- ¹⁴⁵Department of Physics, Shinshu University, Nagano; Japan.
- ¹⁴⁶Department Physik, Universität Siegen, Siegen; Germany.
- ¹⁴⁷Department of Physics, Simon Fraser University, Burnaby BC; Canada.

- ¹⁴⁸SLAC National Accelerator Laboratory, Stanford CA; United States of America.
- ¹⁴⁹Department of Physics, Royal Institute of Technology, Stockholm; Sweden.
- ¹⁵⁰Departments of Physics and Astronomy, Stony Brook University, Stony Brook NY; United States of America.
- ¹⁵¹Department of Physics and Astronomy, University of Sussex, Brighton; United Kingdom.
- ¹⁵²School of Physics, University of Sydney, Sydney; Australia.
- ¹⁵³Institute of Physics, Academia Sinica, Taipei; Taiwan.
- ¹⁵⁴(^a) E. Andronikashvili Institute of Physics, Iv. Javakhishvili Tbilisi State University, Tbilisi; (^b) High Energy Physics Institute, Tbilisi State University, Tbilisi; (^c) University of Georgia, Tbilisi; Georgia.
- ¹⁵⁵Department of Physics, Technion, Israel Institute of Technology, Haifa; Israel.
- ¹⁵⁶Raymond and Beverly Sackler School of Physics and Astronomy, Tel Aviv University, Tel Aviv; Israel.
- ¹⁵⁷Department of Physics, Aristotle University of Thessaloniki, Thessaloniki; Greece.
- ¹⁵⁸International Center for Elementary Particle Physics and Department of Physics, University of Tokyo, Tokyo; Japan.
- ¹⁵⁹Department of Physics, University of Toronto, Toronto ON; Canada.
- ¹⁶⁰(^a) TRIUMF, Vancouver BC; (^b) Department of Physics and Astronomy, York University, Toronto ON; Canada.
- ¹⁶¹Division of Physics and Tomonaga Center for the History of the Universe, Faculty of Pure and Applied Sciences, University of Tsukuba, Tsukuba; Japan.
- ¹⁶²Department of Physics and Astronomy, Tufts University, Medford MA; United States of America.
- ¹⁶³Department of Physics and Astronomy, University of California Irvine, Irvine CA; United States of America.
- ¹⁶⁴University of West Attica, Athens; Greece.
- ¹⁶⁵University of Sharjah, Sharjah; United Arab Emirates.
- ¹⁶⁶Department of Physics and Astronomy, University of Uppsala, Uppsala; Sweden.
- ¹⁶⁷Department of Physics, University of Illinois, Urbana IL; United States of America.
- ¹⁶⁸Instituto de Física Corpuscular (IFIC), Centro Mixto Universidad de Valencia - CSIC, Valencia; Spain.
- ¹⁶⁹Department of Physics, University of British Columbia, Vancouver BC; Canada.
- ¹⁷⁰Department of Physics and Astronomy, University of Victoria, Victoria BC; Canada.
- ¹⁷¹Fakultät für Physik und Astronomie, Julius-Maximilians-Universität Würzburg, Würzburg; Germany.
- ¹⁷²Department of Physics, University of Warwick, Coventry; United Kingdom.
- ¹⁷³Waseda University, Tokyo; Japan.
- ¹⁷⁴Department of Particle Physics and Astrophysics, Weizmann Institute of Science, Rehovot; Israel.
- ¹⁷⁵Department of Physics, University of Wisconsin, Madison WI; United States of America.
- ¹⁷⁶Fakultät für Mathematik und Naturwissenschaften, Fachgruppe Physik, Bergische Universität Wuppertal, Wuppertal; Germany.
- ¹⁷⁷Department of Physics, Yale University, New Haven CT; United States of America.
- ¹⁷⁸Yerevan Physics Institute, Yerevan; Armenia.
- ^a Also Affiliated with an institute covered by a cooperation agreement with CERN.
- ^b Also at An-Najah National University, Nablus; Palestine.
- ^c Also at Borough of Manhattan Community College, City University of New York, New York NY; United States of America.
- ^d Also at Center for High Energy Physics, Peking University; China.
- ^e Also at Center for Interdisciplinary Research and Innovation (CIRI-AUTH), Thessaloniki; Greece.
- ^f Also at CERN, Geneva; Switzerland.
- ^g Also at CMD-AC UNEC Research Center, Azerbaijan State University of Economics (UNEC); Azerbaijan.

^h Also at Département de Physique Nucléaire et Corpusculaire, Université de Genève, Genève; Switzerland.

ⁱ Also at Departament de Física de la Universitat Autònoma de Barcelona, Barcelona; Spain.

^j Also at Department of Financial and Management Engineering, University of the Aegean, Chios; Greece.

^k Also at Department of Mathematical Sciences, University of South Africa, Johannesburg; South Africa.

^l Also at Department of Physics, California State University, Sacramento; United States of America.

^m Also at Department of Physics, King's College London, London; United Kingdom.

ⁿ Also at Department of Physics, Stanford University, Stanford CA; United States of America.

^o Also at Department of Physics, Stellenbosch University; South Africa.

^p Also at Department of Physics, University of Fribourg, Fribourg; Switzerland.

^q Also at Department of Physics, University of Thessaly; Greece.

^r Also at Department of Physics, Westmont College, Santa Barbara; United States of America.

^s Also at Faculty of Physics, Sofia University, 'St. Kliment Ohridski', Sofia; Bulgaria.

^t Also at Hellenic Open University, Patras; Greece.

^u Also at Henan University; China.

^v Also at Imam Mohammad Ibn Saud Islamic University; Saudi Arabia.

^w Also at Institutio Catalana de Recerca i Estudis Avancats, ICREA, Barcelona; Spain.

^x Also at Institut für Experimentalphysik, Universität Hamburg, Hamburg; Germany.

^y Also at Institute for Nuclear Research and Nuclear Energy (INRNE) of the Bulgarian Academy of Sciences, Sofia; Bulgaria.

^z Also at Institute of Applied Physics, Mohammed VI Polytechnic University, Ben Guerir; Morocco.

^{aa} Also at Institute of Particle Physics (IPP); Canada.

^{ab} Also at Institute of Physics, Azerbaijan Academy of Sciences, Baku; Azerbaijan.

^{ac} Also at National Institute of Physics, University of the Philippines Diliman (Philippines); Philippines.

^{ad} Also at Technical University of Munich, Munich; Germany.

^{ae} Also at The Collaborative Innovation Center of Quantum Matter (CICQM), Beijing; China.

^{af} Also at TRIUMF, Vancouver BC; Canada.

^{ag} Also at Università di Napoli Parthenope, Napoli; Italy.

^{ah} Also at University of Colorado Boulder, Department of Physics, Colorado; United States of America.

^{ai} Also at University of the Western Cape; South Africa.

^{aj} Also at Washington College, Chestertown, MD; United States of America.

^{ak} Also at Yeditepe University, Physics Department, Istanbul; Türkiye.

* Deceased